



**HAL**  
open science

## Soft Underwater Adhesives based on Weak Molecular Interactions

Mehdi Vahdati, Dominique Hourdet, Costantino Creton

► **To cite this version:**

Mehdi Vahdati, Dominique Hourdet, Costantino Creton. Soft Underwater Adhesives based on Weak Molecular Interactions. *Progress in Polymer Science*, 2023, 139, pp.101649. 10.1016/j.progpolymsci.2023.101649 . hal-04266864

**HAL Id: hal-04266864**

**<https://hal.science/hal-04266864>**

Submitted on 31 Oct 2023

**HAL** is a multi-disciplinary open access archive for the deposit and dissemination of scientific research documents, whether they are published or not. The documents may come from teaching and research institutions in France or abroad, or from public or private research centers.

L'archive ouverte pluridisciplinaire **HAL**, est destinée au dépôt et à la diffusion de documents scientifiques de niveau recherche, publiés ou non, émanant des établissements d'enseignement et de recherche français ou étrangers, des laboratoires publics ou privés.

# Soft Underwater Adhesives based on Weak Molecular Interactions

Mehdi Vahdati <sup>1,\*</sup>, Dominique Hourdet <sup>2</sup>, Costantino Creton <sup>2</sup>

<sup>1</sup> Polyelectrolytes, Complexes and Materials (PECMAT), Charles Sadron Institute, CNRS (UPR 22), University of Strasbourg, 67200 Strasbourg, France

<sup>2</sup> Soft Matter Sciences and Engineering (SIMM), ESPCI Paris, PSL University, Sorbonne University, CNRS, 75005 Paris, France

\*Email: [mehdi.vahdati@ics-cnrs.unistra.fr](mailto:mehdi.vahdati@ics-cnrs.unistra.fr)

## Abstract

Underwater adhesion has been the focus of many recent developments motivated by potential biomedical applications. Although most literature on underwater adhesives has focused on strong covalent chemistries, soft materials based on weak molecular interactions have gained interest. Instead of relying on potentially toxic chemical crosslinking reactions to form covalent bonds, these materials are often sticky due to their soft, viscoelastic nature, in a similar manner to soft hydrophobic Pressure-Sensitive Adhesives (PSAs). In this review, we critically discuss the state-of-the-art in the design and characterization of soft viscoelastic coacervates and gels based on specific weak molecular interactions for underwater adhesion. From the perspectives of materials science and mechanics, we investigate the relationships between the composition and structure of these materials and their underwater viscoelastic and adhesive properties. An originality of our review lies in the analogies and comparisons we draw with PSAs as well-understood *hydrophobic* self-adhesive counterparts of the *relatively hydrophilic underwater adhesives* discussed here. Considering current literature, a criterion has been proposed to distinguish *hydrophilic* and *hydrophobic* adhesives. The insights from this review are condensed into detailed guidelines for the design of future soft underwater adhesives. We conclude the review with important open questions and the perspectives of the field.

Key words: adhesion; polymers; physical interactions; equilibrium water content; complex coacervates; tack; rheology

## Table of contents

1. Introduction .....	XX
2. Measurement of adhesion in the presence of water .....	XX
2.1. Shear strength .....	XX
2.2. Peel tests .....	XX
2.3. Probe tack test .....	XX
2.4. Underwater rheology .....	XX
3. Soft underwater adhesives .....	XX

3.1. Based on hydrophobic interactions .....	XX
3.1.1. Hydrophobic interactions .....	XX
3.1.2. Bulk hydrophobic interactions .....	XX
3.1.3. Interfacial hydrophobic host-guest interactions .....	XX
3.2. Based on electrostatic interactions .....	XX
3.2.1. Polyelectrolyte complex coacervation .....	XX
3.2.2. General properties of polyelectrolyte complex coacervates .....	XX
3.2.3. Obtaining sticky complex coacervates .....	XX
3.3. Based on H-bonding interactions .....	XX
3.4. Based on other weak interactions .....	XX
4. Tuning underwater adhesiveness .....	XX
5. Challenges and perspectives .....	XX

### List of abbreviations

PSA	Pressure-sensitive adhesive
T <sub>g</sub>	Glass transition temperature
MWD	Molecular weight distribution
MW	Molecular weight
H-bond	Hydrogen bond
LCST	Lower critical solution temperature
UCST	Upper critical solution temperature
CSC	Critical salt concentration
DP	Degree of polymerization
TTS	Time-temperature superposition
TSS	Time-salt superposition
S switch	Salt switch
T switch	Temperature switch
SFA	Surface force apparatus
AFM	Atomic force microscopy

## 1. Introduction

Soft underwater adhesives with medium- to long-term performance are of great interest in the field of biomedical devices [1,2]. The idea of using surgical adhesives and sealants as minimally invasive alternatives to sutures and staples is not intrinsically new [3–5] but important challenges remain, both from the biomedical and the mechanics perspectives. Previous reviews have detailed the state-of-the-art on wet and underwater hydrogel adhesives from the perspectives of materials and chemistry [5–9], biology and bioinspired design [1,2,6,10–13], and biomedical applications [4,14–16]. The present review focuses on the structure-properties relationships of soft underwater adhesives based on weak molecular interactions, potentially useful for biomedical applications. It is not intended to be an exhaustive review of underwater or surgical adhesives, but rather to provide design guidelines by offering insights into the mechanics of soft adhesives in aqueous media.

It is important to clarify the interest of employing *weak* molecular interactions to make *soft* underwater adhesives when, indeed, strong interactions may be used to make strong adhesives. For this, let us consider some of the design requirements for biomedical adhesives (we emphasize that this is not a list of all the requirements): 1) to avoid hazardous chemicals and reactions, 2) to ensure mechanical compatibility with the substrate tissue in terms of stiffness, and 3) to achieve stable adhesion over a given period.

(1) The oldest and most common strategy to achieve tissue adhesion has been to use injectable precursors followed by an in-situ chemical crosslinking reaction [4,7,17]. The reaction may be triggered by light, the presence of oxygen, or upon mixing reactive components just before application. The main concern with such adhesives is the toxicity of the reaction and the unreacted components (monomers, free radicals, etc.). Furthermore, the reaction relies on specific chemistries which may vary from one tissue to another. Therefore, in the past fifteen years, many materials scientists have also looked at the insightful work of marine biologists, such as Herbert Waite and Russell Stewart, for inspirations from organismal adhesion [10–12,18]. Marine organisms such as mussels, barnacles, and sandcastle worms have evolved to develop resilient underwater adhesives for their harsh environments. Although each of these animals has its own tricks and strategies for underwater adhesion, they all use a variety of molecular interactions, including many *non-covalent* interactions, as reviewed by Kamperman's group [2] and shown in Fig. 1 A.

At the onset of this trend, many material scientists hypothesized that catechol chemistry, with its capacity to form various water-mediated weak and strong interactions with different substrates, was the ultimate solution to the challenges of underwater adhesion. Many studies were – and still are – focused on developing catechol-based underwater adhesives, as addressed in several detailed reviews [1,2,5,13,19,20]. However, catechol chemistry is extremely pH dependent, is prone to oxidation, and requires highly oxidizing and usually toxic reagents for hardening. Marine organisms have overcome

these issues by taking advantage of controlled microenvironments (e.g. with local pH control, which is not always feasible in real applications) and a range of other moieties and interactions in the vicinity of catechol functions [12,21–23]. Therefore, several research groups, including ours, started to develop soft underwater adhesives based on simpler model systems to understand the role of specific weak molecular interactions (Fig. 1).

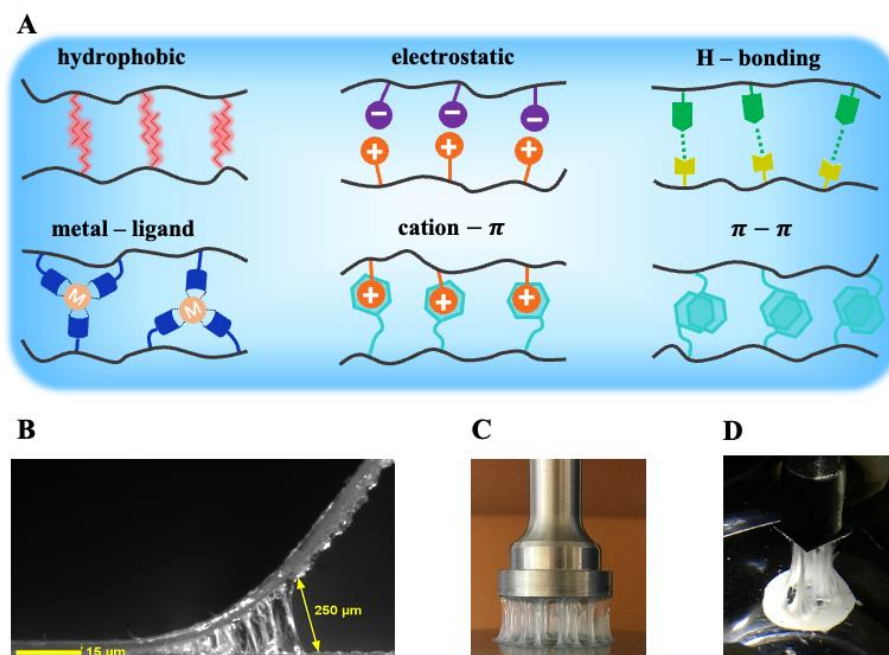


Fig. 1. (A) Weak molecular interactions useful for soft underwater adhesion. (B) The side-view of a hydrophobic PSA tape showing extensive fibrillation in debonding (peeling). [24], Copyright 2017.

Adapted with permission from Royal Society of Chemistry. (C) A soft PSA-like physical hydrogel based on hydrophobic interactions showing extensive fibrillation while debonding in air. The hydrogel features a similar behavior in water (not shown). [25], Copyright 2020. Adapted with permission from American Chemical Society Publications. (D) A soft PSA-like physical hydrogel based on electrostatic interactions showing extensive fibrillation in debonding in 0.1 M NaCl solution. [26], Copyright 2020. Adapted with permission from American Chemical Society Publications.

(2) Matching the mechanical properties of an adhesive with those of the target tissue is important because cells recognize and respond to the mechanical properties of their environment/surroundings [27]. Therefore, soft adhesives for soft and wet, fragile tissues, such as the kidney or the liver, are needed just as much as strong adhesives, for instance, to glue bones. Soft underwater adhesives may be inspired from existing pressure-sensitive adhesives (PSAs) that instantly stick to most surfaces without relying on specific chemistries, a curing reaction or solvent evaporation (Fig. 1 B) [28,29]. However, PSAs are typically made of hydrophobic rubbery polymers and fail to stick to wet and immersed surfaces. This is usually due to poor contact with the substrate. Conversely hydrophilic adhesives may suffer from

excessive swelling of the adhesive and/or hydrolysis [19,30]. Nonetheless, the idea of developing “soft, PSA-like materials with controlled water content” has stimulated important developments in the field of underwater adhesion, as we will see in this review.

(3) The soft underwater adhesive must perform its primary function, that is, adhering to a substrate under wet or immersed conditions for a given period. In practical applications, this can be desirable to prevent or seal a leak, to close and protect a wound, or to hold a medical device in place. Depending on the application and the site where the adhesive is applied, it will experience different stress and strain levels, which must be considered in the design. But first, one needs to address how to quantify and understand the performance of an adhesive in aqueous media. It is also critical to have a clear notion of what is usually meant by *soft*, by *viscoelastic* and by *sticky*. We also believe that it is important to propose a distinction between soft adhesives depending on their level of hydrophilicity.

As reviewed in detail by Creton and Ciccotti [29,31], soft materials include a broad range of materials, such as generic adhesives, gels, rubbers, and soft tissues, with elastic moduli between  $10^3$  to  $10^7$  Pa. The majority of the soft underwater adhesives in the present review are characterized by a large extensibility and low elastic moduli, in the range of  $10^2$  to  $10^5$  Pa. They are thus similar to or slightly softer than conventional PSAs. The stickiness of a classical PSA is due to a careful design of its viscoelastic properties (glass transition temperature and network architecture) in order to easily form an intimate contact with almost any substrate under a light pressure while requiring a large energy per unit area to subsequently detach from the same substrate. This large hysteresis in this contact/debonding process can be achieved with lightly crosslinked high molecular weight polymers with a broad glass transition temperature centered around 20-30°C below the optimal usage temperature. [28] In parallel, the combination of large extensibility and some level of elasticity are needed to avoid flow and to favor detachment without residues [28,29]. In conventional PSAs, strain hardening during fibrillation relies on the presence of a low degree of chemical crosslinking. Due to their viscoelasticity, the adhesive properties of hydrophobic PSAs are highly rate and temperature dependent [29,32]. However, this handicap in industrial applications is much less important in life sciences where the relevant temperature is usually fixed.

But what macromolecular characteristics are needed to feature such a dual character and thereby instant stickiness? PSAs are typically hydrophobic, rubbery polymers – meaning they are above their glass transition temperature ( $T_g$ ) at room temperature – with a wide molecular weight distribution (MWD) and a low degree of crosslinking. They may also contain additives such as plasticizers and low molecular weight (MW) resins to fine tune their viscoelastic and adhesive properties [28]. The mobility of the polymer chains ( $T_g$  below room temperature) enhanced by short chains and small MW components is essential for the viscous dissipation. On the other hand, a network of physical and chemical crosslinks prevents the material from macroscopic flow. A sparse crosslinking means that the

material only starts to resist flow at very large deformations. Most PSAs are thus designed and formulated to be soft viscoelastic solids.

As mentioned above, PSAs are typically hydrophobic. Without going into details at this point, they are made of polymers that dislike water and tend to avoid or minimize their contact with wet surfaces. On the other hand, hydrophilic polymers tend to swell and eventually dissolve in water, unless they are crosslinked. Highly crosslinked gels swell little but become too elastic and thus non-sticky as they lose their liquid-like character while lightly crosslinked gels are still prone to excessive swelling. What is the trick then to make PSA-like underwater adhesives out of hydrophilic polymers?

To answer this question, we need to understand how a polymer chain behaves in a certain solvent depending on its quality. In a so-called good solvent, or in an athermal solvent, the polymer chain conformation displays a self-avoiding walk as it has favorable or neutral interactions with the solvent. ~~In a so-called solvent, the polymer chain conformation displays a self-avoiding walk as it has a lot of favorable interactions with the solvent.~~ As the solvent quality decreases, i.e. as the chains affinity for the solvent reduces, the chain starts to collapse to minimize its contact with the surrounding solvent molecules. After reaching a random coil conformation in theta conditions, the single chain collapse in a globular state in very poor solvent. The polymer solution eventually goes through a phase separation, with a polymer-rich phase in equilibrium with a solvent-rich phase [33]. This is the case, for instance, for mildly hydrophobic polymers in water. The polymer-rich phase is generally referred to as a coacervate. The advantage of a coacervate is that it is concentrated in polymer, sometimes up to 80 wt%, with a degree of swelling mainly controlled by the monomer composition rather than by the degree of crosslinking. The formation of such a concentrated phase will be responsible for dramatic modifications of flow properties since the viscosity of a polymer solution is highly dependent on the polymer concentration [33].

As we will see in this review, different weak intra- and inter-molecular interactions may trigger the phase separation process, possibly in conjunction with an environmental stimulus, such as temperature or salt concentration. Coacervates thus hold great potential for making soft underwater adhesives. Alternatively, phase separation may occur on a microscopic scale if, for instance, the hydrophobic polymer is modified with hydrophilic residues. In this case, the dense hydrophobic domains can contribute to the mechanical properties to make tough or sticky hydrogels [34–36].

Throughout this review, we distinguish conventional *hydrophobic* PSAs from soft *hydrophilic* underwater adhesives based on their equilibrium water contents. We propose that it is reasonable to distinguish *hydrophobic* adhesives, with typical water contents much lower than 20 wt%, from *hydrophilic* adhesives, which often contain more than 20 wt% water. This notion of the water content of an adhesive should not be confused with the “level of hydrophobicity of specific interactions” on molecular level. As an example, a *hydrophilic* underwater adhesive physically crosslinked with

hydrophobic interactions may contain more than 90 wt% water, which we will refer to as “a *hydrophilic* adhesive based on hydrophobic interactions”. We will also see *hydrophobic* underwater adhesives based on hydrophobic interactions. As we will see, the water content is a crucial parameter in the mechanical and adhesive properties of *hydrophilic* systems. Therefore, we also propose to distinguish these systems as *water-rich* and *water-poor hydrophilic* adhesives with 20 – 60 wt% and 60 – 95 wt% water, respectively.

In [Section 2](#), the most common methods of measuring adhesion under wet and immersed conditions as well as their advantages and limitations and the useful information from each method are reviewed. This section also presents the design principles of soft *hydrophobic* adhesives to offer insights for the design and characterization of soft *hydrophilic* underwater adhesives. In [Section 3](#), the state-of-the-art in soft underwater adhesives based on specific weak molecular interactions is critically reviewed. Indeed, some systems rely on multiple weak interactions. This section will end with an overview of other types of weak interactions that have shown great promise for underwater adhesion, although we know of few or no model systems relying on these interactions alone. This review is mainly concerned with bulk, macroscopic underwater adhesion; however, we have not excluded instances of interfacial adhesion where the systems studied hold promise for the development of bulk systems. Based on the current state of the art, [Section 4](#) provides guidelines and suggestions for the design of future soft *hydrophilic* underwater adhesives based on weak molecular interactions. We will conclude this review with a discussion of open questions and some perspectives in [Section 5](#).

## 2. Measurement of adhesion in the presence of water

The adhesive performance of soft *hydrophobic* PSAs is typically assessed in terms of long-term shear strength, peel force upon debonding of a tape, and tackiness upon light contact [37]. These properties are closely linked to the viscoelastic behavior of these materials [28]. In this context where testing is done in air, the characterization methods are well-developed and quantitative, as briefly overviewed in the following [29]. Over the past 10 years, these testing methods have been extended to underwater adhesion testing targeted at *hydrophilic* systems. The state-of-the-art in the evaluation of adhesion in water and the complications associated with it are addressed in this section. We note that some of the results reviewed in this section report on covalently crosslinked adhesives, but we cover them briefly for the sake of introducing the method, knowing that these methods can very well be used to characterize soft adhesives.

As mentioned earlier, a general but very important parameter when making comparisons between different *hydrophilic* underwater adhesives is the *equilibrium water content*. Systems with a large difference in level of hydrophilicity (*water-poor* versus *water-rich* systems) are usually not quantitatively comparable because water generally acts as a plasticizer. In addition, the conditioning time and the testing medium must be considered when comparing different systems. Finally, when



comparing different studies, it is important to note where failure occurred upon debonding: at one of the two interfaces, within the bulk of the glue, or within the bulk of one of the two substrates. Interfacial failure is usually due to a weak bond. This can be due to improper contact from the beginning (no wetting), excessive shrinkage or swelling, and or the diffusion of water at the interface. Adhesive bulk failure, not uncommon with very soft physically cross-linked adhesives, occurs when the bulk of the adhesive has a weak resistance against shear stresses. On the contrary, when the joint and the adhesive are mechanically strong, failure may occur in one of the two substrates or at interfaces. This is unlikely to be the case for most of the adhesives reviewed in this text.

## 2.1. Shear strength

The shear strength of a pressure-sensitive-adhesive is typically measured in a static and or dynamic mode. In a static shear test, an adhesive tape with a given contact area on a substrate is exposed to a constant load and the time to failure is measured. This time is also known as the holding time. Static shear experiments are relatively easy to perform but are time consuming. A dynamic shear test measures the force required for failure under a constant shear rate, as schematized in Fig. 2 A [37]. The data is often reported as the shear strength, defined as the maximum force ( $F_{max}$ ) normalized by the initial contact area. This experiment is typically performed on a uniaxial tensile tester by holding the substrate in place and pulling the adhesive tape apart along the plane of adhesion at a given velocity (the shear rate is the ratio of the velocity by the adhesive thickness). The geometry is similar in both tests, but the information obtained is different. In any case, when failure occurs cohesively, i.e. within the adhesive layer, the shear strength is a measure of the cohesive strength of the material. The reader is referred to the following references for more details about shear tests [37–39].

When the adhesive comes in the form of a bulk viscoelastic sample or a liquid precursor, it is applied between the overlapping surface of two relatively long, flat, and parallel substrates. The overlap area is usually determined in agreement with some standard (for instance, ASTM F2255-05 for tissue adhesives) and must be well controlled. The substrates may be rigid (glass, metal, glassy polymers, bone) [40–42] or soft and flexible (hydrogels, elastomers, soft tissues) [43–46]. Such adhesives often require a certain amount of curing and or conditioning time (this is not the case with *hydrophobic* PSAs). The environmental parameters such as temperature and relative humidity may be controlled, depending on the type of adhesive and the application.

The shear geometry, in its dynamic or static form, has been the most commonly used geometry to test the performance of adhesives under wet and immersed conditions [40–43,46]. In most cases, the samples are prepared on dry or on wet substrates outside the aqueous medium of the test. The sample is then conditioned either in the wet state or directly in the aqueous medium of the test. Few works involving shear measurements have reported a bonding process while fully immersed in water [47]. For dynamic shear experiments in fully immersed conditions, a chamber mounted on the measuring

apparatus is generally used, as reported by the groups of Stewart, Li, and Dhinojwala [40,42,47] and schematically shown in Fig. 2 A. Otherwise, the test is commonly performed on wet samples in air [43,45,46,48]. Static shear tests can be done in aquariums or beakers, simply by hanging a given weight from the sample, or on tensile testers [47,49,50]. In some cases, the holding time is reported [50,51], although these tests usually simply provide visual demonstration of the holding capacity in a qualitative way. In general, comparing the results from tests performed under wet and immersed conditions should be done with care. This is less of a concern when samples are conditioned in an aqueous medium before the test and when evaporation is not significant within the time frame of the experiment.

The main advantages of this method are the simplicity of the sample preparation and the experimental setup as well as the range of substrates which may be used. It is particularly suitable for testing biological tissues soaked with water, phosphate-buffered saline (PBS), mucus, or blood (see standard test method ASTM F2255-05). However, a lap shear test does not provide detailed information about debonding mechanisms, and direct, real-time observation of failure is not always straightforward. Comparisons with the results of other adhesion experiments may cast further light on the performance of the adhesive and the failure mechanism(s).

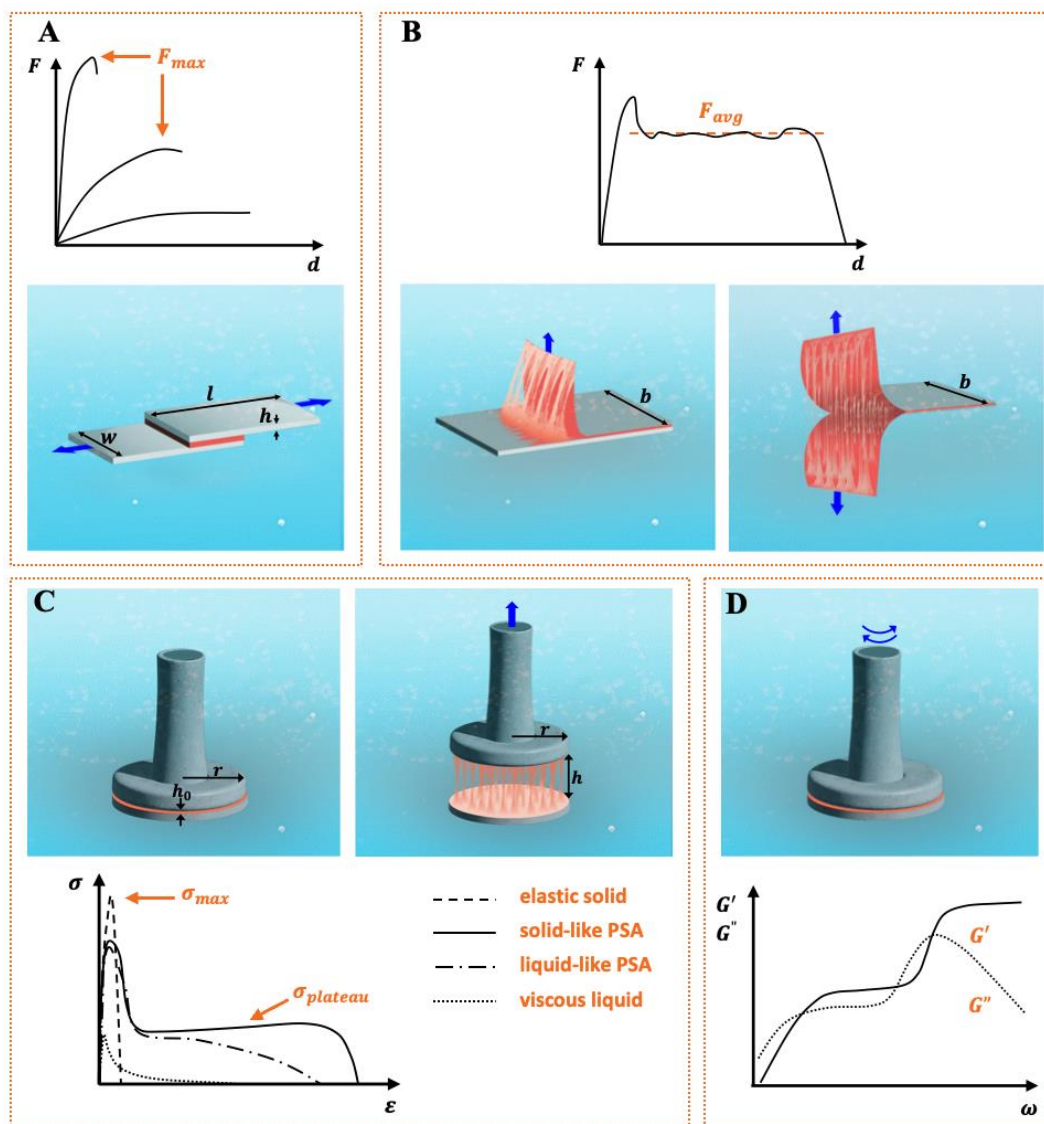


Fig. 2. Schematic illustration of underwater mechanical experiments relevant to the design and characterization of soft hydrophilic adhesives and typical data from each test. (A) lap shear test, (B) peel (left) and T-peel (right) tests, (C) probe tack test, and (D) linear rheology.

## 2.2. Peel tests

Due to their relevance to real applications, peel tests are among the most common testing methods for adhesive tapes and patches in air [28,52]. It should be noted that this test is suitable for soft, viscoelastic adhesives like *hydrophobic* PSAs. A detailed description of peel tests and how to interpret them can be found in reviews [29,53].

Briefly, the test involves peeling a thin strip (in the range of tens of micrometers) of a soft adhesive, typically coated on a backing layer, off a flat substrate. The substrate, usually rigid, may be made of metal, glass, or a glassy polymer and may be untreated or treated, for instance to impart hydrophilicity or specific surface interactions. The backing layer is usually chosen to be flexible enough to allow

peeling at a wide range of peel angles. Yet, it should not be stretchable. More solid-like adhesives in the form of a long strip of given dimensions may be also tested without a backing. In either case, the free end of the adhesive strip is attached to a force measuring apparatus and debonding is done at a constant peeling angle and peeling velocity. The most common testing angle is  $90^\circ$  due to its simplicity and relevance to real applications.

An alternative procedure well-adapted to soft, flexible substrates is the so-called T-peel test. In this case, the two substrates, stuck to one another by the adhesive in between, are pulled apart at a constant debonding rate [28,52]. In the ideal case where the adhesion is relatively strong and the substrates sufficiently flexible, the angle formed at the crack tip is  $180^\circ$ . However, this angle is often difficult to control. The results of such tests, especially with viscoelastic substrates, are more complicated to interpret due to the difficulty to separate the energy dissipated by the adhesive from that dissipated by the substrate [54–56].

Although peel testing on wet substrates including biological tissues is quite common [57–60], underwater peel experiments (Fig. 2 B) are very rare [61]. This is not surprising first because a typical peel test is adapted to soft viscoelastic adhesives, while many current underwater adhesives rely on strong (covalent) interactions and are far more elastic than the average PSA. Second, it seems technically more challenging (e.g., than a lap shear test) to install a peel setup to run in water. In general, these tests are simpler to perform on wet substrates, especially hydrogels and biological tissues. Since peel tests are relevant to real applications such as biomedical adhesives, we expect to see more underwater peel tests as the field of soft underwater adhesives grows.

In air or water, the main data obtained from a peel test is the average steady-state peeling force ( $F_{avg}$ , Fig. 2 B). Knowing the width of the strip,  $b$ , an apparent fracture energy can be calculated from  $\frac{F_{avg}}{b}(1 - \cos \theta)$ . This simplifies to  $F_{avg}/b$  and  $2F_{avg}/b$  in the case of a  $90^\circ$  peel test and a T peel test, respectively. This is in fact the work done by that force (force times distance) divided by the area (width times distance) on which the work was done. This apparent fracture energy is commonly expressed in force per unit distance, equivalent to energy per unit area, and can be considered an adhesion energy (under quasistatic steady state peeling). It should be emphasized that the apparent fracture energy is *not* necessarily a characteristic of the interface between the soft adhesive and the substrate; it is also highly dependent on the peel angle and the thickness of the adhesive. For instance, the swelling of non-equilibrated adhesives in water can change the thickness and the mechanical properties (modulus) of the layer and thereby the outcome of the test [24,29].

Despite the simplicity to perform these tests, they usually involve the formation of a complex fibrillated structure with locally variable stress and strain fields at the peel front [24]. This results from a strong coupling between the local bending of the backing and the viscoelastic properties of the adhesive. The problem is further complicated in the case of soft and flexible substrates. When the

adhesion is strong enough, a part of the *apparent* adhesion energy comes from viscoelastic dissipation in the substrate, which is difficult to decouple from the *actual* adhesion energy. Although the viscoelasticity of the substrate is relevant to many real applications such as soft tissue adhesion, it has not received much attention [54,55].

In developing underwater peel tests, repeatability and reproducibility must be verified to make sure the data is reliable. In addition to force-displacement data and average peel forces usually reported from peel experiments, visual observation of the experiment should be feasible. It is important to note whether the soft adhesive can form stable fibrils in water, as is the case with *hydrophobic* PSAs in air. It is also important to observe the failure mode, to answer questions such as where the failure occurs or whether the adhesive comes off the surface clean.

### 2.3. Probe tack test

A probe tack test measures the adhesiveness of a highly confined layer of a soft viscoelastic material between a flat substrate and a flat-ended cylindrical probe [29,62]. Unlike in lap shear and peel tests, in this method the soft adhesive experiences a well-defined displacement field due to the relatively negligible bending stiffness of the machine [29]. For this, the flat plates must be parallel. The substrate and the probe are rigid and may be made of metal, glass, or glassy polymers. A transparent substrate offers the advantage of direct observation of the confined layer in debonding, for instance using a tilted mirror (at 45 °) and a camera as in the setup of Lakrout and Creton [63] or in the custom-built underwater setup by Sudre and coworkers [64].

In a typical experiment, in air or water, the viscoelastic adhesive is placed on the rigid substrate and compressed to a certain level of force,  $F_{\text{contact}}$ , by a probe of radius  $r$ . The displacement is then kept constant for a given contact time. Importantly, the thickness of the layer,  $h_0$ , is significantly smaller than the radius of the probe,  $r$  (so  $r/h_0 \gg 1$ ); meaning the layer is highly confined [62,65]. The viscoelastic adhesive may relax some of the applied compressive load during the time before the onset of the test. The probe is then pulled off at a constant velocity,  $V_{\text{deb}}$ , and the force of debonding  $F$  is measured as a function of time or displacement ( $h - h_0$ ). A nominal strain rate ( $\dot{\epsilon}$ ) may be defined as the debonding velocity normalized by the initial thickness of the layer ( $V_{\text{deb}}/h_0$ ) [29]. An underwater probe tack test is schematized in Fig. 2 C.

In 2012, Sudre and coworkers reported the first custom-built underwater probe tack setup [64]. As shown in Fig. 3, the setup consists of a temperature-controlled chamber mounted on a tensile tester and a rigid probe attached to the flat end of a cylindrical punch connected to a load cell. The chamber holds a glass slide as the substrate and can be filled with various aqueous media (water, PBS, etc.). The advantage of this setup is that it allows a good control of the alignment between the rigid plates confining the adhesive layer and a direct lateral and axial observation of the debonding process. So far, it has been used in measuring the underwater adhesion between polymer brushes or thin films grafted on the rigid

probe and macroscopic hydrogels [66,67]. More recently, it was also used in measuring the underwater adhesion of soft, *hydrophilic* sticky materials to various rigid probes [68]. Other underwater probe tack setups have since been developed by other groups as well [69–71].

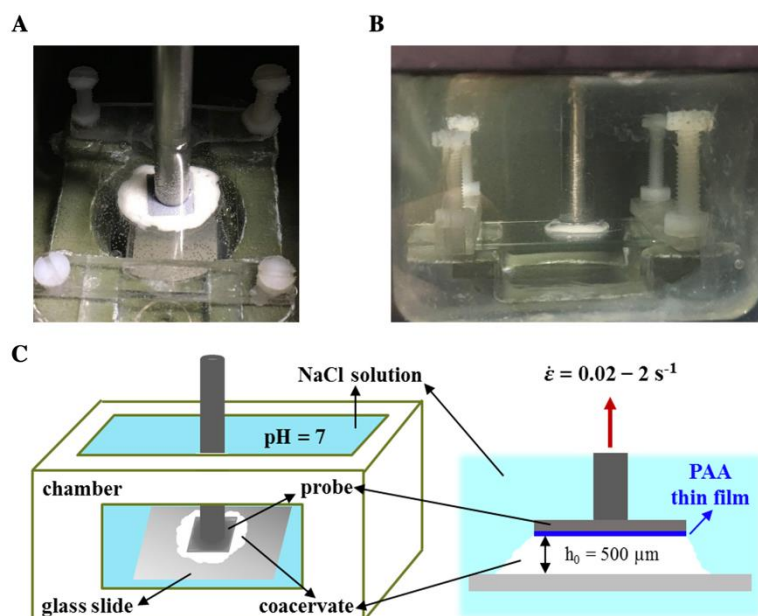


Fig. 3. (A) The top view of the chamber, showing an underwater adhesive between a flat punch (the probe connected to the load cell) and a glass slide. The testing geometry is immersed in an aqueous medium. (B) The lateral view of the same experiment. (C) Schematic representation of the different elements of the underwater adhesion testing setup developed at the SIMM lab at ESPCI Paris. [26], Copyright 2020. Reproduced with permission from American Chemical Society Publications.

Derks and coworkers were the first to use a rheometer equipped with a normal force transducer to perform probe tack tests on confined layers of *hydrophobic* viscoelastic adhesives [72]. Vahdati and coworkers adapted a rheometer to perform probe tack tests on thermoresponsive sticky hydrogels in air and in water [25,36]. The rheometer used is equipped with a sufficiently sensitive axial load cell and a Peltier heating plate offering rapid and precise control of temperature. The thermoresponsive *water-rich* adhesive is injected between the two plates and heated above its gelation temperature. For underwater adhesion measurements, a relatively large amount of preheated water is added into a cup around the measuring geometry, triggering in-situ gelation. When the initial sample is a liquid, the compression step prior to pull-off is not performed but the rest of the test is carried out similarly. Using rheometers as probe tack instruments is not limited to thermoresponsive hydrogels and any soft *hydrophilic* adhesive may be tested as long as the capacity and the sensitivity of the load cell allow such measurements [72].

The force-displacement data obtained is usually expressed in terms of *nominal* stress, defined as the debonding force normalized by the initial contact area ( $\sigma_N = F/\pi r^2$ ), versus *nominal* strain, defined as



the displacement normalized by the initial thickness ( $\varepsilon_N = h/h_0 - 1$ ). Different adhesives may be quantitatively compared based on the maximum force, the maximum strain, as well as the adhesion energy. The latter, defined as the energy required to create unit surface area of the adhesive, is readily calculated as  $W_{adh} = h_0 \int_0^{\varepsilon_{max}} \sigma_N \cdot d\varepsilon_N$  (in  $\text{J}\cdot\text{m}^{-2}$ ). It is worth noting that typical *hydrophobic* PSAs have adhesion energies on the order of 10-1000  $\text{J}\cdot\text{m}^{-2}$  in air and 1-10  $\text{J}\cdot\text{m}^{-2}$  in water and on wet surfaces.[63,71,73,74] As we shall see in this review, current soft *hydrophilic* underwater adhesives based on weak physical interactions have adhesion energies in the range of 0.1-100  $\text{J}\cdot\text{m}^{-2}$ .

The shape of the stress-strain curve contains a wealth of information about the deformation of the layer and the type of failure (cohesive versus adhesive), as shown in Fig. 2 C. For example, the first drop following the peak stress ( $\sigma_{max}$ , Fig. 2C) may be due to the occurrence of peripheral fingering instabilities (elastic or viscous), bulk cavitation, or a combination of both [62,63,65]. In the case of soft viscoelastic liquids, fingering instabilities (also known as Saffman-Taylor instabilities [75]) appear due to the intrusion of a low viscosity medium (air or water) into the highly confined layer of the incompressible adhesive as it is pulled toward the center of the probe in pull-off [72,76]. In the case of solids, the fingering is also due to incompressibility but is more similar to a buckling instability and it is fully reversible [77,78]. Bulk cavitation in incompressible soft elastic solids occurs when the hydrostatic component of the tensile load exceeds atmospheric pressure [36,62]. When the adhesive is too soft or liquid-like, fingering instabilities become predominant causing the stress to drop before it can build up sufficiently for cavitation. Most probably, soft viscoelastic adhesives experience both phenomena, with fingers in the periphery and cavities in the center [36,79,80].

As presented in the schematic stress-strain curve in Fig. 2 C, different material behaviors may be distinguished based on the shape of the curve after the peak of nominal stress ( $\sigma_{max}$ ). This peak may be followed by an abrupt drop (to zero) or the appearance of a stress plateau ( $\sigma_{plateau}$ , Fig. 2 C) [63,81,82]. The abrupt drop of force is usually observed when the bulk of the adhesive is stronger than the interface, leading to the propagation of a crack at or close to the interface (early adhesive failure). In contrast, when the interface is stronger than the bulk, the fingers and cavities grow into fibrils allowing very large deformations. With liquid-like viscoelastic adhesives the fibrils become thinner in their central section and fail cohesively [74]. In this case, the stress continues to drop after the peak but at a slower rate (compared to the case of interfacial crack propagation). However, with solid-like viscoelastic adhesives, the fibrils formed are stable and go through strain hardening. This strain hardening is seen as a second peak in nominal stress and causes tremendous energy dissipation. The failure is usually expected to be adhesive, occurring when the stored energy in the fibrils overcomes the adhesion energy [62,82,83]. In all of these descriptions, it is important to note the temperature and the rate at which the experiments are performed, given the viscoelastic nature of the adhesives addressed in this review.

One limitation of the probe test is that it is not necessarily representative of real applications, for instance biomedical applications. A peel test, in comparison, is a lot more representative of how a bandage is removed in practice. Another limitation is that the probes typically used are rigid, unlike, for instance, soft biological tissues. One may attempt to perform tests by using biological tissues as substrates. However, complications may arise in the interpretation from non-parallel substrates as well as from possible deformation and viscoelastic dissipation in the substrates. One alternative may be using thin layers of highly cross-linked and thus elastic hydrogels in place of the substrates when this is feasible. The hydrogels must be flat and parallel and at their equilibrium degree of swelling in the testing medium. Despite these limitations, a probe tack test provides the most detailed information about the performance of soft underwater adhesives, their mechanisms of adhesion and the failure modes. It is therefore the most informative test for the design of soft (underwater) adhesives.

#### 2.4. Underwater rheology

Designing soft adhesives such as PSAs requires fine-tuning of their viscoelastic properties such that they can form intimate contact with various substrates without relying on specific chemistries at the interface (what we call *generic* adhesion or in this case *stickiness*) while resisting a certain amount of stress in debonding. PSAs are in particular distinguished from other types of adhesives (structural, hot melt, etc.) by intrinsic viscoelastic dissipation mechanisms during debonding [28]. These features have made rheology an indispensable characterization tool in developing soft adhesives. The following overview of linear viscoelasticity is well-established for *hydrophobic* systems, and we will explain how the general principles and methods can be extended to underwater adhesives. At present, nonlinear rheology is used to a smaller extent (a few examples are given in [Section 3](#)).

Linear viscoelastic properties of soft adhesives are quantified via small amplitude oscillatory shear experiments over a range of frequencies to obtain information about the dynamic behavior of the material at different time scales. Small amplitudes ensure remaining in the *linear* regime, with no irreversible change in the internal organization of the material. To test soft solid-like samples and liquid-like samples, which is the case for most adhesives addressed in this review, a cone-plate geometry with a constant (truncation) gap is used. Using a cone ensures applying a homogenous and constant shear rate to the entire surface of the sample. Stiffer, solid-like samples are tested on a plate-plate geometry with sandblasted or roughened plates to avoid interfacial slippage. The experiment can be done at different gap heights in this case. However, a gradient in shear rate is applied to the sample in this geometry, with the outer edge and the center of the sample experiencing the highest shear rate and zero shear rate, respectively [84,85].

The main information from linear viscoelastic measurements are the dynamic moduli, namely, the storage modulus ( $G'$ ) and the loss modulus ( $G''$ ) (see [Fig. 2 D](#)).  $G'$  is a measure of the elasticity of the material, while  $G''$  is a measure of its dissipative character. In simple rheological terms, a viscoelastic



solid is characterized by  $G'(\omega) > G''(\omega)$  when  $\omega \rightarrow 0$  while a viscoelastic liquid is characterized by  $G''(\omega) > G'(\omega)$  when  $\omega \rightarrow 0$  (with  $\omega$  the angular frequency). Whether a solid material is soft or stiff is determined by the magnitude of the so-called complex modulus,  $|G^*(\omega)| = \sqrt{G'(\omega)^2 + G''(\omega)^2}$ . Liquid-like materials may be compared on the basis of their complex viscosity,  $\eta^*(\omega) = G^*(\omega)/\omega$ . At the transition between the liquid and solid regimes, also referred to as the gel point, the viscous response ( $G''$ ) and the elastic response ( $G'$ ) of the material have the same frequency dependence. The tangent of the phase lag between the elastic response and the viscous response of the material,  $\tan(\delta)$ , also known as the loss factor, is the ratio of its loss modulus to its storage modulus,  $G''(\omega)/G'(\omega)$ . It is therefore independent of frequency at the gel point [85,86].

All the above information may be easily obtained in an aqueous medium, using a chamber or a cup around the measuring geometry (schematized in Fig. 2 D), as done by Hamad and coworkers [87] and Vahdati and coworkers [26]. A low-viscosity medium like water or most aqueous media should not interfere with the measurement (i.e., it does not alter the measured torque), although this might have to be verified. Most importantly, one must check whether the adhesive is stable over time in water or whether it is prone to swelling or shrinkage [26,36,88]. This verification can be done via time sweeps. Section 3 contains examples of rheological measurements in aqueous media (water, salt solutions, PBS, etc.).

One of the best-known and simplest criteria in the design of soft *hydrophobic* PSAs is the so-called Dahlquist criterion [89]. Dahlquist noticed that in order for the adhesive to be capable of making good contact with substrates and to form adhesive fibrils upon debonding, its storage modulus must not exceed 0.1 MPa at the frequency corresponding to the contact time (at 1 rad.s<sup>-1</sup> for a contact time of 1 s, for instance) [82]. In water, interfacial forces are weaker and more variable; we thus expect the Dahlquist's criterion to be at a lower modulus. In other words, to be sticky, *hydrophilic* underwater PSAs must generally be softer than their *hydrophobic* counterparts.

Winter and Mours highlighted another rheological criterion for stickiness: “polymers at the gel point are extremely powerful adhesives” [86]. This offers an opportunity to make PSA-like underwater adhesives. The relaxation modulus,  $G(t)$ , of a critical gel takes on a power-law form of  $G(t) = G_0(t/\tau_0)^{-s}$ , where  $\tau_0$  is a material-specific characteristic time [90]. The front factor  $G_0$  is a measure of the stiffness of the critical gel in its unrelaxed state. The exponent  $s$  varies in the range of 0 to 1 for stronger to softer critical gels, respectively [90]. This power-law relaxation means that the material's elastic and viscous responses become frequency invariant at this point, rendering several linear viscoelastic material functions such as  $G'/G^*$ ,  $G''/G^*$ , and  $\tan(\delta)$  independent of frequency [85,91]. In fact, soft materials are stickiest in the *vicinity* of this point, that is, with  $0.3 < \tan(\delta) < 3$ . Commercial *hydrophobic* PSAs are always on the elastic side of the gel point, with  $G'$  slightly higher than  $G''$  and  $\tan(\delta)$  within 0.3 – 0.5. Higher values of  $\tan(\delta)$  lead to increasingly tacky, liquid-like adhesives. This

means that the material can easily wet different substrates (relatively higher  $G''$ ) but at the expense of losing its resistance against creep (relatively lower  $G'$ ). At  $\tan(\delta) > 3$ , the material is basically a tacky liquid prone to creep and therefore not an adhesive in practical terms. This criterion should remain valid in the presence of water.

The ratio  $\tan(\delta)/G'$  (equal to  $G''/G'^2$ ) is another useful parameter obtained from linear rheology to complement adhesion measurements [82,92]. In particular, it is used along with probe tack experiments (see Section 2.3). For a given substrate, there is a critical value of  $\tan(\delta)/G'$  above which crack blunting is favored over crack propagation, allowing bulk deformation to occur preferentially relative to interfacial debonding. At very high values of  $\tan(\delta)/G'$  the adhesive becomes too liquid-like and fibrils form easily but are not load-bearing. To ensure bulk deformation of the layer, a good starting point for the value of  $\tan(\delta)/G'$  based on the Dahlquist criterion and that of proximity to the gel point is  $0.5 \times 10^{-5} Pa^{-1}$  for adhesion on polar surfaces. For adhesion in air on low energy hydrophobic surfaces such as polyolefins or polytetrafluoroethylene (PTFE), soft *hydrophobic* adhesives typically require relatively higher values of  $\tan(\delta)/G'$  to fibrillate. Likewise, given that interfacial forces between two hydrophilic surfaces in water are weaker, adhering to a given substrate in water should require relatively higher  $\tan(\delta)/G'$  values relative to that of a PSA in air.

### 3. Soft underwater adhesives

A summary of the most important data on the underwater and wet performance of soft *hydrophilic* adhesives based on weak molecular interactions is presented in Table 1. In the following review of these works, the main questions that we seek to answer are: (1) From the perspective of materials science, what is the design rationale behind each system? (2) What is the water content of the system? Is this the *equilibrium* water content or would it change in an aqueous medium? (3) What are the structure properties relationships that result from this design? (4) What is the relationship, if any, between the linear rheology and the adhesive properties? (5) What is the significance of each work for the current state of the art? As can be seen in Table 1, not all these questions are answered in each of the studies reviewed here. Nonetheless, we have tried to comment on these important aspects, even if they were not reported in the original work. We must emphasize again that comparing the performance of different *hydrophilic* adhesives can be misleading without noting the water content and the experimental conditions.

*Table 1. Summary of the most important data on underwater and or wet performance of soft hydrophilic adhesives based on weak molecular interactions. The reported values from each work correspond to the system/composition with the strongest mechanical properties.*

ref	interactions <sup>a</sup>	water (wt%)	shear strength (kPa)	tack strength (kPa)	$W_{adh}^b$ (J.m <sup>-2</sup> )	rate <sup>c</sup>	comments <sup>d,e</sup>
-----	---------------------------	-------------	----------------------	---------------------	----------------------------------	-------------------	-------------------------

[36]	HP	92	NA	49	10.8	0.25 s <sup>-1</sup>	UW, T switch, 50 °C, 10 min, SS/SS
[49]	HP	NA	340	NA	NA	1 mm.s <sup>-1</sup>	Wet, interfacial adhesion, contact in water (pH=7.4) under 2 kPa for 1 h, Si/Si
[93]	HP	NA	NA	80	NA	1 mm.s <sup>-1</sup>	Wet, Porcine skin, interfacial adhesion, under 5 kPa for 120 s
[93]	HP	NA	NA	35	NA	1 mm.s <sup>-1</sup>	UW, interfacial adhesion, contact in water, under 25 kPa for 120 s, PP/PP
[68]	HP	91	0.85 (0.1 s <sup>-1</sup> )	5	1.9	0.2 s <sup>-1</sup>	UW, T Switch, 50 °C, 0.75 M NaCl, G/G
[94]	HP	77	NA	20	4.6	0.2 s <sup>-1</sup>	UW, T Switch, 50 °C, 0.7 M NaCl, G/G
[26]	ES	56	NA	50	65.2	2 s <sup>-1</sup>	UW, NO switch, 0.1 M NaCl, G/PAA
[26]	ES	62	NA	7.5	3.5	0.2 s <sup>-1</sup>	UW, S switch, 0.1 M NaCl, 1 h, G/PAA
[95]	ES	26	450	NA	NA	2.2 s <sup>-1</sup>	Wet, NO switch, contact in MiliQ water under 24 kPa for 3 h, G/G
[96]	ES	NA	29.6	NA	NA	0.17 mm.s <sup>-1</sup>	UW, NO switch, contact in water under 35 kPa for 15 min, PEEK/PEEK
[40]	ES	24	36	NA	NA	0.17 mm.s <sup>-1</sup>	UW, pH switch, contact in water under 35 kPa for 2 h, SS/SS
[97]	ES + HP	93	NA	25	7.2	0.2 s <sup>-1</sup>	UW, T + S switch, 50 °C, 0.1 M NaCl, 1 h, G/PAA
[94]	ES + HP	77	NA	70	60.6	0.2 s <sup>-1</sup>	UW, T + S Switch, 37 °C, 0.1 M NaCl, 1 h, G/G
[98]	HB	NA	NA	180	NA	0.02 mm.s <sup>-1</sup>	Wet, Porcine skin, under 20 N for 1 min, UW adhesion not reported
[99]	HB	NA	NA	70	NA	0.02 mm.s <sup>-1</sup>	UW, contact in water under 5 N for 30 s, SS/SS
[100]	HB	19	NA	98	NA	0.2 mm.s <sup>-1</sup>	Wet, porcine skin, UW adhesion not reported
[101]	HB + ES	NA	70	NA	NA	0.3 mm.s <sup>-1</sup>	Wet, Porcine skin, UW adhesion not reported
[102]	HB + HP	25	NA	600	NA	1.7 mm.s <sup>-1</sup>	UW, contact in water under 30 N for 10s, PMMA/PMMA
[103]	HB + HP	NA	NA	70	NA	0.08 s <sup>-1</sup>	UW, immediate pull-off, Al/Al
[103]	HB + HP	NA	NA	155	NA	25 s <sup>-1</sup>	UW, immediate pull-off, Al/G
[21]	CP + HP	88	NA	6	30	0.1 mm.s <sup>-1</sup>	UW, in 0.7 M NaCl, 10 s under pressure equivalent to gel's modulus, G
[104]	CP + ES	NA	158	NA	NA	0.3 mm.s <sup>-1</sup>	UW, in 0.15 M NaCl, delivered UW, 30 s of contact, G/G
[105]	ML + HB	34	50	NA	NA	3.3 mm.s <sup>-1</sup>	Wet, after 1 h in water, under 20 kPa for 2 min, G/G

<sup>a</sup> **HP**, **ES**, and **HB**, **CP**, and **ML** denote hydrophobic, electrostatic, and hydrogen bonding, Cation -  $\pi$ , and metal - ligand interactions, respectively. <sup>b</sup> The work of adhesion from wet or underwater probe tack experiments. <sup>c</sup> Note that the rate is either the (nominal) strain rate in s<sup>-1</sup> or the debonding velocity in mm.s<sup>-1</sup>. <sup>d</sup> The following acronyms have been used: **UW** for underwater, **T switch** for temperature switch, **S switch** for salt switch, **SS** for stainless steel, **Si** for silicon, **G** for glass, **PP** for poly(propylene), **PAA** for poly(acrylic acid), **PEEK** for poly(ether-ether-ketone), **PMMA** for poly(methyl methacrylate), **Fe**

for iron, **Al** for aluminum surfaces. <sup>e</sup> In the references where adhesion to different substrates was tested, the value reported corresponds to the best performance.

### 3.1. Based on hydrophobic interactions

#### 3.1.1. Hydrophobic interactions

Hydrophobic interactions play a crucial role in many (biological) processes, such as protein folding and biological membrane structures. In simple terms, the hydrophobic effect is the low solubility of hydrophobic solutes in water [106,107]. Hydrophobic interactions are the “solvent-mediated” attraction between hydrophobic molecules to minimize the exposure of their hydrophobes to water [108]. Most water-soluble polymers are comprised of hydrophilic (e.g. amide) and hydrophobic (e.g. vinyl backbone) moieties. The hydrophilic residues provide the main driving force for dissolution in water via hydrogen bonding, while the hydrophobic residues minimize their contact with the neighboring water molecules by organizing them into a structured hydration layer. This comes at the expense of entropy loss.

Most polymers can be distinguished based on their overall solubility in water. Hydrophilic polymers form extensive H-bonds with water molecules and stay in an extended coil state, while hydrophobic polymers remain in a collapsed globular state. Certain polymers with an amphiphilic nature – on the level of a monomer or chain segment – feature a temperature responsive behavior [108–110]. The transition temperature above which a polymer becomes hydrophobic is called the Lower Critical Solution Temperature (LCST), corresponding to the minimum on the coexistence curve of the phase diagram, as schematically shown in [Fig. 4 A](#). The inverse behavior is called UCST for Upper Critical Solution Temperature [108,111].

LCST polymers such as poly(N-isopropyl acrylamide) (PNIPAM) and poly(oligo(ethylene glycol)) (meth)acrylates (POEGMA) are of particular interest due to the small dependence of their LCST on the molecular weight, concentration, or the architecture of the homopolymer [108,112]. PNIPAM shows a sharp coil-to-globule transition in water just below body temperature (~ 32 °C), where amide-water H-bonds are disrupted and replaced by water-water and amide-amide H-bonds. This endothermic process is marked by an enthalpy of 4 – 6 kJ.mol<sup>-1</sup> of NIPAM [113–115]. The LCST of POEGMA can be tuned from 26 to 90 °C by varying the number of ethylene glycol units in the side chains from 2 to 9, respectively.

Heating aqueous solutions of LCST polymers usually leads to macrophase separation and precipitation. Therefore, these polymers are sometimes crosslinked to make chemical hydrogels, but they are prone to a volume phase transition, i.e. shrinkage, upon heating [34,116,117]. Otherwise, they are copolymerized with hydrophilic monomers to form thermoresponsive hydrogels, i.e. viscous solutions and physical hydrogels below and above the LCST, respectively [110,118]. For this thermally

triggered sol to gel transition, the monomer composition, copolymer topology, and architecture must be carefully designed [25,119,120].

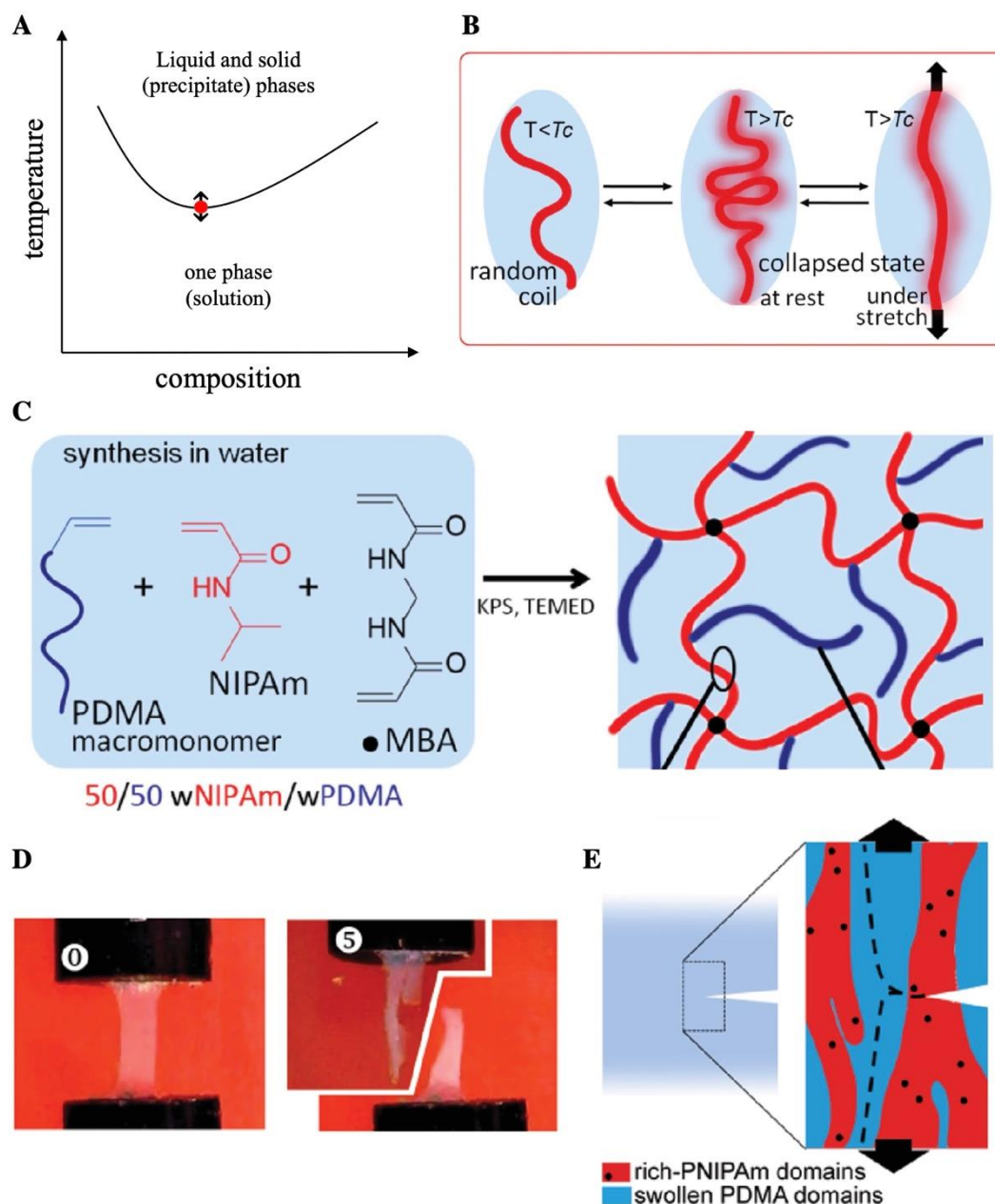


Fig. 4. (A) The schematic phase diagram of a LCST polymer as a function of its composition. The red dot represents the LCST. (B) The macromolecular rationale in the thermal toughening strategy developed by Guo and coworkers. PNIPAM chains tend to collapse to minimize their contact with water above the transition temperature. Stretching them out of their collapsed state requires energy. (C) The synthetic pathway to make a chemical network of PNIPAM grafted with PDMA. (D) The hydrogel during fracture experiments, (0) the notched sample at rest, (5) the sample post failure, where the crack propagation pathway is observed. (E) The nanostructure suggested to explain the crack bifurcation leading to thermal toughening. The blue and the red phases schematize the swollen

*hydrophilic phase and the collapsed hydrophobic phase, respectively. [34], Copyright 2016. Adapted with permission from John Wiley & Sons Inc.*

As shown in [Fig. 4 B – E](#), Guo and coworkers [34,121] combined the above strategies by introducing grafted chemical networks of thermoresponsive PNIPAM and hydrophilic poly(*N,N*-dimethyl acrylamide) (PDMA) comonomers. This macromolecular design enabled a microscopic phase separation while working under isochoric conditions, i.e. without macroscopic volume change, above the transition temperature. This led to significant thermal toughening (resistance to crack propagation) in a similar way to what is observed in natural rubber due to strain induced crystallization [122–125]; however, the requirements to make tough hydrogels are not exactly the same as those to make sticky hydrogels [31,34].

In [Section 3.1.2](#), we will present examples of wet and or underwater sticky hydrogels based on hydrophobic interactions in the bulk. These hydrogels are generally water-rich (with 50+ wt% water). Hydrophobic host-guest interactions for interfacial adhesion will be briefly introduced in [Section 3.2.2](#).

### [3.1.2. Bulk hydrophobic interactions](#)

Over the past decade, a growing body of literature has marked the important role of hydrophobic interactions in organismal adhesion [23,126,127]. However, these works either reported microscopic adhesion experiments or combinations of hydrophobic and strong interactions, and therefore fall outside the scope of the present review. [Fig. 5](#) gives a schematic overview of the systems using only hydrophobic interactions showing promise for underwater adhesion, as reviewed in the following.



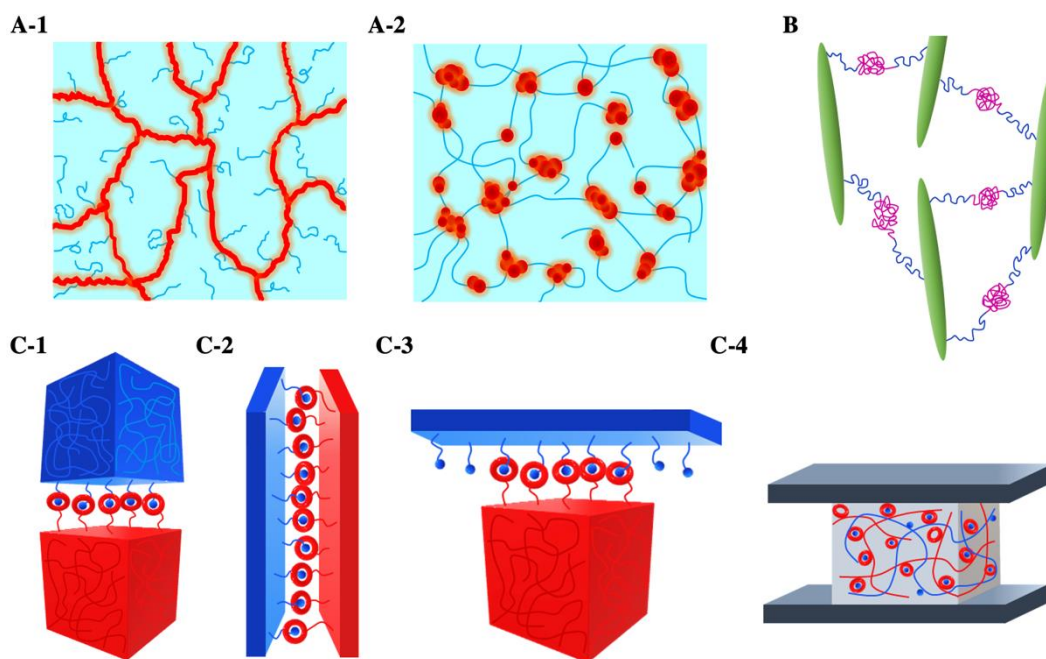
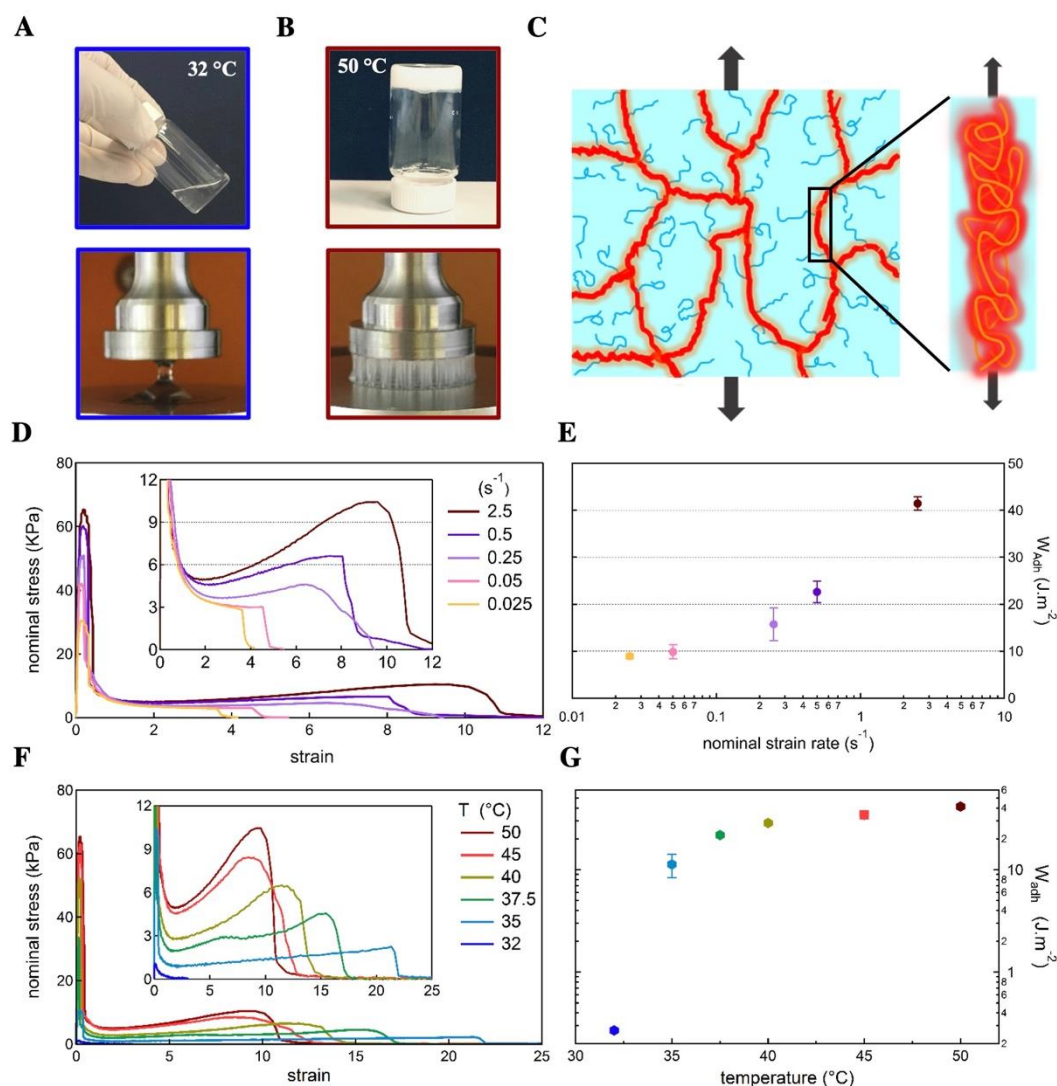


Fig. 5. Examples of hydrophobic interactions to achieve wet and underwater adhesion. (A-1) The continuous hydrophobic nanostructure proposed for PNIPAM-g-PDMA physical hydrogels above the LCST of PNIPAM. The red zones are hydrophobic associations of long PNIPAM backbones (A-2) The nanostructure proposed for the physical hydrogel with the inverse topology, PDMA-g-PNIPAM. The red zones are hydrophobic associations of short PNIPAM side chains. [25], Copyright 2020. Adapted with permission from American Chemical Society Publications. (B) Physical hydrogels made of a network of LCST POEGMA copolymers connected to cellulose nanocrystals (in green) through acylhydrazone bonds. [128], 2021. Adapted with permission from American Chemical Society Publications. (C-1) macroscopic self-assembly (adhesion) of hydrogels through interfacial host-guest interactions between the host (in red) and the guest (in blue) hydrogels, (C-2) Adhesion of host and the guest surfaces (C-3) Adhesion of a host hydrogel onto a rigid guest surface (C-4) A bulk adhesive hydrogel based on host-guest interactions.

Vahdati and coworkers developed a soft and injectable *water-rich* underwater adhesive based on a thermoresponsive graft copolymer showing a reversible sol to gel transition under isochoric conditions above the overlap concentration ( $c^*$ ), as shown in Fig. 6 A – B [36]. The copolymer, PNIPAM-g-PDMA, consisted of high MW ( $440 \text{ kg}\cdot\text{mol}^{-1}$ ) PNIPAM backbones bearing relatively short ( $14 \text{ kg}\cdot\text{mol}^{-1}$ ) PDMA side chains at 50 – 50 wt%. Above  $34 \text{ }^\circ\text{C}$ , the formation of a percolating (bicontinuous) network of strong hydrophobic PNIPAM domains across a swollen PDMA matrix led to a macroscopic hydrogel (see Fig. 6 C). At higher temperatures, the hydrophobic domains became increasingly concentrated and thus stronger with the disruption of additional hydrogen bonds with water molecules. This manifested itself in the increase of the storage modulus,  $G'$ , reaching a pseudo-plateau of  $1.3 \text{ kPa}$  around  $50 \text{ }^\circ\text{C}$ , with

a  $\tan(\delta)$  as low as 0.1 (at 92 wt% water content). The hydrogel is stable at observable times scales, but the loss modulus is still frequency dependent, implying that the material retains some dissipative nature.



**Fig. 6.** (A) The injectable solution of PNIPAM-g-PDMA (8 wt% in water) in a tilted vial and during a probe tack test. (B) The PNIPAM-g-PDMA hydrogel (at 92 wt% water content) in an inverted vial and during a probe tack test on a rheometer. Extensive fibrillation is visible in this case as opposed to the test at 32 °C. (C) The proposed nanostructure for PNIPAM-g-PDMA physical hydrogel. The red phase represents the continuous hydrophobic domains made up of PNIPAM backbones within the swollen PDMA phase in blue. (D) Nominal stress-strain curves from probe tack experiments on 8 wt% PNIPAM-g-PDMA at 50 °C at different nominal strain rates (in  $s^{-1}$ ). The inset is a magnification of the plateau region. (E) The corresponding adhesion energies obtained at different nominal strain rates. (F) Nominal stress-strain curves from probe tack experiments on 8 wt% PNIPAM-g-PDMA at different temperatures at  $2.5 s^{-1}$ . The inset is a magnification of the plateau region. (G) The corresponding adhesion energies as a function of the test temperature. [36], 2020. Reproduced with permission from John Wiley & Sons Inc.



Like a soft *hydrophobic* PSA in air, the *water-rich* PNIPAM-g-PDMA hydrogel (92 wt% water) showed a rate and temperature dependent adhesion energy in probe tack experiments. Well above the LCST, the hydrogel featured a marked increase in both stiffness and viscous dissipation with strain rate (Fig. 6 D – E). At strain rates below  $0.2 \text{ s}^{-1}$ , the hydrogel detached adhesively from the probe without extensive deformation and strain hardening, whereas above  $0.2 \text{ s}^{-1}$ , it went through substantial fibrillation up to large deformations ( $> 900 \%$ ) before cohesive failure occurred. The fibrillation was associated with peripheral fingering instabilities and cavitation in the center of the probe. Meanwhile, the strain hardening, observed in both pull-off and constant shear rate (stress growth) experiments, was due to the very slow dynamics of PNIPAM in the hydrophobic domains and the tendency of this nanostructure to minimize its contact with water (Fig. 6 C).

Interestingly, these PSA-like features were observed as soon as the transition temperature was crossed, i.e. at  $35 \text{ }^\circ\text{C}$  (Fig. 6 F – G). The shape of the stress – strain curves and the extent of strain hardening were similar at higher temperatures; however, the stress levels and the maximum deformation increased and decreased, respectively, as the hydrogel became more cohesive at higher temperatures. This suggested that a load-bearing hydrophobic nanoscaffold (Fig. 6 C) forms immediately above the LCST and becomes stronger (more hydrophobic) with temperature. At body temperature, for example, the hydrogel featured extensive fibrillation and strain hardening up to very large strains ( $1700 \%$ ) with an adhesion energy of  $21.8 \text{ J.m}^{-2}$  (at  $2.5 \text{ s}^{-1}$ ) [36].

It is worth noting the essential role of copolymer topology and concentration in the nonlinear mechanical properties [25]. With the same monomer composition and architecture and at the same polymer concentration/water content, the inverse topology (PDMA backbones bearing PNIPAM grafts, PDMA-g-PNIPAM), had comparable mechanical properties in small deformations as resolved by linear rheology. However, it did not feature any strain hardening, neither in probe tack tests nor in stress growth experiments. This was associated with the formation of isolated hydrophobic domains (see Fig. 5 A-2) as opposed to a percolating hydrophobic nanoscaffold (see Fig. 5 A-1). As a result, the adhesion energy was notably lower at the same  $G'$ . Moreover, at very high polymer concentrations ( $> 10 \text{ wt}\%$ ), the solution is too viscous at low temperature compromising the injectability while the gel is too stiff at high T compromising the adhesive properties.

Underwater rheology and probe tack tests were used to study the underwater performance of  $8 \text{ wt}\%$  PNIPAM-g-PDMA, as presented in Fig. 7. Upon in-situ immersion in hot water ( $50 \text{ }^\circ\text{C}$ ), the hydrogel was formed almost instantaneously, and the dynamic moduli reached a stable plateau after 5 minutes. No swelling or shrinkage was observed in water. In underwater probe tack tests on stainless steel substrates, the hydrogel maintained its generic PSA-like behavior regardless of the applied strain rate,

although the stress levels and the extent of strain hardening were somewhat lower compared to the tests in air. Yet, the adhesion energy (even after 15 h of immersion) was only 30% lower than that in air. This is significant next to conventional *hydrophobic* PSAs, which lose up to 95% of their adhesion energy on wet substrates [36,129]. It was concluded that the hydrophobic nanoscaffold was insensitive to the presence of water, highlighting the potential of hydrophobic interactions to make *water-rich* bulk underwater adhesives.

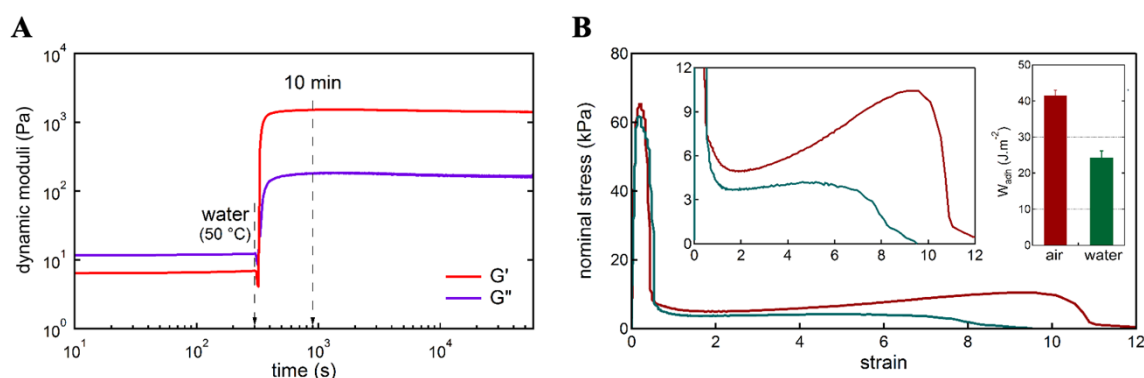


*Fig. 7. (A) Time sweep experiment on 8 wt% PNIPAM-g-PDMA. Preheated water (50 °C) was added around the geometry after 5 minutes. The dynamic moduli reach a stable plateau by 10 min from immersion, where they remain for longer immersion times (16 h shown here). (B) The comparison of the probe tack curves in air and water both at 50 °C and at 2.5 s<sup>-1</sup>. The experiment in air was performed 10 min after immersion. The left inset magnifies the plateau region. The right inset presents the corresponding adhesion energies. [36], 2020. Adapted with permission from John Wiley & Sons Inc.*

Nasseri and Tam [128] reported thermoresponsive sticky hydrogels based on POEGMA copolymers attached to dialdehyde cellulose nanocrystals via acylhydrazone dynamic covalent bonds, as shown in Fig. 8 A (also see Fig. 5 B). The POEGMA copolymers were prepared at different ratios of comonomers with 2 and 4-5 PEG groups on the side chain, allowing the LCST to be tuned between 40 and 58 °C. At a 50:50 molar ratio between the two comonomers and using a high enough concentration of dialdehyde cellulose nanocrystals, the material was a soft gel ( $G' \approx 0.01$  kPa) at room temperature with a LCST at 45 °C. Above this temperature, a gradual stiffening was observed with  $G'$  and  $G''$  reaching 1 and 0.1 kPa, respectively, by 70 °C [130].

The authors studied the adhesive properties of these hydrogels in probe tack experiments on stainless steel substrates in air (Fig. 8 B – C) [128]. The hydrogels showed the highest adhesion energy ( between 1.6 and 4.3 J.m<sup>-2</sup> at 0.25 s<sup>-1</sup>) and fibrillation to large strains (700 – 800 %) when tested at their respective LCST temperature. According to the authors, higher temperatures weakened the acylhydrazone bonds

and led to lower adhesion energies. Given that the dynamic moduli of these hydrogels continue to increase above the LCST temperature [130], it is more likely that the higher degree of elasticity and the weaker interface must have hindered the formation of fibrils at higher temperatures ( $\tan(\delta)/G'$  too low); an explanation that is comparable to that of the effect of polymer concentration discussed above [25].

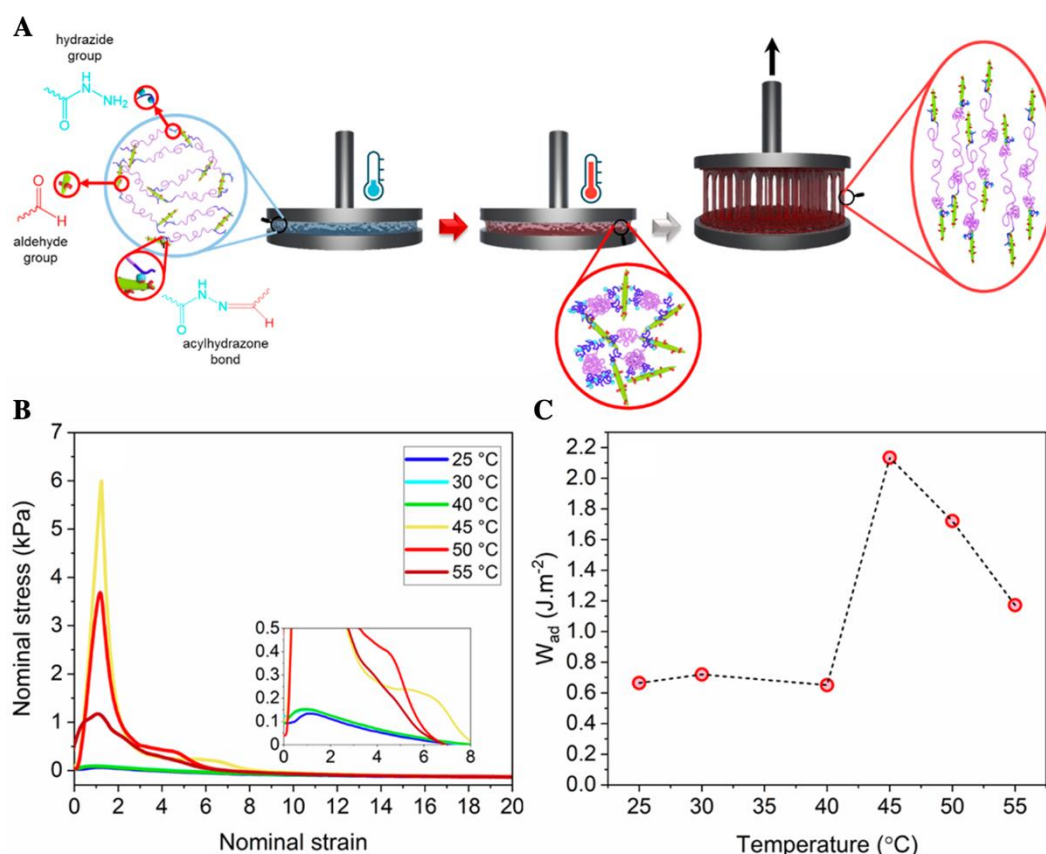


Fig. 8. (A) The schematic representation of the strategy developed by nasseri and Tam. (B) Typical nominal stress-strain curves obtained at different temperatures. (C) The corresponding adhesion energies. [128], 2021. Reproduced with permission from American Chemical Society Publications.

The underwater mechanical properties of these or other POEGMA based hydrogels have not been reported so far, but they are intuitively expected to be weaker in water than in air, as is the case for most adhesives. These hydrogels are also expected to be more prone to swelling and dissociation than PNIPAM based hydrogels. This is due to one of the unique features of PNIPAM which is forming hydrophobic aggregates with very slow dynamics (or long lifetimes). This is mainly related to the concentrated domains of PNIPAM being close to their glass transition unlike other LCST polymers like POEGMA or poly(alkylene oxide) derivatives which have very low  $T_g$  values, well below room temperature.

Systems combining such hydrophobic interactions with other weak interactions will be addressed in the next sections.

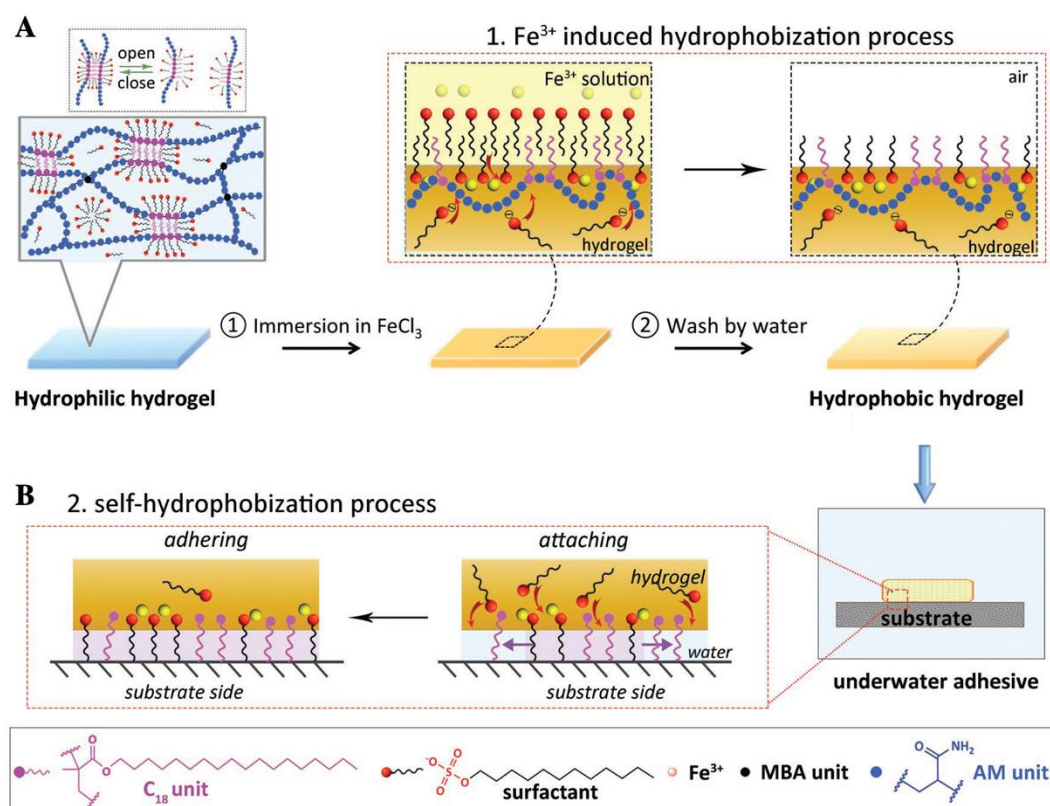


Fig. 9. Schematic illustration of (A) the underwater adhesion strategy based on self-hydrophobization of PAM hydrogels, and (B) how the self-hydrophobization process leads to underwater adhesion between the hydrogel and substrate. [93], Copyright 2020. Reproduced with permission from John Wiley & Sons Inc.

As a last example in this part, Han and coworkers [93] reported nonspecific wet interfacial adhesion of hydrophobically-modified, dynamic poly(acrylamide) (PAAm) hydrogels. The PAAm network contained a small amount ( $< 20$  wt%) of hydrophobic stearyl methacrylate ( $\text{C}_{18}$ ), which formed a hydrophobic bilayer on the *surface* when treated with ferric dodecyl sulfate (FDS) surfactant, as schematized in Fig. 9. The so-called self-hydrophobization of the hydrogel's surface was determined via water contact angle, which reached  $115^\circ$  after 80 min of immersion in the presence of FDS (from  $22^\circ$  before immersion). In a consistent fashion with the water contact angle, the interfacial underwater probe tack strength of the hydrogel against a poly(propylene) (PP) substrate increased from a completely non-adhesive state (0 kPa before FDS treatment) to around 35 kPa after 80 min of FDS treatment (under a preload of 25 kPa, a contact time of 120 s, debonding velocity  $1 \text{ mm}\cdot\text{s}^{-1}$ ). As expected, the modified hydrogel showed stronger underwater adhesion to hydrophobic surfaces, as opposed to hydrophilic ones

like glass or metal. Increasing the contact time and the preload increased the adhesion strength. The hydrogel also featured adhesion to wet porcine skin with a strength of about 30 and 80 kPa after 2 minutes and 1 day of contact (under 5 kPa). The increase in adhesion strength over time was attributed to the favorable self-adaptability of the dynamic surface of the hydrogel. The advantages of the FDS-modified hydrogel are that it was tough ( $4 \text{ kJ}\cdot\text{m}^{-2}$ ) while sticky, and that it showed negligible swelling and therefore stable and repeatable wet adhesion (50 cycles studied). However, this hydrogel is not injectable. We note that the authors did not report the water content of these hydrogels, but they are most probably water-rich, *hydrophilic* systems.

### 3.1.3. Interfacial hydrophobic host-guest interactions

Macrocyclic-based host-guest interactions between a host macrocycle and a guest molecule can involve a variety of different weak molecular interactions such as hydrogen bonding, electrostatic interactions, and hydrophobic interactions to form host-guest complexes [9,131]. Host-guest interactions have been widely studied in the context of molecular recognition and supramolecular polymeric materials for several applications including self-assembled hydrogels, self-healing hydrogels, and adhesive supramolecular materials [9,50,131,132]. Recently, Ji and coworkers thoroughly reviewed macrocycle-based host-guest supramolecular adhesives [9]. Here, we highlight a few examples, mainly based on hydrophobic host-guest interactions, with regards to adhesion in water or on wet surfaces.

Hydrophobic interactions between hydrophobic guest molecules and the hydrophobic cavity of water-soluble hosts have great potential for achieving wet and underwater adhesion. The main macrocyclic hosts studied in this context are cyclodextrins (CDs) and cucurbiturils (CBs). CDs show a moderate binding to guest molecules in water, with association constants in the range of  $10^1 - 10^6 \text{ M}^{-1}$ , depending on the size of the hydrophobic cavity and the guest molecule. CBs have generally higher association constants, between  $10^5 - 10^{15} \text{ M}^{-1}$ , making their complexes more promising candidates for strong underwater adhesion [49,133].

Interfacial wet adhesion based on host-guest interactions was first reported by Harada's group between acrylamide gels bearing either host or guest moieties (Fig. 5 C-1). They showed that host gels and guest gels formed "macroscopic" assemblies in the presence of a small amount of water. The strength of these assemblies followed the trend in association constants between different hosts and guests. For instance, the wet adhesion strength between the  $\beta$ -CD gel (host) and the adamantane gel (guest) with  $K_a$  of  $1500 \text{ M}^{-1}$  was 1 kPa, while that of the  $\alpha$ -CD gel (host) and the *n*-butyl gel (guest) with  $K_a$  of  $57 \text{ M}^{-1}$  was 0.25 kPa. For couples with lower association constants, no adhesion (assembly) was observed. These assemblies were selective when multiple host and guest gels were present, again in line with the association constants [134].



Kim's group [49] reported strong interfacial underwater adhesion between silicone surfaces modified with cucurbit[7]uril (CB7) and aminomethylferrocene (Fc), in a similar manner to a Velcro, as shown in Fig. 10 (also schematized in Fig. 5 C-2). The binding strength of this host-guest complex in water is on the order of  $10^{12} \text{ M}^{-1}$  making it very stable. In a lap shear configuration prepared in water by pressing the host and guest surfaces together, the joint had a wet adhesion strength of 0.34 MPa at  $1 \text{ mm}\cdot\text{s}^{-1}$ . The hydration step is necessary for the formation of host-guest interactions. When the samples prepared in water were removed and dried in air for 12 h, the adhesion strength was 1.1 MPa. The adhesion strength dropped to 0.13 MPa upon the oxidation of Fc into  $\text{Fc}^+$  using NaClO solution followed by drying (12 h). This was expected due to the much lower association constant of the ferrocene cation with CB7.

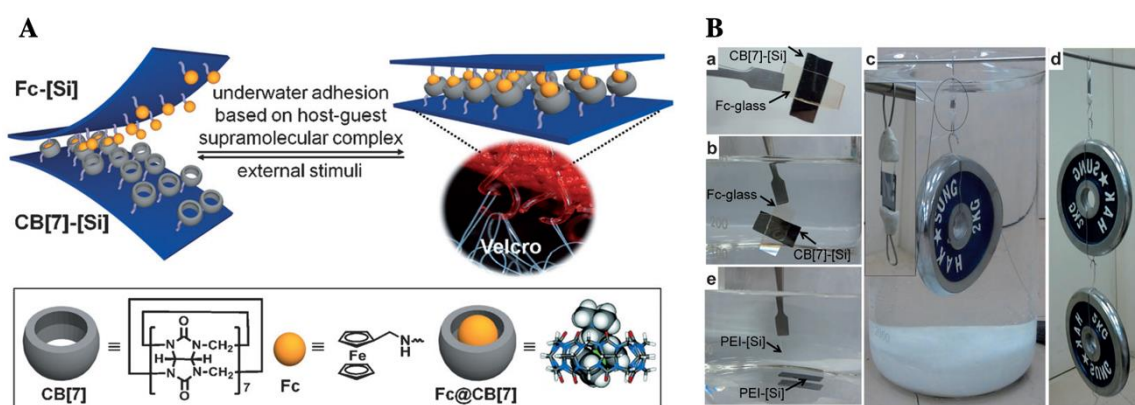


Fig. 10. The Velcro-inspired underwater adhesion mechanism based on the strong host-guest interactions of cucurbit[7]uril (CB7) and aminomethylferrocene (Fc). (B) Visual examples of underwater adhesion between surfaces modified with the host and the guest functions. Note that the unmodified surfaces (shown as PEI-[Si]) do not adhere to each other. [49], Copyright 2013.

Reproduced with permission from John Wiley & Sons Inc.

A similar strategy with glass substrates bearing CD and azobenzene moieties was reported by Roling and coworkers [132]. Host-guest interactions have also been used to bond hydrogels to hard surfaces (schematized in Fig. 5 C-3) [135]. A nontrivial limitation of these strategies is that the adhesion is interfacial; more specifically, between surfaces and/or chemical hydrogels bearing very specific host and guest moieties. This is a practical limit for the use of these interactions in achieving adhesion to surfaces in real applications. Most surfaces do not bear such functionalities, at least not at relevantly high concentrations. To address these issues, Liu and Scherman reported a supramolecular acrylamide hydrogel dynamically crosslinked via interactions of CB8 (cucurbit[8]uril) units hosting two benzyl-imidazolium guests (schematized in Fig. 5 C-4). The dynamic host-guest interactions contributed to the

bulk cohesion and the toughness of the hydrogel while interfacial adhesion to various substrates was associated with non-specific, van der Waals interactions [50].

The *water-rich* (88 wt % water) hydrogel bonded glass slides with a *wet* shear adhesion strength of 1.1 MPa at 1.67 mm.s<sup>-1</sup>. The mechanical properties of this hydrogel were very sensitive to the water content. Upon lowering the water content, the wet adhesion strength gradually increased, reaching 2.3 MPa at a water content of 35 wt%, while water contents lower than 10 wt% led to brittle interfacial failure. On the other hand, the authors reported a 10-fold drop in the shear strength upon immersion of the joint in water for 2 h (98.5 wt% water). The hydrogel entirely lost its strong adhesive properties as it swelled and eventually dissolved in water [50]. This example highlights the significance of the *equilibrium* water content for underwater adhesion.

We note that despite their great potential, there are currently no reports of stable bulk underwater adhesives based on host-guest interactions.

### 3.2. Based on electrostatic interactions

This section focuses on the design of soft viscoelastic underwater adhesives based on permanently or non-permanently charged polymers.

#### 3.2.1. Polyelectrolyte complex coacervation

In the broadest sense, the term complex coacervation applies to a *liquid-liquid* phase separation driven by weak molecular attractive interactions, such as electrostatic, hydrophobic, or H-bonding interactions [136–138]. The equilibrium co-existence of two liquid phases is ubiquitous in natural systems. The most relevant example to this review is the freshly secreted *water-rich* glue of the sandcastle worm used to hold together grains of sand debris to serve as the worm's shelter. The castle is then fortified against the harsh marine environment as the glue hardens via complementary metal-coordination and covalent crosslinking. However, the fact remains that it initially relies on complex coacervation of oppositely charged biopolymers (polyelectrolytes) kept in separate granules until secretion. The reader may find further details of the biological aspects of the sandcastle worm glue in several recent reviews [2,18,22].

Coacervation in biological systems is usually quite complicated and can involve several interaction types [136,139]. For this reason, we will focus on well-defined and simple model systems and in particular synthetic polyelectrolytes, where the phenomenon is called *polyelectrolyte* complex coacervation. Polyelectrolyte complex coacervation is widely believed to occur via an ion exchange process whereby the entropically favorable release of small counterions, i.e. salt ions, favors macroion pairing between the oppositely charged monomers of the polyelectrolytes [138,140–142]. Macroscopically, this leads to the formation of a dense, polymer-rich phase in equilibrium with a polymer-depleted supernatant [136,141].

### 3.2.2. General properties of polyelectrolyte complex coacervates

With respect to underwater adhesion, we are mainly concerned with the dense phase, which can be a viscous liquid, a viscoelastic sticky material, or an elastic solid. The most important parameters known to control the bulk mechanical properties of this phase are the concentration of salt, the type of salt, the chemical composition of the monomers involved, the MW of the polyelectrolytes, and the charge balance [85,91,136,143,144]. The impact of these parameters is schematically shown in Fig. 11. In the following discussion, we will keep referring to the equilibrium water content as a key player in the mechanical properties, as is the case with other soft materials such as polymer solutions, hydrogels, and biological tissues. Being at equilibrium water content is especially important in applications where the material is going to be immersed in an aqueous medium [26,94].

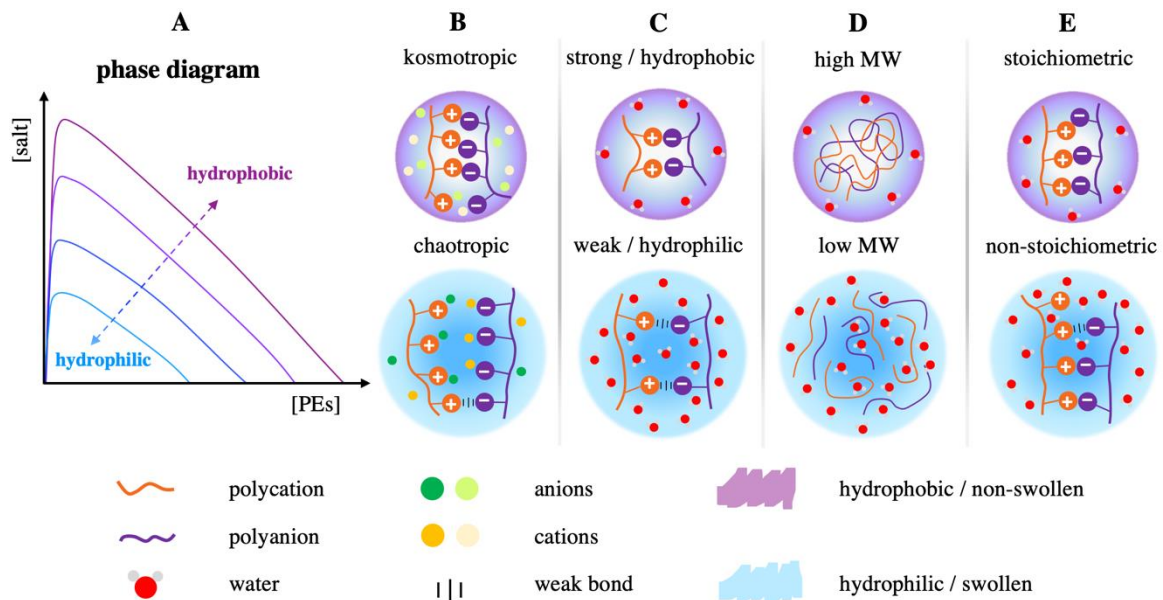


Fig. 11. Schematic representation of the impact of the main parameters determining the general properties of complex coacervates. (A) The general effect of hydrophobicity on the phase separation behavior projected on the salt – polyelectrolytes plane. (B) The type of counterions: kosmotropic or strongly hydrated counter ions versus chaotropic or weakly hydrated counterions; water molecules are not shown for simplicity. (C) The type of chargeable monomers: strong and/or hydrophobic versus weak and/or hydrophilic; the counterions are not shown for simplicity. (D) The molecular weight; the counterions as well as the charged groups of the polyelectrolytes are not shown for simplicity. (E) Stoichiometry versus non-stoichiometry; the counterions are not shown for simplicity.

#### 3.2.2.1. Salt concentration

We must first briefly draw the reader's attention to fundamental differences in the dynamics of polymer melts/solutions and complex coacervates. The dynamics of unentangled polymer solutions is mainly controlled by hydrodynamic interactions on the scale of blobs made of self-avoiding walk chains



and is well described by the Rouse model. At larger molecular weights, the occurrence of entanglements between polymer chains further restricts chain motion. This is qualitatively described by the Reptation model, which considers the wiggling movement of a flexible polymer chain through a tube of entanglements. Now, in polyelectrolyte complex coacervates, the dynamic formation of multiple macroion pairs (called *stickers*) per chain significantly slows down the chain motion. As we will explain in the following, the salt-dependent occurrence of these stickers shifts the viscoelastic response of complex coacervates to longer time scales compared to their neutral/uncharged analogues (without the stickers). Similar to other systems of associating polymers [33,145,146], the dynamics of unentangled and entangled complex coacervates can be well described by the Sticky Rouse [84,147] and the Sticky Reptation models [84,87].

In principle, complex coacervates can be regarded as physical hydrogels/associations with the macroion pairs between the oppositely charged polyelectrolytes acting as the transient crosslinks. The dynamic formation of these stickers is an activated process, where the lifetime of a sticker scales with the exponential of the activation energy,  $E_a$ ; or  $\tau \propto \exp(\frac{nE_a}{kT})$ , which in turn scales with the square root of the salt concentration as  $E_a = A - B \cdot C_s^{1/2}$  [85,147,148].  $A$  and  $B$  are constants for a given system, and  $n$  is the number of macroion pairs per bonding site [26,84,87]. Over longer time scales, the polymer dynamics is determined by the association lifetime. In the *unentangled* regime described by the Sticky Rouse model, the longest relaxation time is  $\tau_{SRouse} \sim \tau \cdot f^2$ , with  $f$  the number of dominant binding sites per chain. In the *entangled* regime described by the Sticky Reptation model, the longest relaxation time is  $\tau_{SRep} \sim \tau_{SRouse} N/N_e$ , where  $N$  and  $N_e$  are the number of Kuhn segments in the chain and between two entanglements [84,87]. Relevant time scales of different relaxations in complex coacervates as well as Sticky Rouse and Sticky Reptation relaxation mechanisms are schematized in Fig. 12. For detailed descriptions of these models and their application to the dynamics of complex coacervates, the readers are referred to the seminal papers by Rubinstein and Semenov [145,149] and to the review by Lutkenhaus [84], respectively.

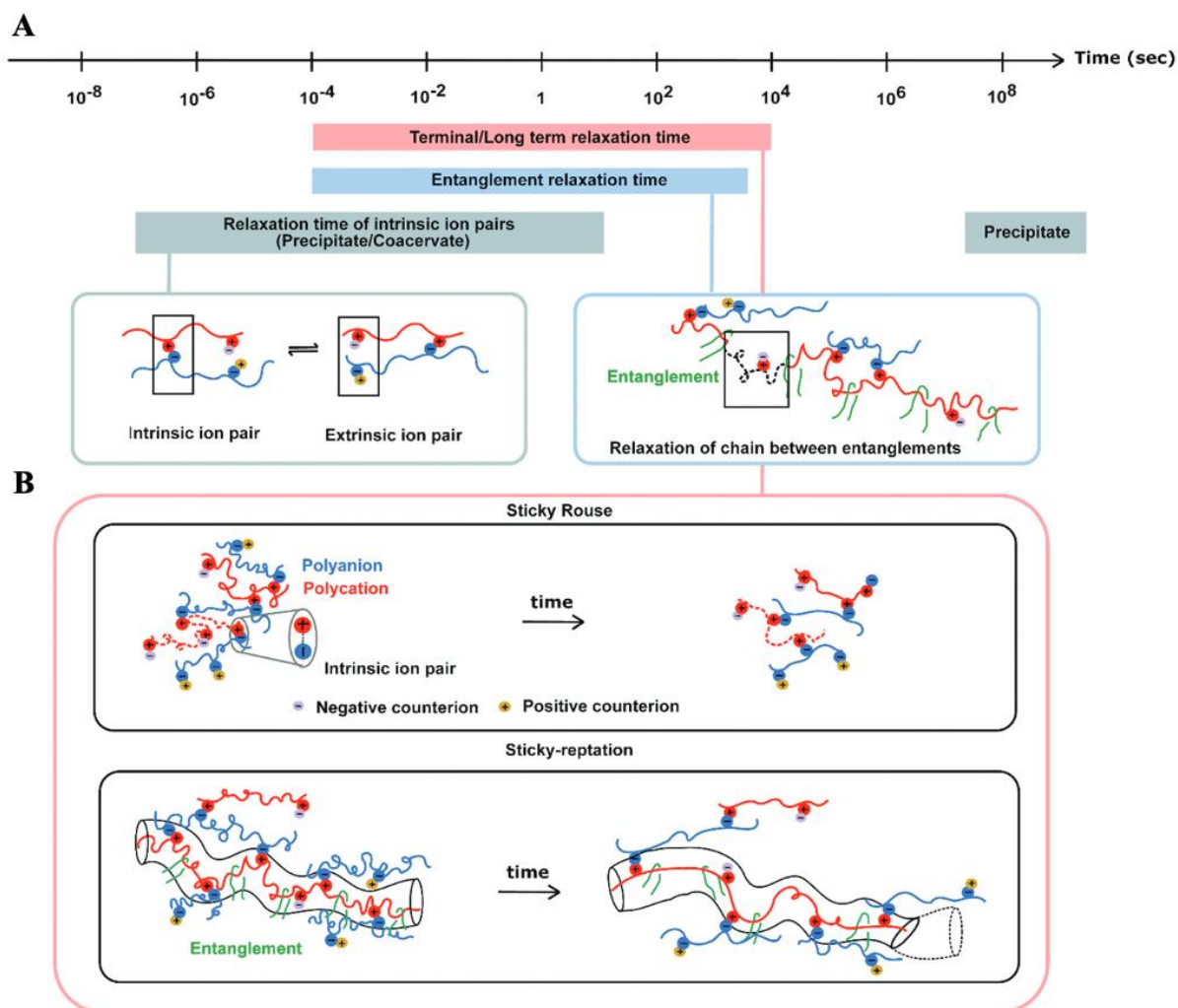


Fig. 12. (A) Relevant time scales of different relaxations in complex coacervates. (B) Schematic representation of relaxation mechanisms for complex coacervates consisting of short and long chains described by Sticky Rouse and Sticky Reptation models, respectively. [84], Copyright 2020. Adapted with permission from Royal Society of Chemistry.

Although considering macroion pairing as an activated process is simplistic in many ways, it sets a good starting point to explain the role of salt concentration on the physical and mechanical properties of complex coacervates, as presented in Fig. 13. At relatively low salt concentrations, macroion pairing is favored and the material may be a solid polymer network, usually called a *complex*. Higher salt concentrations reduce the activation energy and screen macroion pairing, resulting in more swollen, softer solids [136]. At a certain salt concentration, the material reaches a critical gel state, marking a rheological gel to sol transition (the crossover of  $G'$  and  $G''$  in Fig. 13 C) [84,91]. In the vicinity of this point, the material is highly viscoelastic and expected to be *sticky*. Higher salt concentrations yield a liquid *coacervate* with higher water contents and lower polymer volume fractions and therefore lower viscosities. This makes coacervates potentially useful as *injectable* underwater adhesives. Highly

swollen coacervates resemble polyelectrolyte solutions with a terminal behavior, where the loss and storage moduli scale with the first and second power of the angular frequency ( $G'' \sim \omega$  and  $G' \sim \omega^2$ ) at long time scales (small frequencies) [26,84]. In hydrophilic systems, complexation is eventually suppressed above a so-called Critical Salt Concentration (CSC) where all macroions are doped by small counterions, producing a salty polyelectrolyte solution [136]. This point corresponds to the highest point on the binodal curves in the phase diagram in Fig. 11 A.

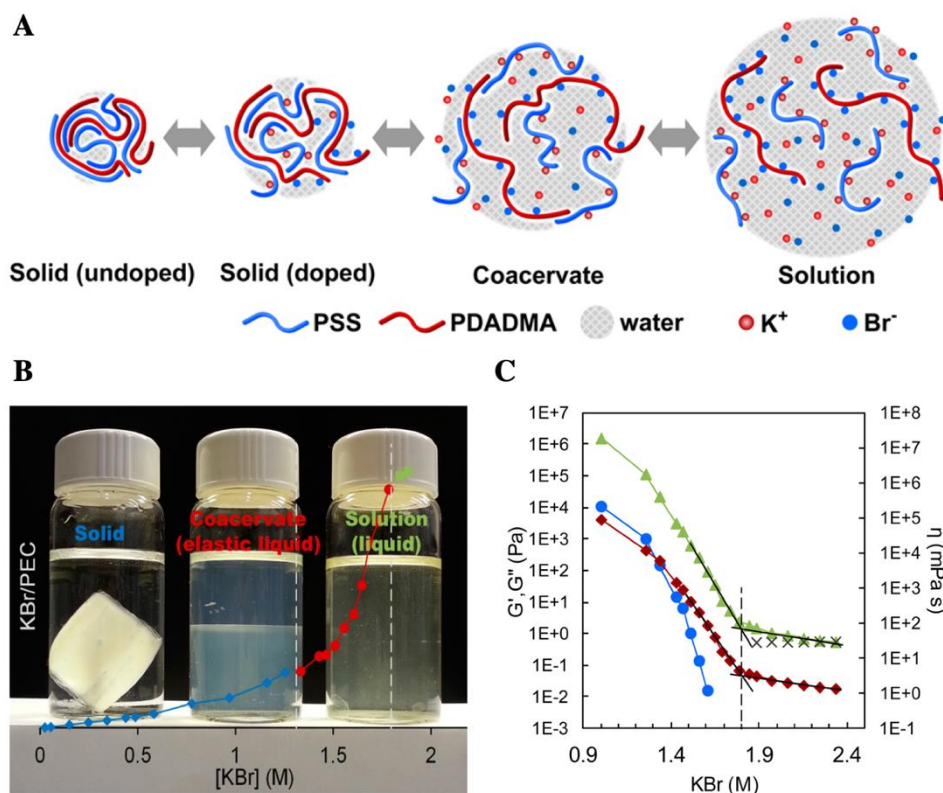


Fig. 13. (A) Schematic illustration of the polyelectrolyte complex/coacervate continuum on the molecular scale. (B) A polyelectrolytes complex, coacervate, and salty solution formed at different KBr concentrations. The KBr/PEC data points in blue, red, and green correspond to these three regimes, respectively. (C) The evolution of  $G'$  (blue circles),  $G''$  (red diamonds), and viscosity (green triangles) as a function of KBr concentration. The crossover of the dynamic moduli marks the sol to gel transition. The dashed line corresponds to the CSC. [136], Copyright 2014. Reproduced with permission from American Chemical Society Publications.

The effect of salt on the relaxation spectra of complex coacervates is analogous to the effect of temperature on the dynamics of polymer melts, described by the so-called Time-Temperature Superposition (TTS). Since salt affects the relaxation times of all modes (ionic bonds) to the same extent, by  $\tau \propto \exp(A - B \cdot C_s^{1/2})$ , adding (or removing) salt shifts *all* the relaxation spectra towards higher (or lower) frequencies [85,147]. This means that the dynamic moduli of complex coacervates prepared at

different salt concentrations can be rescaled onto a master curve using salt-dependent shift factors in a so-called Time-Salt Superposition (TSS). TSS allows access to a wide range of time scales which are not typically accessible by experiment. More importantly, it gives a good approximation of the viscoelastic properties of complex coacervates at intermediate salt concentrations without the need to prepare the corresponding samples. The readers will find more detailed discussions in the following reviews [84,85,150].

#### 3.2.2.2. Type of salt

The effect of the type of salt can be explained in the light of the Hofmeister series, with a few exceptions [151,152]. As schematically shown in Fig. 11 B, less hydrated (chaotropic) counter ions are more effective in dissociating macroion pairs. This means that at a given salt concentration, a coacervate prepared with less hydrated counter ions should have a higher water content than one prepared with strongly hydrated (kosmotropic) counter ions. For instance, for a given pair of polyelectrolytes, sodium salts ( $\text{Na}^+\text{X}^-$ ) become increasingly stronger at breaking macroion pairs as  $\text{X}^-$  is changed from  $\text{Cl}^-$  to  $\text{Br}^-$  to  $\text{I}^-$  to  $\text{SCN}^-$  [151].

Changing the counter ion thus provides a means of targeting a certain window of mechanical properties at lower or higher salt concentrations, as shown by Sadman and coworkers [143]. This of course depends on the final application. For instance, in certain biomedical applications where high salt concentrations are not tolerated, using NaBr instead of NaCl will allow working at lower salt concentrations. Nonetheless, an important conclusion from the work of these authors was that the mechanical properties of a polyelectrolyte complex coacervate are governed by its degree of swelling and not the salt used to swell it.

#### 3.2.2.3. Chemical composition of the monomers

As schematized in Fig. 11 C, relatively hydrophobic polyelectrolytes form hard, *water-poor* solid precipitates with water contents between 20 – 60 wt% while more hydrophilic polyelectrolytes tend to form *water-rich* liquid-like coacervates with water contents between 60-95 wt% [87,143]. In other words, the hydrophobic/hydrophilic (amphiphilic) nature of the oppositely charged monomers plays a crucial role in determining the equilibrium water content and thereby the mechanical properties of the resulting complex coacervates. Sadman and coworkers compared well known Polystyrene Sulfonate (PSS) / Polydiallyldimethylammonium (PDADMA) complex coacervates with a series of increasingly hydrophobic polycations, namely methyl-, ethyl-, and propyl-substituted poly(4-vinylpyridine), as shown in Fig. 14 A. These authors showed that the swelling degree is less sensitive to the presence of salt (KBr) in *water-poor* complex coacervates [143].

Another factor here is the affinity of the oppositely charged monomers for one another. As demonstrated in the series in Fig. 14 B, complex coacervates made of stronger polyelectrolytes generally tend to pair more strongly (i.e. with higher lifetimes) and have lower water contents. As a result, they

are less sensitive to the presence of counter ions. Likewise, weaker polyelectrolytes form weaker complex coacervates more liable to doping. A comprehensive example may be found in the work of Fu and coworkers [153].

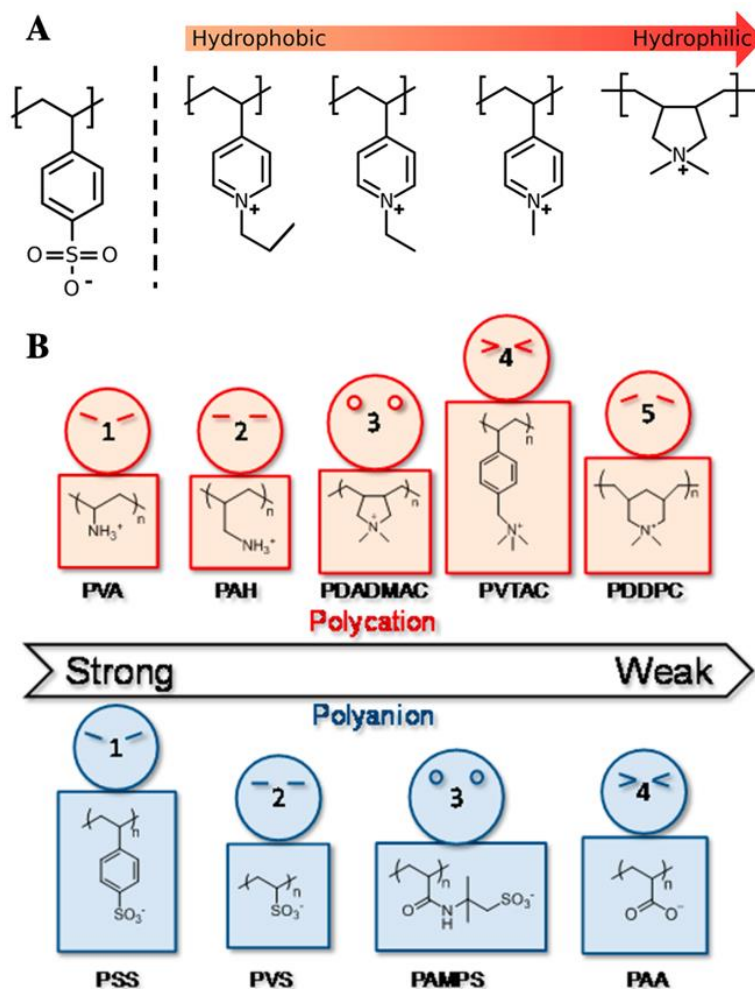


Fig. 14. (A) Complex coacervate pairs of polystyrene sulfonate (PSS) with a series of polycations of varying hydrophilicity. [143], Copyright 2017. Reproduced with permission from American Chemical Society Publications. (B) A list of strong to weak polyelectrolyte complex coacervates. [153], Copyright 2017. Reproduced with permission from American Chemical Society Publications.

#### 3.2.2.4. Molecular weight

Lowering the MW increases the solubility of polyelectrolytes in water (their entropy of mixing with water is higher). It also lowers the maximum number of stickers per chain in the Sticky Rouse model (see Section 3.2.2.1.). As a result, the complex coacervates formed are softer and more *water-rich* (Fig. 11 D). Spruijt and coworkers [141] studied the rheological properties of complex coacervates having different degrees of polymerization (DP), as depicted in Fig. 15 A. Fig. 15 B presents the corresponding phase diagrams (also see Fig. 11 A) They showed that for DP less than about 300, the water content of



polyacrylic acid (PAA) / poly(*N,N*-dimethylaminoethyl methacrylate) (PDMAEMA) complex coacervates becomes increasingly sensitive to the MW. At DP close to 10, complex coacervation is suppressed, even in deionized water, while at DP larger than 300, the water content remains almost constant at about 65 %. Based on similarities in the water contents and the TSS master curves for complex coacervates from different polyelectrolyte chemistries with  $50 < DP < 150$  (Fig. 15 C), Vahdati and coworkers [26] suggested that the above MW dependent trends should be true for *water-rich* complex coacervates. All these complex coacervates were found to be in the semi-dilute, unentangled regime (with both  $G'$  and  $G''$  scaling with  $\omega^{0.5}$  at high frequencies).

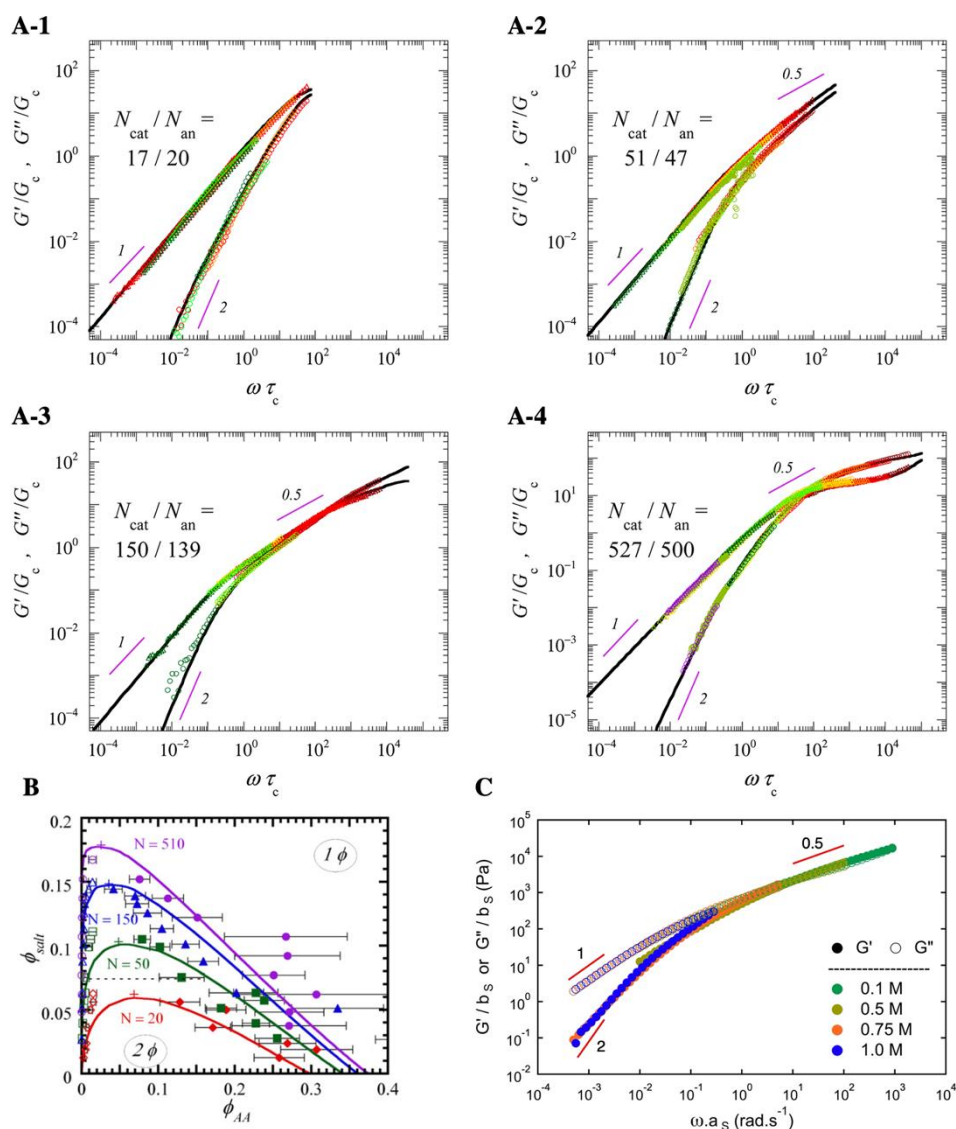


Fig. 15. (A) TSS master curves for PAA/PDMAEMA complex coacervates from polyelectrolytes of different DP indicated (as  $N$ ) on each graph. [148], Copyright 2013. Adapted with permission from American Chemical Society Publications. (B) The corresponding phase diagrams for PAA/PDMAEMA complex coacervates. [141], Copyright 2010. Adapted with permission from American Chemical Society Publications. (C) TSS master curve for a pair of water-rich

*polyelectrolytes with DP around 100. [26], Copyright 2020. Adapted with permission from American Chemical Society Publications.*

Above the entanglement molecular weight, a rubbery plateau appears at high frequencies. As mentioned earlier, the longest relaxation time is longer by a factor of  $N/N_e$  compared to the Sticky Rouse model [145,154]. We note that a certain level of entanglements is essential for the performance of classic *hydrophobic* PSAs. To fit the Dahlquist's criterion, the plateau modulus is often adjusted using low MW tackifiers to dilute the entanglements (increasing  $N_e$ ) [28]. This may be achieved by combining high and low MW polyelectrolytes in the case of coacervate based underwater adhesives.

### 3.2.2.5. Charge balance

Polyelectrolyte complex coacervates are often prepared at stoichiometric charge ratio to have a one-to-one balance between the oppositely charged monomers. But how realistic is the one-to-one picture and what would happen if one polyelectrolyte is in excess?

Spruijt and coworkers [148] reported that the dynamic moduli and the zero-shear viscosity of their PAA/PDMAEMA coacervates remained unaffected by deviations from stoichiometry. They argued that excess polyelectrolytes end up in the supernatant phase and that the coacervates have a "preferred" composition. In contrast, Chen and coworkers [144] found that increased nonstoichiometry in PSS/PDADMA complexes had a plasticizing effect, lowering the  $T_g$  values and the dynamic moduli. This was attributed to the enhanced water content associated with the so-called extrinsic sites where the macroions are *not* paired. This contradiction may be because these works have investigated either liquid coacervates or solid complexes, and not the entire viscoelastic spectrum. That said, the role of nonstoichiometry merits further studies.

In any case, it is now known that some level of nonstoichiometry is inevitable [87,144,148]. This means that even when the complex coacervates are prepared at stoichiometric ratio, the final complex coacervate is very likely to be slightly off stoichiometry (this aspect is not shown in Fig. 11 E for simplicity). This can be due to kinetic trapping, charge density mismatch, backbone flexibility mismatch (steric hindrance), and or the effective size of the monomer group [87]. Overall, slight (5 – 10 %) deviations from stoichiometry should not have a large impact on bulk properties while larger deviations may be useful for tuning the mechanical properties in solid-like systems.

A last comment on the general properties of complex coacervates is that some of the above-mentioned features, such as the sol-gel transition or the CSC, may not be observed in certain systems. In general, we expect the two-phase region of the salt vs. polymer phase diagram to shrink with any factor enhancing the dynamics and contributing to the solubility of the complex coacervate (see the phase diagram in Fig. 11 A) [26,141]. For instance, polyelectrolytes that are very water soluble, due to their small molecular weight and or due to the chemical composition of their monomers, may never

produce a solid complex, remaining in a liquid coacervate state at all concentrations of a sufficiently doping salt. In extreme cases, coacervation may be suppressed all together. On the other hand, very hydrophobic polyelectrolytes may form solid complexes over a wide range of salt concentration. This may happen with large molecular weight polyelectrolytes ( $DP > 1000$ ) or when the affinity between the macroions is so strong that they are never fully doped with salt (i.e. no CSC is observed with certain salts). These materials, called saloplastics, are then more interesting for applications such as artificial tissues and porous membranes rather than underwater adhesion [155,156].

### 3.2.3. Obtaining sticky complex coacervates

Fig. 16 compares different strategies reported so far to obtain sticky complex coacervates based on electrostatic interactions. Although the focus of the literature has been mainly on polyelectrolyte-based complex coacervates, adhesives based on polycations complexed with multivalent anions and based on short (oligomeric) chains complexed with hyper-charged polyoxometalates have shown great promise as well. These will be reviewed in the following with a critical focus on the mechanical properties.

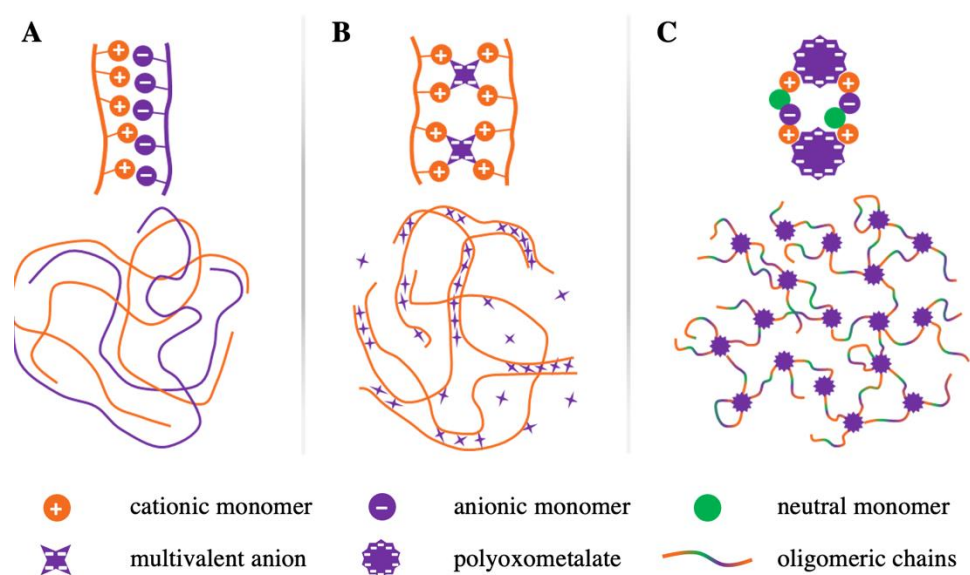


Fig. 16. Different types of complex coacervates based on electrostatic interactions involving (A) oppositely charged polyelectrolytes, (B) a polyelectrolyte and a multivalent ion, and (C) short peptides and polyoxometalates.

Inspired by their research on the sandcastle worm's glue, Russell Stewart's group was the first to study complex coacervates as *bulk* underwater adhesives [11,157]. Given the limitations of obtaining large enough samples from the animals, they developed polymers with residues resembling the proteinaceous secretions of the worm, as demonstrated in Fig. 17 A [2,42,158]. Their biomimetic synthetic complex coacervates, mainly based on modified polyphosphates and polyamines, were responsive to different environmental stimuli namely salt concentration, pH, the presence of divalent



cations, and temperature [11,42]. Under optimized conditions (pH, divalent cation concentration, etc.), the thermally triggered complex coacervates featured bond strengths up to 650 kPa at 37 °C in underwater lap shear tests on aluminum substrates. The water content in these materials was about 60-70 wt/vol %.

Stewart's group also reported complex coacervates based on pharmaceutical grade biopolymers, such as polycationic salmine sulfate and polyanionic sodium inositol hexaphosphate [159]. The complex coacervates prepared at 1.2 M NaCl were successfully applied as endovascular embolics upon a so-called *salt switch*, as depicted in Fig. 17 B. A salt switch involves injecting a salty liquid coacervate into a low salt medium to diminish the concentration of salt in the material. When the gradient is large enough, this can trigger a sol to gel transition, solidifying the adhesive [26]. However, these authors did not report any quantitative adhesion tests.

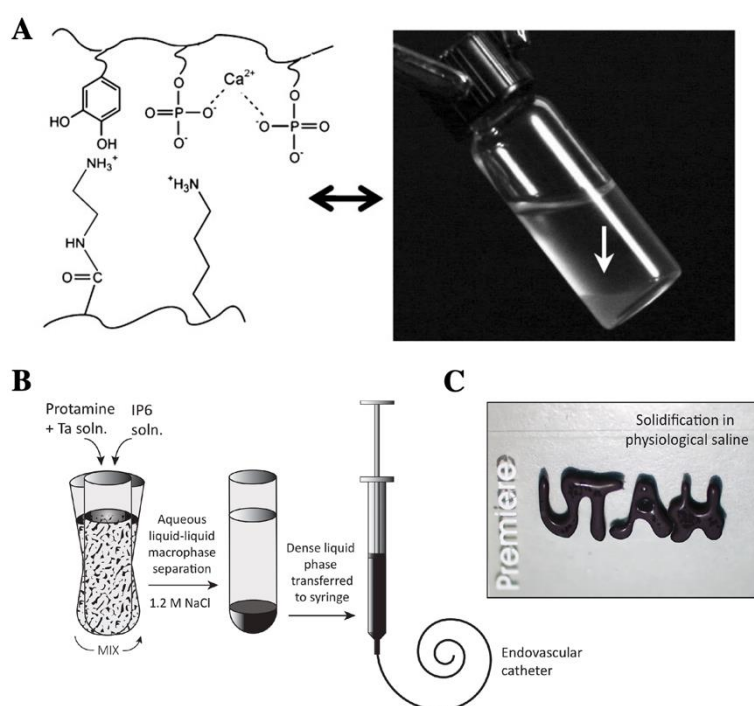


Fig. 17. (A) The biomimetic polyelectrolytes developed by Stewart's group and the resulting complex coacervate. [42], Copyright 2010. Reproduced with permission from John Wiley & Sons Inc. (B) The salt switch strategy introduced by the same group using pharmaceutical grade biopolymers. [159], Copyright 2016. Reproduced with permission from John Wiley & Sons Inc.

Dompé and coworkers [68,97,160] reported a series of insightful studies on multiresponsive underwater adhesives based on *water-rich* complex coacervates. Interestingly these authors developed simple model systems based on synthetic polyelectrolytes, namely poly(dimethylaminopropyl acrylamide) (PDMAPAA) and PAA. In parallel, they developed analogous graft copolymers with the same polyelectrolytes grafted with different contents of short, thermoresponsive PNIPAM side chains

(10 – 40 wt%). In the following discussion, we will refer to the complex coacervates made of the homopolymers and of the copolymers as the homo and graft systems, respectively. Both materials were injectable liquids at 0.75 M NaCl and room temperature.

The equilibrium water content of the coacervate based on graft copolymers slightly increased with PNIPAM content. At 0.75 M NaCl and room temperature, for example, the water content increased from 85 to 93 wt% as the fraction of PNIPAM grafts was changed from 0 to 40 wt% [160]. This was due to the combined effect of the hydrophilic PNIPAM side chains and the effective dilution of the charged groups. Upon a temperature switch (from room temperature to 50 °C) which turns PNIPAM into a hydrophobic polymer, no significant change in the overall water content was observed, while a slight increase was reported after a salt switch. In both cases, the authors proposed a porous structure with trapped water to rationalize the small change in water content [68,160].

The underwater adhesiveness of these complex coacervates between a glass slide and different probes were studied by underwater probe tack tests upon salt, temperature, and combined switch experiments [97]. In all experiments, the aqueous medium was added immediately after contact with the probe was established.

Upon a *temperature switch* (T switch; from room temperature to 50 °C), the graft complex coacervates (containing 30 wt% PNIPAM and prepared at 0.75 M NaCl) showed a highly rate dependent adhesion to a negatively charged PAA probe, characteristic of soft viscoelastic adhesives, as seen in [Fig. 18 A](#), while the homo complex coacervates were non-sticky under the same conditions ( $W_{adh} \approx 0 \text{ J.m}^{-2}$ ) [68]. The adhesion energy of the graft coacervates on PAA increased with PNIPAM content, reaching  $3.9 \text{ J.m}^{-2}$  for 40 wt% PNIPAM, highlighting thus the role of hydrophobic interactions [160].

Upon a *salt switch* (S switch), both the homo and the graft complex coacervates (initially prepared at 0.75 M NaCl) turned into opaque hydrogels when placed in a 0.1 M NaCl medium at room temperature [97]. The homo system had larger dynamic moduli compared to the more swollen graft copolymer, but both hydrogels were very soft ( $G' \approx 0.1\text{-}1 \text{ kPa}$ ) and viscoelastic. In underwater probe tests they displayed extensive fibrillation upon debonding. Because of the higher water retention of the hydrophilic PNIPAM at room temperature, the graft system showed a better balance between interfacial interactions and viscoelastic dissipation and was thus deformed to a larger extent ( $W_{adh} = 6.5 \text{ J.m}^{-2}$ , [Fig. 18 B – C](#)) before cohesive failure, while the homo system failed adhesively ( $W_{adh} = 3.2 \text{ J.m}^{-2}$ ). The adhesion energy of the graft system is noticeably larger than  $1.6 \text{ J.m}^{-2}$  in the T switch. It is also interesting to note that the value of  $G'$  after a salt switch was almost half that of  $G'$  after a temperature switch (see [Fig. 18 D](#)).

The graft complex coacervates (30 wt% PNIPAM at 0.75 M NaCl) were also studied in *combined temperature – salt switch* experiments [97]. Interestingly, it was found that the order in which the two interactions are triggered impacts the final bulk mechanical properties. As seen in [Fig. 18 E](#), the dynamic

moduli were one decade larger when the material was immediately heated to 50 °C followed by the salt switch (T + S switch), compared to when it was heated after the salt switch (S + T switch). In S + T switch, the increased number of macroion pairs formed between the large polyelectrolyte backbones at 0.1 M NaCl reduces the mobility of the short PNIPAM side chains. In contrast, the formation of hydrophobic PNIPAM domains in T + S switch does not prevent the subsequent formation of macroion pairs. For this reason, and to replicate the real conditions in biomedical applications, the underwater adhesion tests were done upon T + S switch. The measured adhesion energy ( $7.2 \text{ J}\cdot\text{m}^{-2}$ ) was only slightly higher than the salt switch alone (Fig. 18 B – C). Nonetheless, the main advantage of this system was a quick initial adhesion followed by a more gradual stiffening mechanism.

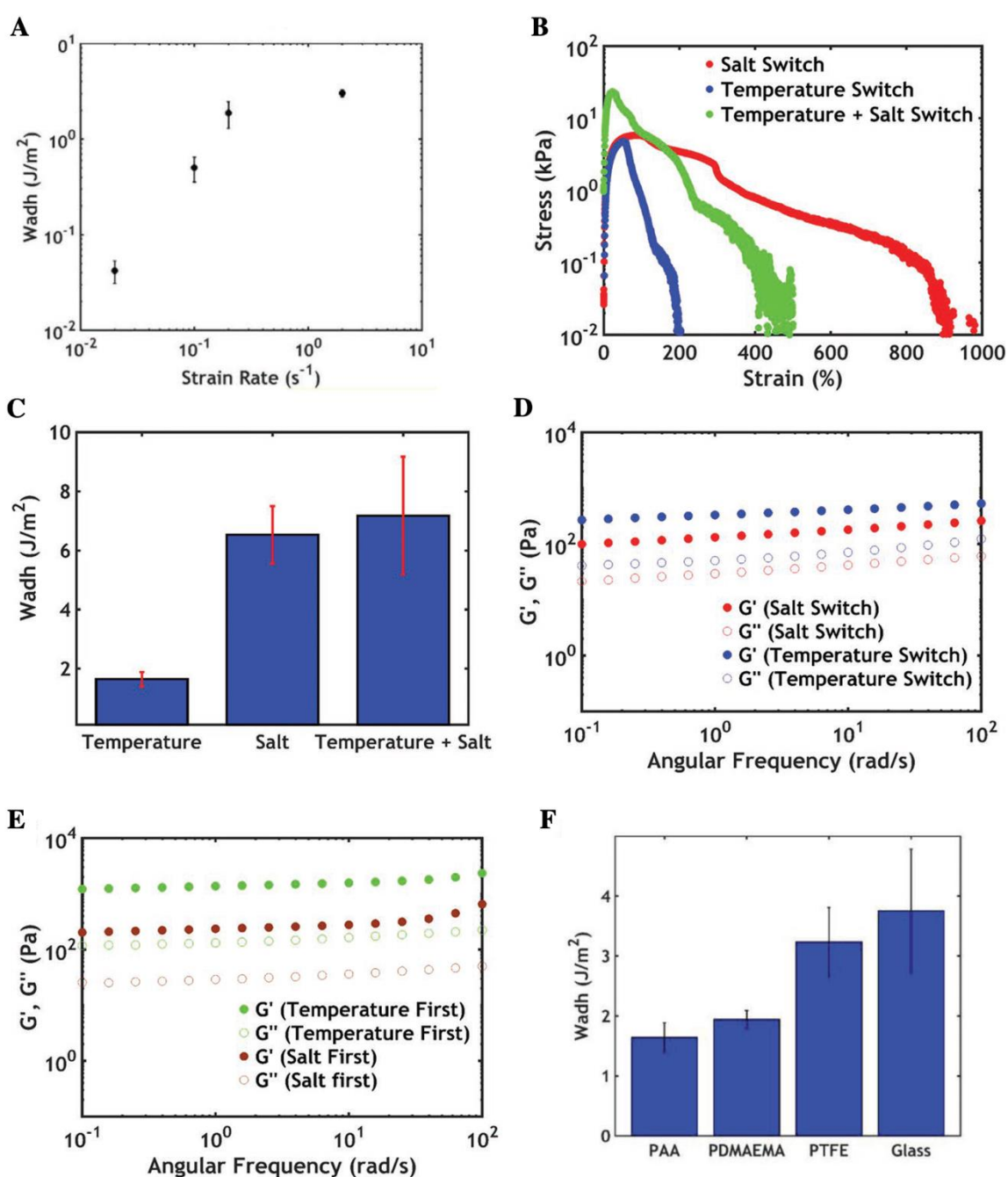


*Fig. 18. (A) The adhesion energy of the thermoresponsive graft complex coacervate upon temperature (T) switch in underwater probe tack tests against a PAA surface as a function of the nominal strain rate. (B) Representative nominal stress-strain curves from underwater probe tack experiments on the graft system at  $0.2\text{ s}^{-1}$  upon T switch, salt (S) switch, and a combined T + S switch and (C) the corresponding adhesion energies. (D) The linear rheological properties of the graft system upon S switch and T switch. (E) The linear rheological properties of the graft system upon T + S switch versus S + T switch. (F) The adhesion energies from underwater probe tack experiments on the graft system using different probes at  $0.2\text{ s}^{-1}$  upon T switch. [68], Copyright 2019. Reproduced with permission from John Wiley & Sons Inc. [97], Copyright 2020. Reproduced with permission from John Wiley & Sons Inc.*

These works highlight the importance of macromolecular design and type of interactions on the bulk mechanical properties of soft materials [97,160]. The incorporation of different interactions was also beneficial for versatile adhesion to various surfaces in water, namely charged and uncharged as well as hydrophobic and hydrophilic surfaces, as seen in Fig. 18 F. This versatility was attributed to the dynamic nature of electrostatic interactions allowing local polarization at the interface and the amphiphilic nature of the material [44,68]. Nevertheless, the fact remains that such adhesion energies are almost 2 decades lower than *hydrophobic* PSAs in air mainly because of the high water contents in these hydrophilic coacervates.

An unexpected finding was that the complex coacervates based on the inverse topology, i.e. oppositely charged polyelectrolytes grafted onto large PNIPAM backbones, lost their thermoresponsiveness. Unlike the case of uncharged hydrophilic grafts (PNIPAM-g-PDMA, described in Section 3.1.2), the macroion pairs formed between relatively short polyelectrolyte grafts ( $DP = 100$ ) prevented the PNIPAM backbones from collapsing onto one another and thus from forming hydrophobic domains [161]. This difference is schematized in Fig. 19. As a result, the PNIPAM backbones did not contribute to the enhancement of the mechanical properties upon T switch; in fact, they rendered the coacervates even more *water-rich*. The complex coacervate prepared at 0.1 M NaCl was a viscous liquid ( $G'' > G'$ ) and the adhesion energy measured in a similar probe tack test was below  $1.2\text{ J.m}^{-2}$ . This example shows that the interplay between weak molecular interactions on different length and time scales can be rather subtle and understanding the role played by macromolecular design is crucial when developing soft underwater adhesives.

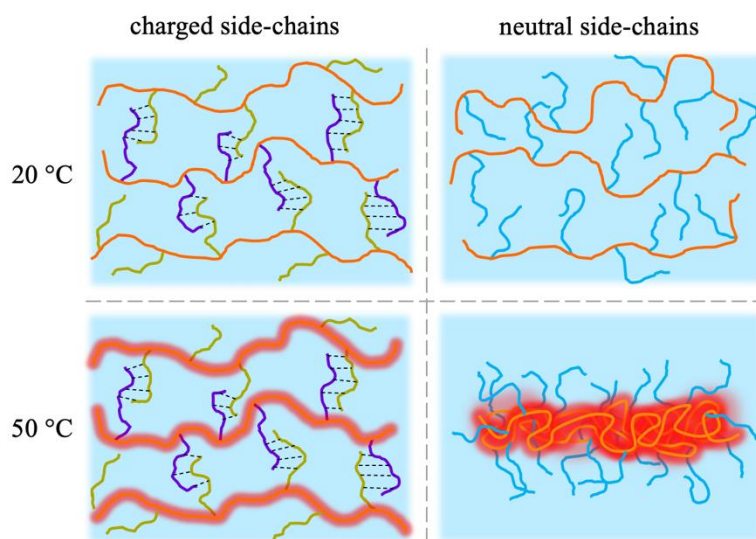


*Fig. 19. Schematic representation of graft copolymers with PNIPAM backbones grafted with oppositely charged side chains as opposed to neutral side chains below and above the LCST of PNIPAM. Reprinted from [161].*

Dompé and coworkers also investigated the impact of lowering the water content via extrusion on the mechanical properties [94]. After 9 minutes of extrusion at 50 °C, the material became increasingly elastic as the polymer volume fraction (and thus the density of elastically active chains) increased, leading to a 10-fold increase in the storage modulus. The optimal adhesion/cohesion balance ( $\tan(\delta) / G'$ ) was obtained at a water content of 77 wt% after 3 minutes of extrusion. This allowed extensive deformation of the material with a significant adhesion energy of 60.6 J.m<sup>-2</sup> before cohesive failure upon a T + S switch (compared to 7.2 J.m<sup>-2</sup> and a water content of 88 wt% before extrusion). The adhesive obtained after 3 minutes of extrusion was stable with little shrinking or swelling in physiological conditions for 5 days, which is sufficiently long for many applications. Longer extrusion times rendered the material too elastic ( $\tan(\delta)$  too small;  $\tan(\delta) / G'$  too low) causing early adhesive detachment from the probe. As a result, the adhesion energies were the same or even lower than the unextruded coacervate.

In practice, using a salt switch to develop injectable underwater adhesives has several limitations, as noted by our group [26]. Firstly, the salt concentration in the coacervate must not be too different from physiological conditions. This must be considered when choosing the monomer composition of the polyelectrolytes and their MW to obtain an injectable (liquid) coacervate. Secondly, complex coacervates prepared at higher salt concentrations have a lower polymer volume fraction and hence lower mechanical properties after equilibration into a low salt medium (compared to a complex coacervate prepared in this medium). A large salt concentration gradient is also very likely to lead to trapped water in closed pores [97,155,162]. Therefore, there is a nontrivial trade-off between the



injectability of polyelectrolyte complex coacervates and their final mechanical properties upon a salt switch.

To clarify this point, Vahdati and coworkers [26] studied complex coacervates of poly(2-acrylamido-2-methylpropanesulfonic acid) (PAMPS) and poly(N,N- [(dimethylamino) propyl] methacrylamide) (PMADAP) with 100 monomer units. The coacervate at 0.75 M NaCl was an injectable fluid with a water content of 63 wt%. After 1 h of salt switch in physiological conditions, an adhesion energy of  $4 \text{ J.m}^{-2}$  was measured against a charged PAA probe in an underwater probe tack test at  $0.2 \text{ s}^{-1}$ , as shown in Fig. 20. This value is comparable to previous literature reports [68,97]. In contrast, when prepared at 0.1 M NaCl, the same polyelectrolytes formed an instantly sticky complex coacervate due to their optimized water content (55 wt%) [26]. Although not injectable, the adhesion energy of this material was  $16 \text{ J.m}^{-2}$  under the same experimental conditions and reached  $65 \text{ J.m}^{-2}$  (close to Post-It® notes and soft healthcare adhesives) at  $2 \text{ s}^{-1}$  (see Fig. 20 B). This underwater adhesive could be applied directly under water and featured repeatable underwater adhesion without relying on a salt switch. Nonetheless, complex coacervates based on such low molecular weights soften in large deformations due to the absence of entanglements, like uncrosslinked, *hydrophobic* PSAs.

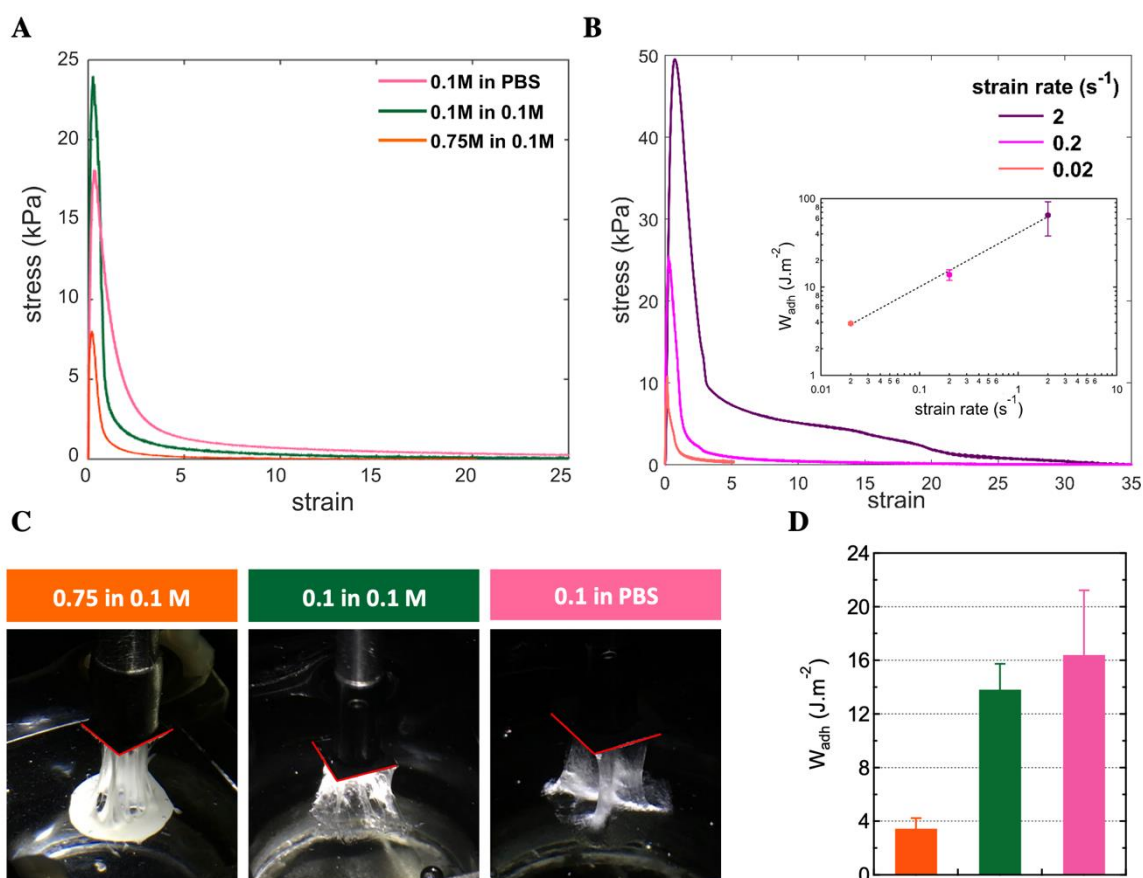


Fig. 20. (A) Nominal stress-strain plots from underwater adhesion experiments in a low salt medium, either 0.1 M NaCl or PBS at a nominal strain rate of  $0.2 \text{ s}^{-1}$ . All experiments were performed after 1 h



*of immersion in the aqueous medium. (B) The effect of the nominal strain rate on the underwater adhesion of the 0.1 M sample tested in a 0.1 M NaCl medium. The inset presents the corresponding adhesion energies. (C) Images taken from the underwater adhesives during debonding at large deformations. (D) The corresponding adhesion energies. [26], Copyright 2020. Adapted with permission from American Chemical Society Publications.*

Another type of polyelectrolyte complex-based underwater adhesive was introduced by the Lapitsky group [95], who developed *water-poor* physical hydrogels based on poly(allylamine) (PAH) physically crosslinked with strongly binding multivalent anions, pyrophosphate (PPi) and tripolyphosphate (TPP). The design and properties of the PAH/TPP system is demonstrated as an example in [Fig. 21 A](#). These hydrogels are sensitive to the ionic strength and the pH of the medium. They take up more water and become more viscoelastic upon addition of salt, changing the preparation pH of the parent solutions, or upon exposure to highly acidic or basic media. However, under all the reported preparation conditions ( $0.0 \text{ M} < [\text{NaCl}] < 0.5 \text{ M}$ , and  $6 < \text{pH} < 8$ ), the water content in these complexes was very low between 25 and 38 wt% [48,95].

Under physiological conditions, i.e.  $\text{pH} = 7$  and  $0.15 \text{ M NaCl}$ , both PAH/PPi and PAH/TPP were stiff viscoelastic hydrogels slightly above the gel point, with  $G'$  and  $G''$  around 200 and 80 kPa (at  $1 \text{ rad}\cdot\text{s}^{-1}$ ) (see [Fig. 21 B](#)). Deviation from this pH at preparation changed the charge balance and led to softer materials. However, once prepared at a certain pH, the complexes were relatively insensitive to moderate fluctuations in the pH of their medium (by 1 – 2 pH units). Salt affected both materials in a similar manner to polyelectrolyte complexes (between oppositely charged polymers). In general, PAH/TPP was characterized by stronger binding and was less sensitive to the above factors [48,95].

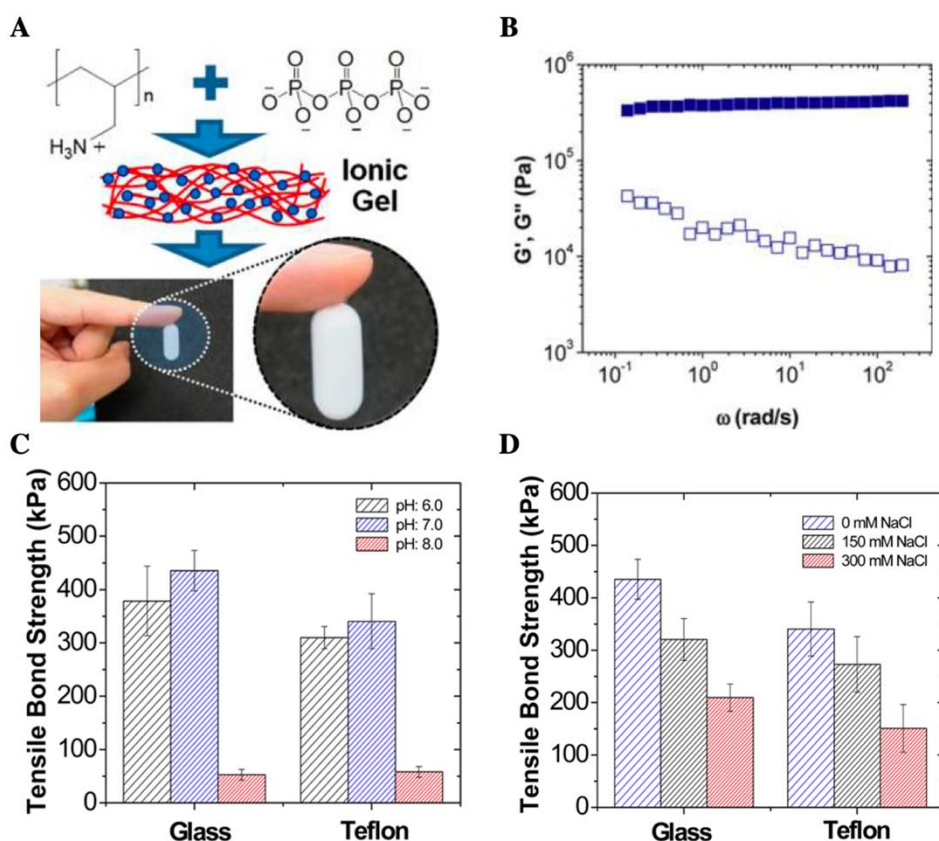


Fig. 21. (A) PAH/TPP cocervate as a wet adhesive. (B) The dynamic behavior of PAH/TPP physical hydrogel prepared at pH 7 with no added salt. [95], Copyright 2015. Reproduced with permission from American Chemical Society Publications. (C) The lap shear strength of the PAH/TPP cocervate prepared at different pH without added salt and (D) prepared at different NaCl concentrations at pH 7. [48], Copyright 2015. Reproduced with permission from American Chemical Society Publications.

The wet adhesive properties of PAH/PPi and PAH/TPP were measured by lap shear tests. The results for the PAH/TPP cocervates are presented in Fig. 21 C – D. The samples were directly prepared in deionized water on both hydrophilic (glass) and hydrophobic (PTFE) substrates followed by 3 – 4 h of immersion. They were then removed and immediately tested in the wet state at  $0.85 \text{ mm}\cdot\text{s}^{-1}$  (or  $2.2 \text{ s}^{-1}$ ). In agreement with their linear viscoelastic behavior, the highest adhesion strengths (350 – 450 kPa) were reported for the samples prepared at 0.0 M NaCl and pH = 7 [95]. The adhesion strength was almost independent of substrate chemistry, but the failure mode was cohesive on glass versus adhesive on Teflon. As seen in Fig. 21 C – D, the softening resulting from the addition of salt or alteration of the pH lowered the adhesion strength. The lowest adhesion strengths ( $< 100 \text{ kPa}$ ) were reported for the complexes prepared at pH = 8 (0.0 M NaCl) or 0.3 M NaCl (pH = 7) [48].

As mentioned earlier, when both components are polymers, several macroion pairs must break/dissociate at once to allow relaxation on the scale of a chain segment. The relatively small size of the oppositely charged crosslinker (PPi or TPP) may thus explain the high sensitivity of these complexes

to the presence of counter ions. Needless to say that entanglements are less likely to contribute to the creep resistance of these adhesives [150]. On the other hand, using smaller crosslinkers may help to reduce the free volume in the material and favor lower water contents.

Underwater adhesives were also reported based on hybrid (organic - inorganic) supramolecular assemblies (coacervates) of short, cationic peptides and polyoxometalates, as demonstrated in Fig. 22 [96]. Polyoxometalates are metal oxide clusters known for their rigid conformation, single MW distribution, and being highly negatively charged in water [163]. Due to the polyampholyte nature of the peptides used, the samples were prepared well below their isoelectric point at pH = 2 (above pH = 2.5, a clear solution, rather than a coacervate, was obtained). The complex based on SiW (H<sub>4</sub>SiW<sub>12</sub>O<sub>40</sub>) and Pep1 (Ac-EEMQRRAD-NH<sub>2</sub>, containing two arginine (RR) and two glutamic acid (EE) residues, pI = 4.7) had a 2:1 Pep1:SiW ratio and formed a stiff viscoelastic gel with  $G'$  and  $\tan(\delta)$  around 1 MPa and 0.4 (at 5 rad.s<sup>-1</sup>), respectively. The underwater adhesion of Pep1:SiW in lap shear tests at 10 mm.s<sup>-1</sup> was around 25 – 30 kPa regardless of the substrate (glass, aluminum, and polyether-ether-ketone (PEEK)). As seen in Fig. 22 D, the failure mode was cohesive in all cases. These authors showed that the mechanical properties of these materials were insensitive to the type of polyoxometalate used; rather, they were mainly controlled by the net charge and the size of the peptide. For instance, the material lost its underwater adhesiveness as the cationic arginine moieties were replaced with anionic glutamic acid moieties. The authors did not comment on the long-term stability of this adhesive; the tests were performed after 15 min of immersion in deionized water. Finally, the addition of salt weakened the adhesive properties, as expected [96].

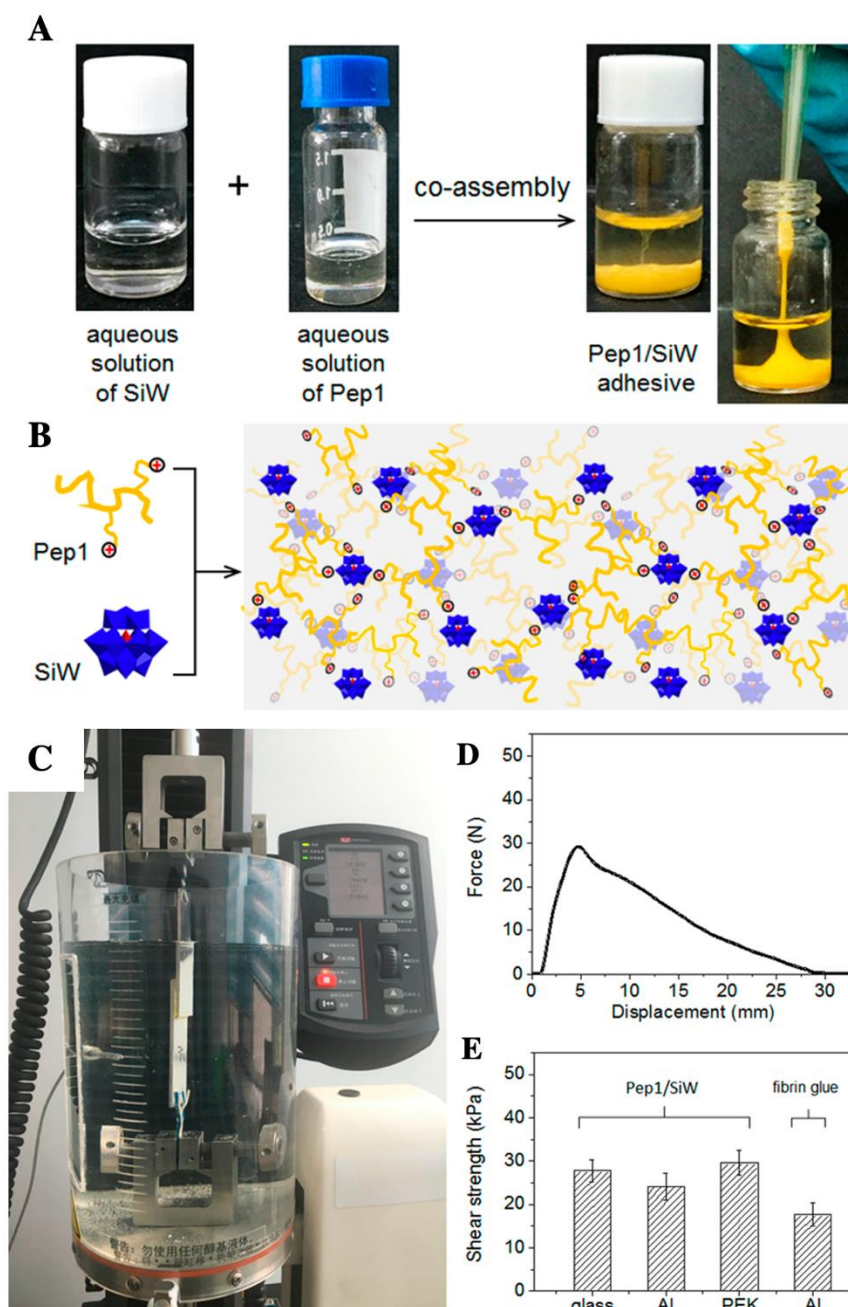


Fig. 22. (A) The preparation of Pep1:SiW coacervate from initially homogeneous solutions of each component. (B) Schematic representation of the co-assembled network of the coacervate phase. (C) The underwater lap shear setup used in this work. (D) A typical force-displacement curve from the underwater lap shear test on aluminum substrates. (E) The underwater adhesive performance of Pep1:SiW coacervate on different substrates and in comparison to a commercial tissue adhesive tested under similar conditions on aluminum substrates. [96], Copyright 2017. Reproduced with permission from American Chemical Society Publications.

Similar materials based on a shorter peptide (tripeptide) and a similar polyoxometalate ( $\text{SiW}_{11}$ ) were designed to respond to the pH and to the presence of metal ions [40]. This material started out as an *water-poor* but still injectable coacervate with a water content of 23 – 26 wt% at a tripeptide: $\text{SiW}_{11}$  ratio

of 2.4:1 at pH = 6.5. It then turned into a viscoelastic hydrogel upon lowering the pH (at pH = 4.5: water content = 15 – 17 wt%,  $G' \approx 100$  kPa,  $\tan(\delta) \approx 0.35$  at  $1 \text{ rad.s}^{-1}$ ) or addition of metal ions such as  $\text{Co}^{2+}$  or  $\text{Ni}^{2+}$  (at 0.1 M  $\text{Co}^{2+}$ :  $G' \approx 100$  kPa,  $\tan(\delta) \approx 0.15$  at  $1 \text{ rad.s}^{-1}$ ). The underwater shear strength on various substrates was measured to be 30 – 36 kPa at pH = 4.5 and 15 – 21 kPa at 0.1 M  $\text{Co}^{2+}$  (pH = 6.5). The failure mode was cohesive in all cases with little dependence on the substrate type, characteristic of soft liquid-like PSAs with low resistance to creep. This is not unexpected, given the small molecular components and the dynamic interactions involved in this coacervate-based adhesive. Nevertheless, these features work in favor of making their underwater adhesion repeatable (over a few attachment / detachment cycles).

We note that polyoxometalates are also capable of forming other interactions, as we will see in the following section.

### 3.3. Based on H-bonding interactions

Hydrogen bonding is one of the strongest ( $1 - 50 \text{ kT}$ ) physical interactions and therefore holds great potential for making soft, but resilient underwater adhesives [8,164]. However, the main challenge with using H-bonding for underwater adhesion is winning the competition against water itself. This is simply because water molecules act as both H-bond donors and H-bond acceptors. If the H-bonding partners have a larger affinity for water molecules than for one another, the material will swell and possibly dissolve in water over time. As we will see in the examples reviewed in the following, current systems reporting H-bonding for underwater adhesion usually take advantage of complementary weak interactions.

Tannic acid (TA) is a naturally-occurring, bulky polyphenolic compound capable of forming multiple weak interactions, mainly H-bonds, with both natural and synthetic polymers such as gelatine, poly(ethylene glycol) (PEG), and poly(vinyl alcohol) (PVA) [99,165,166]. The TA molecule can be seen in Fig. 23. Mixing solutions of these polymers with a TA solution at certain ratios leads to an H-bonding-driven complex coacervation with a polymer-rich phase and a water-rich supernatant. The coacervate is usually a highly viscous liquid (more viscous than the parent solutions) potentially useful as a wet and or underwater adhesive. It has been suggested that the presence of TA promotes interfacial interactions with substrates [99].

Lee's group [98] reported tissue adhesives based on the complexation of TA and a 4-arm PEG and named them TAPE. In probe tack tests of TAPE between porcine skin substrates (at  $0.02 \text{ mm.s}^{-1}$  in air), a high adhesion strength of 180 kPa was measured with a shape of the force – displacement curve, consistent with liquid adhesives, suggesting a cohesive failure mode. However no clear data was provided for the underwater adhesiveness of TAPE and the adhesion strength decreased by 50 % in the presence of a  $20 \mu\text{l}$  drop of water. Furthermore, TAPE was prepared at pH = 2 where H-bonding was abundant; deprotonation of TA at neutral or basic pH produced non-adhesive gums or liquids. It is



therefore not clear whether TAPE would keep its adhesiveness if immersed in water (equilibrium water content of the adhesive was not reported) or in physiological fluids.

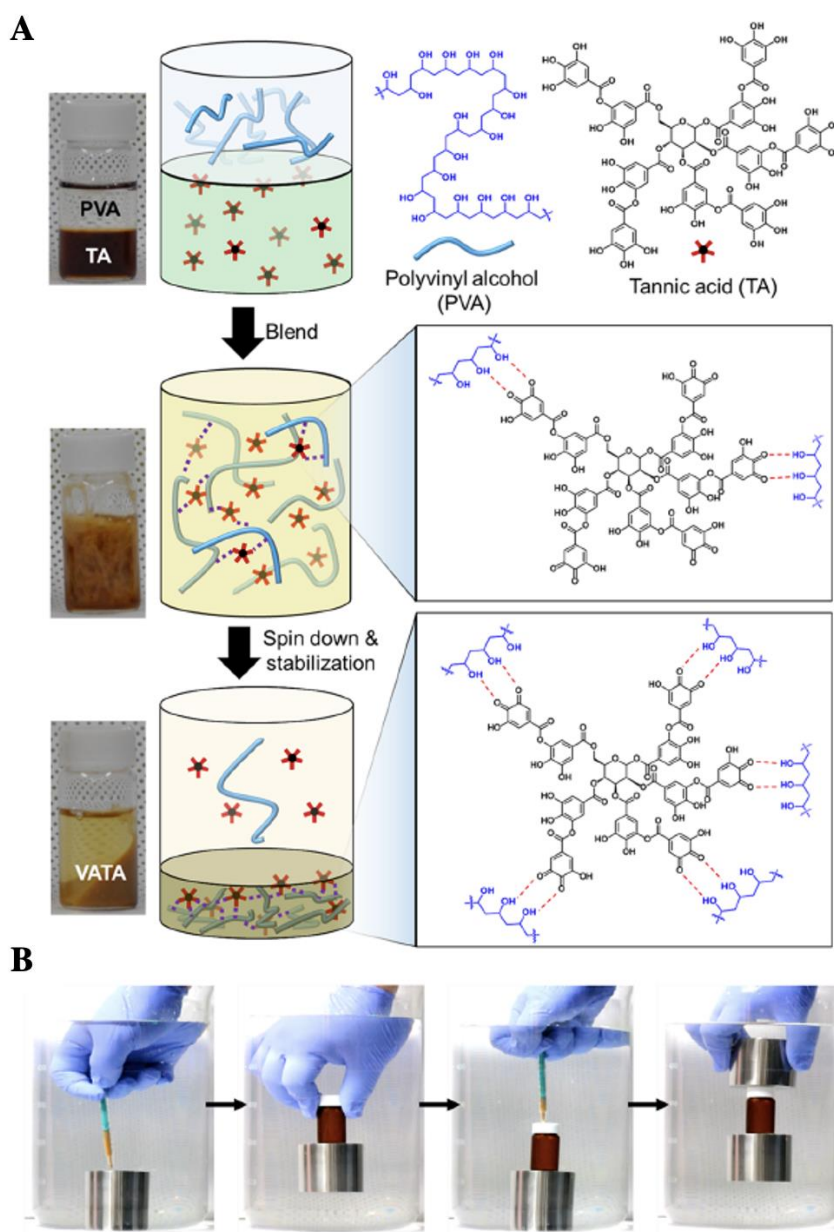


*Fig. 23. (A) The preparation of the underwater adhesive based on PVA and TA. The formation of numerous H-bonds between the PVA chains and TA leads to the formation of a physical hydrogel, which the authors called VATA. (B) Visualization of VATA's performance as an underwater adhesive directly applied under water. [99], Copyright 2020. Reproduced with permission from American Chemical Society Publications.*

The same group reported high strength underwater adhesives based on H-bonding-driven coacervation of TA and PVA in water (named VATA), as illustrated in Fig. 23 [99]. When prepared



from 20 wt% solutions of each component, VATA 20-20, the adhesive was a highly viscous, *water-poor* liquid with dynamic moduli around 10 kPa. The tensile strength in underwater probe tack tests at  $0.02 \text{ mm}\cdot\text{s}^{-1}$  was around 70 kPa, even when the contact was made 24 hours after immersion, suggesting a stable water content (although the water content was not reported by the authors). The adhesion strength did not change in acidic pH but decreased by half at  $\text{pH} = 10$ .

Peng and co-workers [102] performed an extensive study on coacervates from TA and commercially available amphiphilic block copolymers of PEG and poly(propylene glycol) (commercially called F68, PEG<sub>77</sub>-PPG<sub>29</sub>-PEG<sub>77</sub>, MW =  $8400 \text{ g}\cdot\text{mol}^{-1}$ ), as shown in Fig. 24 A. The authors concluded that coacervation was mainly due to H-bonding interactions between TA and PEG, but that the hydrophobic PPG cores of F68 micelles also contributed to the mechanical properties. This scenario is schematized in Fig. 24 B. The coacervates were highly viscous, very *water-poor* adhesives (water contents of 13 – 33 wt%). The best adhesive properties corresponded to TA40+F68-10 coacervate with a water content of 25 wt% and a viscosity of 590 Pa.s. The underwater adhesion strength of this coacervate depended strongly on the substrate, with 600 kPa measured on hydrophobic PMMA and 132 kPa on hydrophilic glass in pull-off tests at  $1.7 \text{ mm}\cdot\text{s}^{-1}$  upon application of 30 N for 10 s. A higher compression force in contact increased the bonding strength. Similarly, repeated pull-off tests (tens to hundreds of cycles) increased the adhesion strength before reaching a plateau. We believe these observations may be due to the high viscosity of the adhesive formulation, limiting the contact area even upon a non-negligible contact force of 30 N. The underwater adhesion of TA40+F68-10 was optimal when prepared at  $\text{pH} 4 - 5$  and its performance was insensitive to the presence of NaCl (up to 1.0 M) in the medium.

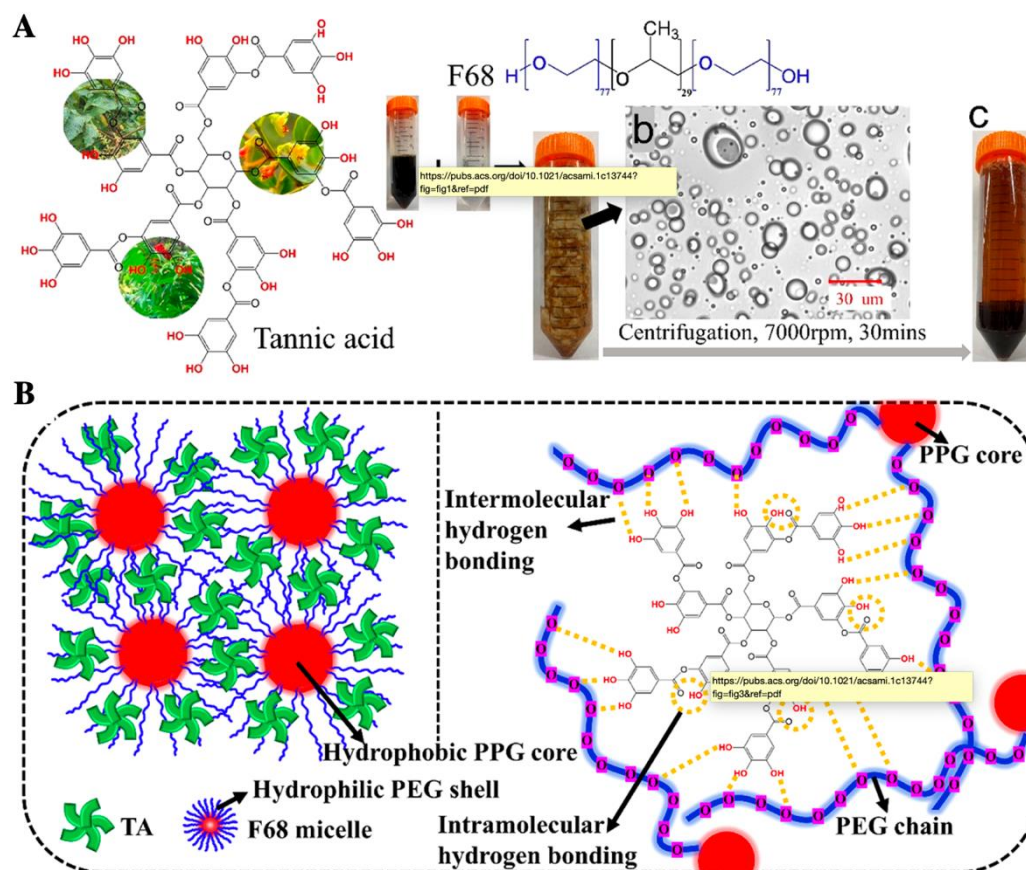


Fig. 24. (A) The coacervation of TA and PEG-PPG-PEG (F68) leading to the formation of liquid droplets rich in polymer and TA. Upon centrifugation, the droplets coalesced into a dense phase at the bottom of the tube. (B) The schematic illustration of the weak interactions responsible for the coacervation of TA-F68. [102], Copyright 2021. Reproduced with permission from American Chemical Society Publications.

The same group reported a wet adhesive based on H-bonding-driven coacervation of SiW, a polyoxometalate, and PEG at acidic pH ( $< 4$ ) [100]. The oxygens of SiW and the ether oxygens of PEG formed H-bonds mediated by hydrated protons. No electrostatic interactions were involved in coacervation. These highly viscous coacervates prepared at different mixing ratios were extremely *water-poor* (16 – 22 wt% water). The adhesion strength of this adhesive to pork skin in probe tack tests at  $0.2 \text{ mm}\cdot\text{s}^{-1}$  was 76 kPa. Addition of a small amount of water at the joint increased this value to 98 kPa. This enhancement was attributed to the facilitation of H-bonding in the presence of water molecules and the increased mobility of PEG chains. Underwater adhesion tests were not reported. However, we speculate that this adhesive should swell in the presence of excess water, compromising its performance.

Inspired by this work, Cui and co-workers [101] developed wet adhesives taking advantage of H-bonding and electrostatic interactions between low MW ( $1800 \text{ g}\cdot\text{mol}^{-1}$ ) branched polyethyleneimine (PEI) and a polyoxometalate called PW12. Optimal viscosity ( $0.8 \text{ Pa}\cdot\text{s}$ ) and adhesive properties were found at a nearly equimolar ratio at pH = 9 where both interactions were present. The dry lap shear

strength of this adhesive measured at a crosshead velocity of  $0.3 \text{ mm}\cdot\text{s}^{-1}$  (adhesive thickness not specified) was in the range of 164 to 319 kPa on hydrophilic substrates such as glass and wood. The wet shear strength was around 70 kPa for porcine skin. Even though the authors claimed underwater adhesiveness, no measurements were performed to quantify this, nor the long-term stability of this adhesive in water.

Wang and co-workers [103] recently reported a *hydrophobic* underwater PSA based on poly(2-methoxyethyl acrylate) (PMEA) and poly(N-allylthiourea) (PATU) at 85 and 15 mol%, respectively. As shown in Fig. 25, the distinguishing feature of the PMEA-PATU adhesive is the synergistic contributions of H-bonding and hydrophobic interactions, resulting in a *temperature-insensitive* loss factor of 1 between 1 and 100 °C (see Fig. 25 C). The dynamic moduli scaled with the square root of frequency ( $G' \approx G'' \sim \omega^{0.5}$ ) over a wide range ( $10^{-5} - 10^3 \text{ Hz}$ ), indicating a segmental Rouse mode due to the decelerating impact of the reversible associations. The storage modulus of this adhesive fell in the window between a high enough modulus to resist shear and the Dahlquist's criterion ( $1 \text{ kPa} \leq G' \leq 100 \text{ kPa}$ ) within the time scales of bonding ( $\sim 1 \text{ s}^{-1}$ ) and debonding ( $\sim 25 \text{ s}^{-1}$ ) (see Fig. 25 C).

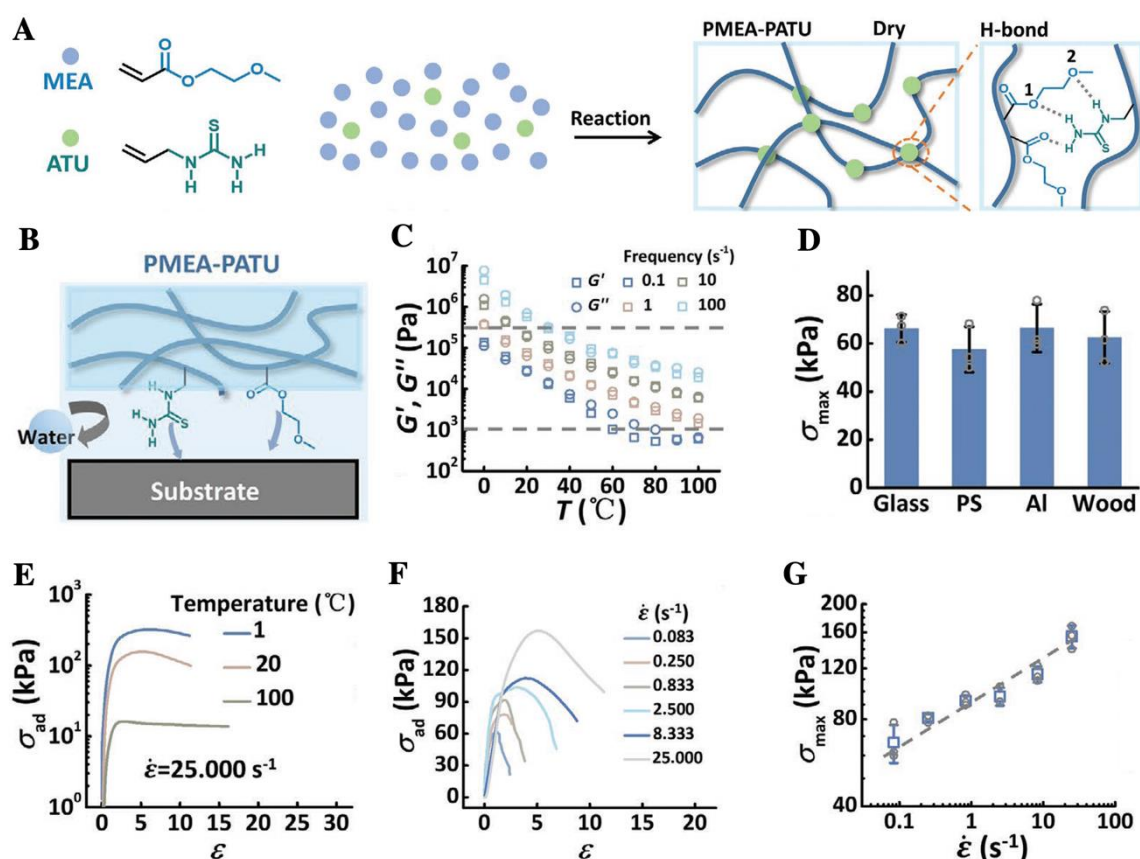


Fig. 25. (A) The solvent-free preparation of the PMEA-PATU underwater adhesive. (B) The hydrophobic drainage of water from the interface in the underwater adhesion of PMEA-PATU. (C) Evolution of the dynamic moduli of PMEA-PATU with temperature at different frequencies. The two dashed lines mark the minimum required modulus for resistance against shear and the Dahlquist's

*criterion. (D) The underwater adhesion strength of the adhesive on different substrates in probe tack tests at  $0.083\text{ s}^{-1}$  at  $20\text{ }^{\circ}\text{C}$ . (E) The stress-strain curves from underwater adhesion tests on glass at  $25\text{ s}^{-1}$  at different temperatures, and (F) at different strain rates at  $20\text{ }^{\circ}\text{C}$ . (G) The strain rate dependence of the adhesion strength. [103], Copyright 2021. Adapted with permission from John Wiley & Sons Inc.*

As expected from the above properties, PMEA-PATU showed generic underwater adhesion to various surfaces, with an adhesion strength of 60 – 70 kPa and cohesive failure in underwater pull-off tests at  $0.08\text{ s}^{-1}$  at  $20\text{ }^{\circ}\text{C}$  (Fig. 25 D). The adhesion strength against glass dropped with immersion time, reaching a plateau at 50 kPa after 4 days. This was probably due to the partial swelling of the adhesive in water. As expected for a viscoelastic gel, the adhesion strength was temperature and rate dependent, as shown in Fig. 25 E – G. It reached 155 kPa at  $25\text{ s}^{-1}$  at  $20\text{ }^{\circ}\text{C}$  on a glass substrate. At the same rate, the adhesion strength was 307 and 16 kPa at 1 and  $100\text{ }^{\circ}\text{C}$ , respectively [103]. The authors did not report the corresponding adhesion energies.

Most recently, Niu and coworkers [167] reported a simple, *dry* PSA based on random copolymers of AA and BA (butyl acrylate) for robust underwater adhesion, as presented in Fig. 26 A. The viscoelastic properties of this PSA were fine-tuned by varying the molar ratio of the comonomers, as shown in Fig. 26 B. At an optimal BA : AA molar ratio of 2.8 : 1.0, called P(BA<sub>2.8</sub> – AA<sub>1.0</sub>), the dry adhesive at room temperature was a highly viscoelastic material close to the gel point with the dynamic moduli just below 0.1 MPa (Dahlquist's criterion) and a  $T_g$  of  $-8.4\text{ }^{\circ}\text{C}$ . The authors attributed the cohesive properties of P(BA<sub>2.8</sub> – AA<sub>1.0</sub>) to the abundant H-bonding interactions of the AA comonomers with the BA and other AA comonomers (see Fig. 26 A) [167]. We note that this composition is similar (with more acrylic acid) to commercial *hydrophobic* PSAs (which can contain up to 10 mol % in acid functions). In this work, higher and lower ratios of BA : AA led to liquid like samples with low shear resistance and solid like samples with too high elasticity, respectively.



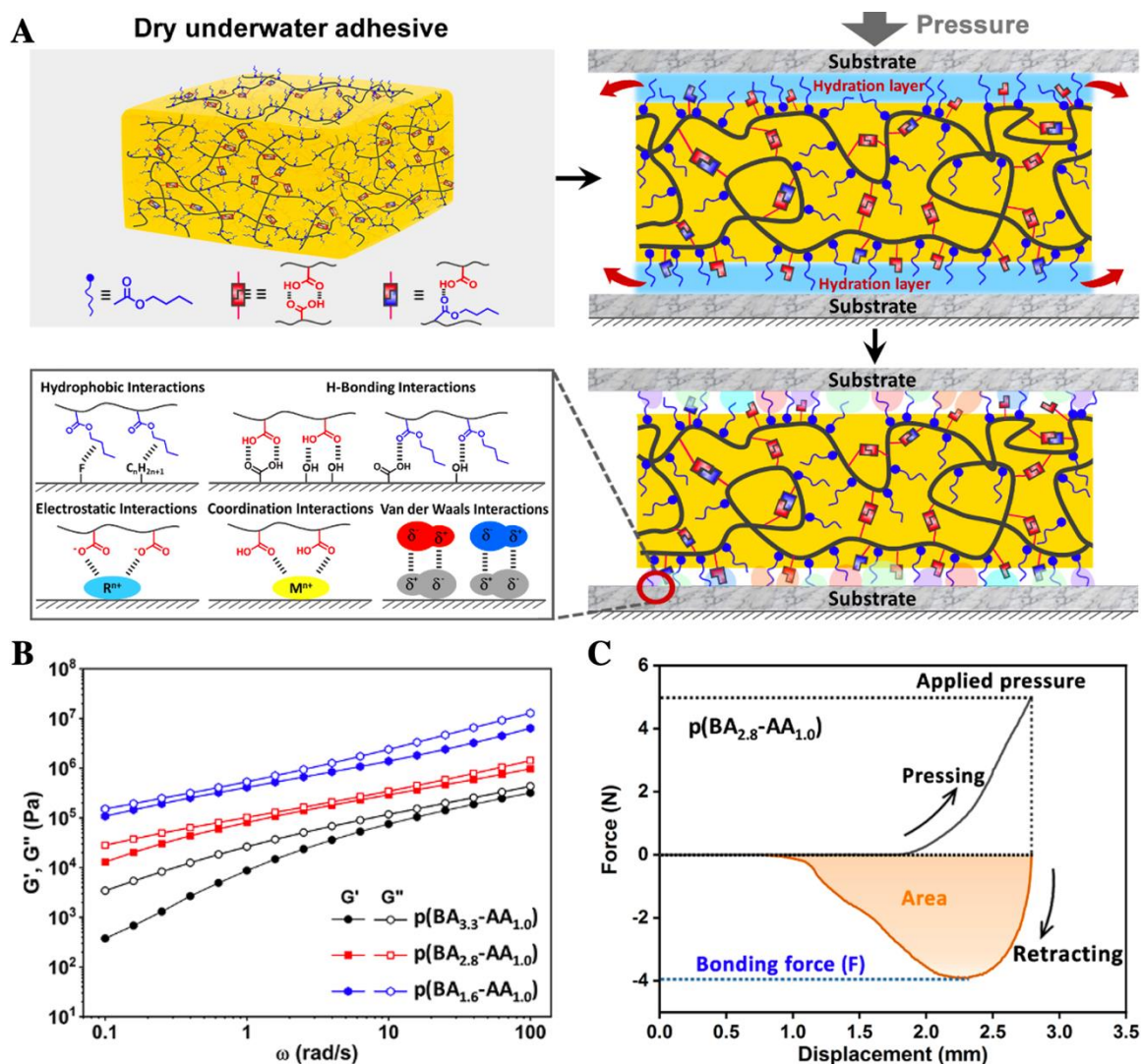


Fig. 26. (A) The design of dry underwater PSAs based on extensive hydrogen bonding and hydrophobic interactions. Other weak interactions may also contribute to the interfacial adhesion. (B) The adjustment of the viscoelastic properties of the dry PSAs by varying the comonomer compositions. (C) A typical force - displacement curve from an underwater probe tack test on  $P(BA_{2.8} - AA_{1.0})$ . [167], Copyright 2022. Reproduced with permission from American Chemical Society Publications.

In water, this material showed limited swelling with a saturated water uptake of 16.8 wt%, making it a *hydrophobic* PSA adhesive. Indeed, this stable water content is promising for long-term underwater adhesion. As schematized in Fig. 26 A, this PSA is capable of forming various weak molecular interactions with immersed substrates, notably H-bonding and hydrophobic interactions (among others suggested by the authors, but not elucidated; for instance, electrostatic interactions in the case of PAA are pH dependent, but this was not studied/reported) (see Fig. 26 A). The hydrophobic n-butyl functions of the BA comonomer were suggested to help to remove the water layer at the interface upon contact under the application of some pressure. This also helps to limit its swelling in water.

The P(BA<sub>2.8</sub> – AA<sub>1.0</sub>) PSA featured a tack strength of 57 kPa against stainless steel (SS) with an adhesion energy of 45 J.m<sup>-2</sup> upon the application of 63 kPa of bonding pressure for 60 s (Fig. 26 C). Without the debonding rate or strain rate reported, it is difficult compare these values with those from other systems. The tack strength increased almost monotonously with the pre-stress applied, reaching 320 kPa for a pre-stress of 640 kPa. This is probably due to the high storage modulus of the adhesive, compromising good contact formation. Nevertheless, at a pre-stress of 250 kPa, the P(BA<sub>2.8</sub> – AA<sub>1.0</sub>) PSA had tack strengths of 115 – 150 kPa on various hydrophilic and hydrophobic substrates under artificial seawater. The performance of this *hydrophobic* underwater adhesive was repeatable over 30 cycles of attachment/detachment. When stored in water for several days, the bonding strength of the adhesive decreased to some extent (around 110 kPa) but remained relatively constant afterwards, consistent with the slight water uptake of the adhesive [167].

### 3.4. Based on other weak interactions

A growing body of experimental evidence has underlined the importance of other weak molecular interactions, namely  $\pi$ -type ( $\pi - \pi$  and cation –  $\pi$ ) interactions and metal-ligand coordination, in the underwater performance of organismal adhesives [168–171]. The majority of these insights are based on micro- and or nano-scale adhesion experiments (mainly Surface Force Apparatus (SFA) measurements and some Atomic Force Microscopy (AFM)), probing the strength of these interactions at a single-molecule level and or at interfaces between ultrathin films. Until recently, no study had developed bulk model systems based on these weak interactions (without covalent interactions involved) to quantify their possible contributions to macroscopic underwater adhesion. In this section, we briefly review the few pioneering works which encourage further developments in this direction.

Cation –  $\pi$  interactions are the result of the non-covalent attractive force between an electron-rich  $\pi$  system and positively charged cations or moieties in their vicinity [164]. Fan and coworkers [21] synthesized a series of alternating copolymers with adjacent cationic-aromatic sequences, named poly(cation-adj- $\pi$ ), as shown in Fig. 27 A. These copolymers are soluble in salt-free water due to the electrostatic repulsion between the positively charged comonomers. At 0.7 M NaCl where the repulsive forces between the like (positive) charges are sufficiently screened, the copolymers form *water-rich* physical hydrogels stabilized by the cation –  $\pi$  and hydrophobic interactions as well as chain entanglements. The physical hydrogels with the acrylate-based and the methacrylate-based model monomers had different equilibrium water contents (88 and 69 wt%, respectively) due to the more hydrophobic nature of the latter monomer. This can be seen in the tensile behavior and the linear rheological properties of the physical hydrogels (Fig. 27 B – C). Unlike the stiffer methacrylate-based system, the acrylate-based hydrogel was relatively soft (Young's modulus  $\sim$  5 kPa), highly dissipative ( $\tan(\delta) \sim$  0.5), and highly stretchable (maximum strain  $\sim$  11). This hydrogel had a tack strength of  $\sim$  6 kPa and an adhesion energy of  $\sim$  30 J.m<sup>-2</sup> against negatively charged glass surfaces in underwater (in 0.7 M NaCl) probe tack tests at 100  $\mu$ m.s<sup>-1</sup>. The hydrogel featured a finger-like, fibrillar structure and



went through extensive deformation and strain-hardening leading to interfacial failure with little residue on the glass surface (Fig. 27 D – E). The authors demonstrated the universality of their strategy using other cationic and aromatic comonomers. They argued that cation -  $\pi$  and hydrophobic interactions play complementary roles in both the interfacial adhesion (via removing surface salt ions and breaking the hydration layer) and the bulk energy dissipation (cohesion).

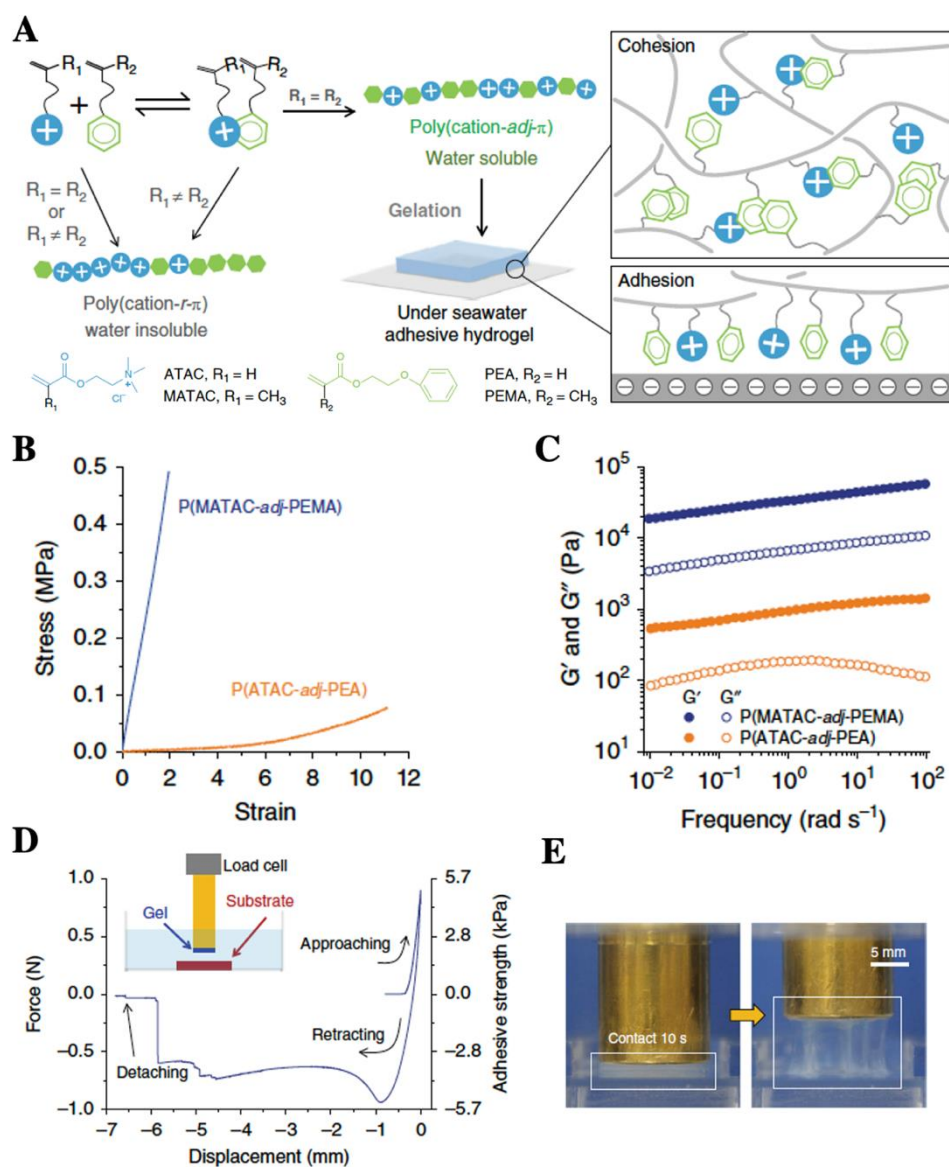


Fig. 27. (A) The design of poly(cation-adj- $\pi$ ) interactions producing sticky physical hydrogels in saline water. (B) The tensile behavior of the physical hydrogels based on the acrylate- and the methacrylate-based comonomers and (C) their linear viscoelastic behavior. (D) Schematic illustration of the underwater (0.7 M NaCl) probe tack test as well as the stress - displacement curve of the acrylate-based system. Signs of strain-hardening can be seen at large deformations. (E) Images showing extensive bulk deformation and fibrillation of the acrylate-based system in 0.7 M NaCl. [21],

Copyright 2019. Adapted with permission from Springer Nature.

Reporting on chemical hydrogels rich in monomers bearing aromatic groups inspired by the composition of barnacle cement, Fan and coworkers [172] highlighted the role of cation- $\pi$  and  $\pi-\pi$  interactions in both the cohesion of the hydrogels by providing energy dissipation mechanisms and the interfacial adhesion by breaking the hydration layer using hydrophobic interactions. Interestingly, the gels containing 80 – 85 mol % aromatic moieties featured superior adhesion in “water”, whereas those containing 70 mol % aromatic groups performed better in “0.7 M NaCl”. Once again, this highlights the importance of salt concentration in finding the right balance between electrostatic repulsion and the cohesion provided by  $\pi-\pi$  interactions, all considering the composition of the comonomers. Another insightful work from this group demonstrated the role of comonomer distribution along the chain (at a given comonomer ratio; equimolar in this case). [173] In a 0.7 M NaCl medium, the copolymer hydrogel with adjacent cationic and aromatic comonomers (an alternating copolymer) had a better underwater adhesion performance compared to its counterpart with block sequences of those same comonomers. The authors argued that the multi-block copolymer forms large hydrophobic aggregated structures in water, with trivial or no contribution to the stabilization of the cationic moieties. We emphasize that the hydrogels developed in both of these works are chemically crosslinked. Physical hydrogel analogues of these chemically crosslinked hydrogels merit further investigation.

Inspired by the cation- $\pi$  interactions of model proteins leading to liquid-liquid phase separation, Zhu and coworkers [104] synthesized a poly(ionic liquid), poly(1-benzyl-3-vinylimidazolium chloride) (P-Ben), as shown in Fig. 28 A. P-Ben is a strong polycation with an aliphatic backbone, bearing a dangling cation-methylene-phenyl (C-M-P) sequence. A C-M-P type sequence allows salt-induced coacervation at different salt concentrations depending on the monomer composition and concentration. At a P-Ben concentration of 0.1 M, coacervation occurs at NaCl concentrations above 0.1 M (see Fig. 28 B). The coacervate phase is a viscoelastic fluid ( $1 < \tan(\delta) < 2$ ) with the dynamic moduli in the range of a few kPa (see Fig. 28). When directly applied on glass substrates under water in physiological conditions (0.15 M NaCl), P-Ben has an instant lap shear strength of about 20 kPa. As expected, higher salt concentrations further screen repulsive electrostatic interactions, which, in this case, lead to stronger cation- $\pi$  interactions and higher shear strengths ( $\sim 40$  kPa in seawater). In order to enhance the interfacial adhesion of the formulation, the C-M-P monomer was randomly copolymerized with two comonomers bearing catechol and vinyl functions (the copolymer called P-Cat-3). The synergy of these functions enhanced the underwater lap shear strength to 160 kPa on glass and 40 kPa on porcine skin (0.15 M NaCl, pH = 6.8). The underwater adhesion remained almost unchanged up to pH = 9. However, highly basic pH led to a reduction in the adhesion strength, which was attributed to the oxidation of the catechol function.

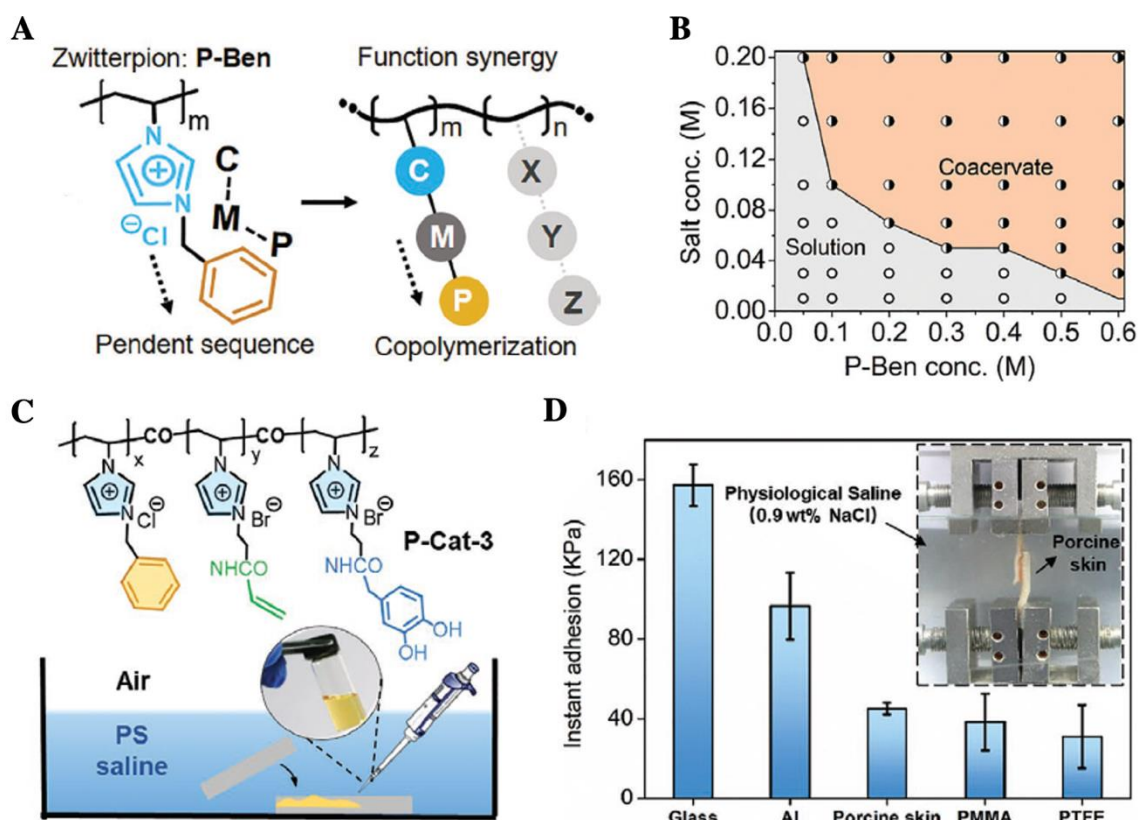


Fig. 28. (A) The structure of P-Ben with the design of C-M-P units into the pendant group and the possibility for synergy with functions on other comonomers. (B) The phase diagram of P-Ben coacervation as a function of NaCl concentration. (C) The synergistic design of the C-M-P monomer (P-Ben) with other comonomers for enhanced interfacial adhesion. (D) The underwater lap shear strength of the copolymer in C on various substrates. [104], Copyright 2022. Reproduced with permission from John Wiley & Sons Inc.

Metal – ligand coordination is another type of weak interaction extensively cited to play a nontrivial part in organismal underwater adhesion [2,174,175]. These interactions are based on the exchange of electron pairs between a metal ion (a Lewis acid) and an organic ligand (a Lewis base). Depending on the nature of the metal ions and the organic motifs (ligands), the binding strength of these interactions can be widely tuned [164]. Surprisingly, very few works have developed bulk underwater adhesives based on metal – ligand coordination alone. Recently, Wei and coworkers [105] reported interpenetrating networks of hydroxypropyl methylcellulose (HPMC) and PDMAEMA. As shown in Fig. 29, the HPMC network was crosslinked via coordination complexation with SiW (tungstosilicic acid) while the PDMAEMA was crosslinked via metal coordination with  $\text{Fe}^{3+}$  ions, as confirmed by FTIR spectroscopy. Hydrogen bonding between the two polymers can also contribute to the network strength. The *water-poor* HPMC/SiW–PDMAEMA/ $\text{Fe}^{3+}$  hydrogel (at the optimal ratio between the components) had a  $G'$  on the order of 10 kPa and a  $\tan(\delta)$  of 0.5. After 1 h of immersion in water, the hydrogel had a wet shear strength of  $\sim 50$  kPa to glass. This value dropped to less than 30 kPa and then

20 kPa after 3 h and 18 h of immersion in water, respectively, indicating an increase in the water content of the hydrogel over time.

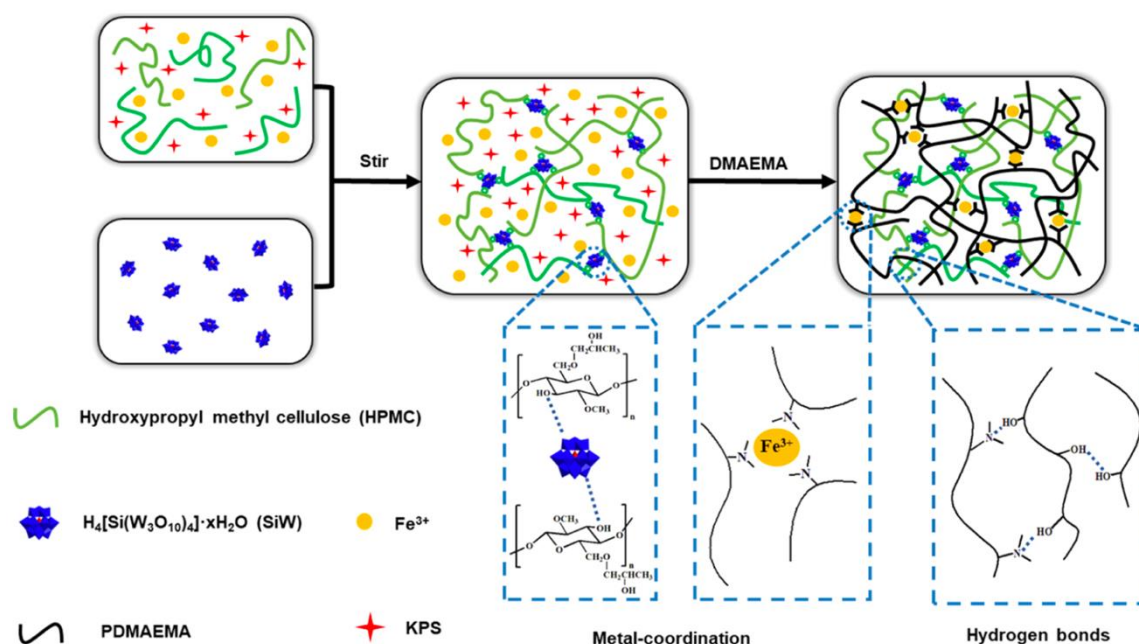


Fig. 29. Schematic representation of the preparation of an HPMC/SiW/ $Fe^{3+}$  hydrogel and the physical interactions involved. [105], Copyright 2021. Reproduced with permission from American Chemical Society Publications.

#### 4. Tuning underwater adhesiveness

Considering the state-of-the-art reviewed above, we propose the following guidelines for future works aiming to obtain soft PSA-like coacervates:

(1) It is important to explore combinations of weak molecular interactions in well-defined model systems. Multiple weak interactions can provide complementary, orthogonal, or synergistic contributions to the adhesive properties. Meanwhile, they can possibly offer adhesion on different time scales and or via different mechanisms for more robust, more versatile adhesion. As reviewed above, obtaining a synergy between different interactions necessitates careful design of the MW, the monomer composition, the copolymer topology, and the grafting density. Otherwise, one interaction may interfere with or impede other interactions, as shown by different groups [21,160,161]

(2) Equilibrium water content is a determining factor in the viscoelastic and adhesive properties of soft underwater adhesives. Lower water contents lead to stiffer coacervates and hydrogels with stronger mechanical properties. In all cases, the water content must be stable over time to ensure consistent performance. The adhesive must therefore be at an equilibrium degree of swelling or thermodynamically immiscible with water. For instance, *water-poor* and *water-rich* polyelectrolyte coacervates become

relevant for real wet and underwater applications at water contents below 35 and 75 wt%, respectively. In principle, *water-poor* complex coacervates are more interesting in terms of adhesion strength, but their injectability may be limited due to high viscosity.

(3) When using hydrophobic interactions in designing underwater adhesives, the stability of the hydrophobic domains is critical. For instance, we speculate that POEGMA based hydrogels must have a lower underwater stability against excessive swelling relative to PNIPAM-based hydrogels because PNIPAM hydrophobic domains are known to have much longer lifetimes due to their very slow dynamics above the transition temperature [108]. Another important factor is the molar mass of the hydrophobic moieties; the energy barrier against removing a long PNIPAM chain from a hydrophobic association is much larger compared to that for a short one [25]. We remind the reader that other well-known thermoresponsive polymers such as POEGMA are well above their  $T_g$  at room temperature. As a result, their hydrophobic domains remain in the rubbery state.

As for host-guest interactions, the mechanical properties are closely related to the association/dissociation constant of the host and guest molecules. Although these interactions have been mostly studied at interfaces, they may be useful for making soft underwater adhesives if the number and or the lifetime of the interactions can be controlled to produce *water-rich* viscoelastic gels instead of elastic ones. Obviously, the association constant must be sufficiently high to control the equilibrium water content. So far, combinations of these interactions with other weak molecular interactions have not been studied for the purpose of underwater adhesion.

(4) Different triggers, such as temperature (as discussed above) but also salt concentration and pH, may be employed in the development of soft injectable underwater adhesives. The use of high salt concentrations in the case of polyelectrolyte complex coacervates is limited due to (i) the tolerance of body tissues in biomedical applications and (ii) the trade-off in mechanical properties due to the decrease in polymer volume fraction. Similarly, in the case of thermoresponsive underwater PSAs, the polymer concentration in the initial solution cannot exceed a certain value, depending mainly on the MW, if injectability is a requirement. This also limits the polymer volume fraction in the final hydrogel unless a macroscopic phase separation (coacervation) takes place.

(5) Tuning the MW is critical in the design of soft adhesives, in water like in air. As mentioned earlier, a broad MWD and a low degree of crosslinking impart generic stickiness to *hydrophobic* PSAs. In the case of soft underwater adhesives, the crosslinking is provided by abundant weak interactions which are usually dynamic. The number density of these interactions as well as their lifetime (if tunable) can be utilized to tune the viscoelastic and adhesive properties of the material.

We do not know of a work focusing on the MWD of soft underwater adhesives. Nonetheless, relatively small MW polyelectrolytes ( $N = 100 - 300$ ) can possibly produce self-adhesive coacervates without needing a salt switch, as shown by Vahdati and coworkers [26]. The shortcoming in this strategy



is the absence of entanglements and the lack of strain hardening in large deformations. The same is true in the case of electrostatically driven complex coacervates where one or both polyelectrolytes are replaced with smaller, non-macromolecular molecules (for examples see Fig. 21 and 22). Inspired by *hydrophobic* adhesives, this challenge might be addressed by using polyelectrolytes of large polydispersity or a combination of small and large MW polyelectrolytes.

Intriguingly, all the systems reviewed in the section on H-bonding interactions similarly rely on relatively low MW ( $< 20 \text{ kg}\cdot\text{mol}^{-1}$ ) polymers. The reason for choosing such small molecular weights was not clearly reported; however, we speculate this is due to the lower viscosity and the better processability of the formulations. In fact, most of the present works have reported highly viscous liquid adhesives. Therefore, higher MWs must have produced solid precipitates or heterogeneous materials. This is reminiscent of high MW, hydrophobic polyelectrolytes which make *water-poor* solid precipitates over a wide range of salt concentrations. By analogy with electrostatic interactions which can be doped using salt, the addition of small molecules capable of disrupting H-bonds (like urea) is an idea worth exploring.

(6) The few reported investigations on cation –  $\pi$  interactions have clearly highlighted their promise for bulk underwater adhesion. In a series of works on physical and chemical hydrogels based on these interactions, Fan and coworkers [21,172,173] demonstrated how the chemistry, fraction, and sequence of the two comonomers (bearing cationic or  $\pi$  moieties) can be designed to achieve adhesion in pure or salty water. The work of Zhu and coworkers [104] was based on monomers with a pendant group bearing both the cationic and the  $\pi$  residues separated by a methylene. Using SFA measurements on model short-sequence peptides, Chang et. al. [176] showed the significance of the sequence topology and composition on the cation- $\pi$  interactions which eventually determine the underwater adhesive properties. All these works mark the importance of (i) “how” the cationic and  $\pi$  residues are positioned with respect to one another (within each monomer unit or along the copolymer), and (ii) “at what ratio” they are incorporated in the copolymer. The former point is reminiscent of the work of Vahdati and coworkers on thermoresponsive graft copolymers discussed in section 3.1.2 (see Fig. 5 A).

Another point to consider when using  $\pi$  – type interactions is that a *minimum* salt concentration to screen electrostatic repulsion is *indispensable* before these interactions can effectively contribute to the mechanical properties (see Fig. 27 B). This minimum salt concentration is expected to be lower when the copolymer is rich in aromatic groups. This is due to both the lower electrostatic repulsion at smaller concentrations of cationic groups and the larger contribution of  $\pi$  –  $\pi$  and hydrophobic interactions. Therefore, unlike polyelectrolyte complex coacervates, the systems based on cation- $\pi$  interactions hold great potential for applications in high salinity media such as seawater.

(7) Future work on *hydrophilic* underwater adhesives based on metal – ligand coordination may draw inspirations from the existing literature on metal – coordinate crosslinked hydrogels [177–179]



that have clearly demonstrated the tunability of the dynamics of these systems by changing the metal ion, the ligand chemistry, and or their (molar) ratio.

(8) A less explored strategy to enhance the performance of soft underwater adhesives is to incorporate rigid particles into them, as done for *hydrophobic* PSAs [92]. Dompé and coworkers [180] showed the feasibility of this strategy using hybrid polyelectrolyte complex coacervates based on thermoresponsive polyelectrolytes and silica nanoparticles. However, they mentioned that due to the strong polymer-particle interactions involved in their system, obtaining a macroscopically homogeneous material was strongly dependent on the preparation method. They also reported a strong partitioning behavior, with most of the nanoparticles ending up in the coacervate phase. It is thus critical to find a reproducible preparation method and to determine the partitioning behavior in the case of phase separation.

The seminal work of Rose and coworkers [181] showed the potential of nanoparticle suspensions to act as adhesives for gels and biological tissues. With optimal design of the gel network mesh size and the particle surface chemistry, the formation of weak molecular interactions between multiple monomers (per network strand) and the surface of the nanoparticles may also provide an efficient adhesion strategy. In this general strategy, shown for carbon nanotubes, cellulose nanocrystals, and silica nanoparticles, the particles connect the two adherend gels while the polymer chains bridge the nanoparticles, as shown in Fig. 30 A. This strategy was shown to be effective in bonding *water-rich* hydrogels and wet biological tissues. Inspired by this work, Michel and coworkers [182] used coatings of coagulation-promoting nanoparticles to achieve adhesion between hydrogels and soft tissues both in the absence and the presence of blood (Fig. 30 B and C, respectively).

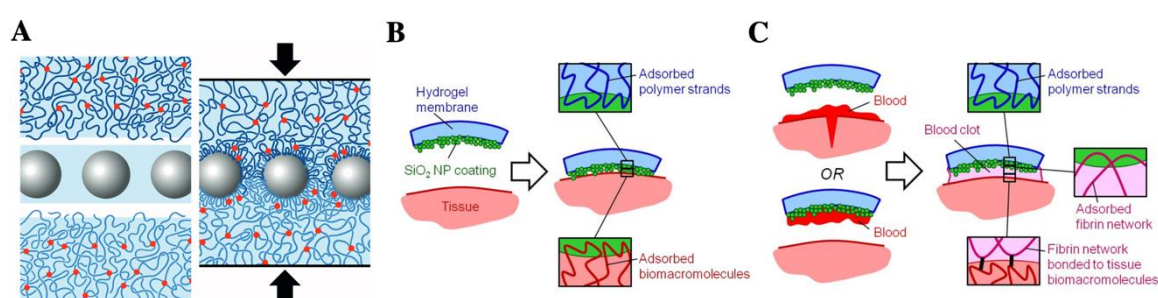


Fig. 30. (A). Schematic representation of the general strategy of gluing together swollen gels using nanoparticles as intermediates. [181], Copyright 2014. Reproduced with permission from Springer Nature. An example of the extension of this strategy to biological tissues (B) in the absence and (C) in the presence of blood. [182], Copyright 2020. Reproduced with permission from American Chemical Society Publications.

## 5. Challenges and perspectives

As we have seen in this review, weak molecular interactions have great potential for developing *hydrophilic* materials with inherent or on-demand stickiness while fully immersed in aqueous media or exposed to a high level of humidity. Nonetheless, research on soft underwater adhesives still has several important challenges to deal with. Current *hydrophilic* underwater adhesives based on weak physical interactions (i) are softer compared to their *hydrophobic* self-adhesive counterparts (PSAs), (ii) are limited in scope due to a nontrivial compromise between injectability and adhesive properties, and (iii) are still mostly based on synthetic model polymers. Considering these aspects, the perspectives of the field are summarized in Fig. 31 and discussed below.

Naturally, the first perspective in this field is to develop soft but more robust underwater adhesives, with adhesion energies exceeding  $100 \text{ J.m}^{-2}$  (Fig. 31). Achieving this goal requires elaborate materials design, given the viscoelastic nature of these adhesives. As discussed extensively in this review, developing a too elastic material (too small  $\tan(\delta)$ ) will favor debonding too easily from substrates while a too viscous material will fail cohesively due to creep. Ideally, one would like to enhance both the storage and the loss moduli of the adhesive, without exceeding neither the Dahlquist's criterion ( $G' < 0.1 \text{ MPa}$ ) nor a  $\tan(\delta)$  value of 0.5. However, in many systems, the equilibrium water content and the interplay between different weak molecular interactions may limit the enhancement of the moduli and or the optimization of the loss factor.

One way to overcome this challenge may be to develop *hydrophobic* adhesives with a thermodynamically limited and stable water content (below 20 wt%), as reported by Wang and coworkers [103] and Niu and coworkers [167]. These systems combine relatively strong hydrophobic interactions with other weak molecular interactions such as H-bonding and electrostatic interactions. Hydrophobic interactions are beneficial for removing the water at the interface, making way for other interactions to form as well. In a similar way,  $\pi$ -based interactions may benefit from the hydrophobicity of the  $\pi$  moieties to break the layer of bound water at interfaces, as suggested by Fan and coworkers [21].

An alternative strategy can be to find ways to reduce or limit the water content in *hydrophilic* adhesives. There exists a good understanding of water content control for systems based on electrostatic interactions, as discussed in Section 3.2.2 (see Fig. 11). Similarly, the works of Vahdati and coworkers [25,36] (see Fig. 5 – 7) and Fan and Gong [21,172] (see Fig. 27) provide preliminary but important insights for systems based on hydrophobic and  $\pi$ -type interactions, respectively. These works may inspire similar investigations on the roles of copolymer composition, architecture and topology as well as monomer composition for the design of soft underwater adhesives based on these and other weak molecular interactions. In all these cases, the challenge is to reduce the water content *while* optimizing the viscoelastic properties, because a mere reduction in the water content often leads to rigid, non-sticky materials. Another possibility is to reduce the water content *after* preparation, e.g. via extrusion as

reported by Dompé et. al [94]. However, this mechanically reduced water content must be stable on the time scale relevant to the application; else, swelling will compromise the underwater performance.

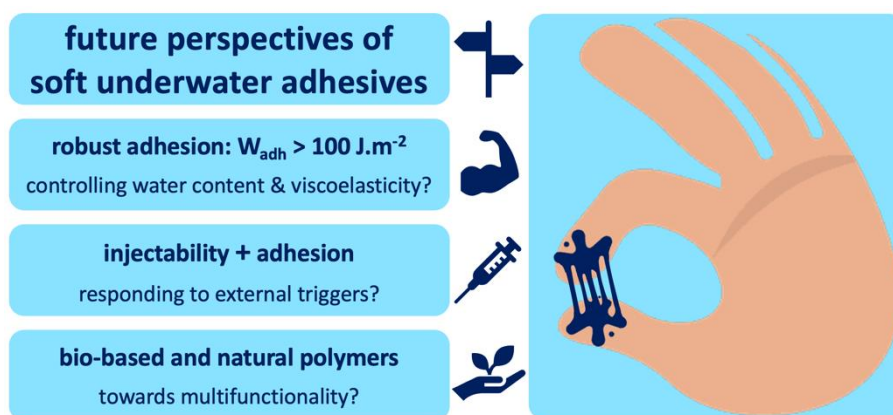


Fig. 31. The most important challenges and perspectives for soft underwater adhesives based on weak molecular interactions.

The second perspective for research on soft underwater adhesives is to address the nontrivial compromise between *injectability* and *adhesive properties* (Fig. 31). As discussed in Section 3, the challenge is often in the conflicting macromolecular designs required for easy injectability and strong nonlinear mechanical properties. Let us put this into perspective with a simple example. Solutions of lower MW polymers generally have lower viscosities and should be more easily injectable compared to solutions of their high MW counterparts (at a given polymer concentration). Meanwhile, lowering the molecular weight reduces the contributions of the entanglements and the number of weak molecular interactions (stickers per chain) to the final mechanical properties once the system is in the gel state. One possibility is to explore systems where the solubility and therefore the size of the (co)polymer is widely tunable upon an external trigger, allowing significant modification of the mechanical properties on demand.

In principle, most hydrophobically modified polymers designed with various architectures (multiblock copolymers, telechelic polymers, or copolymers with random or blocky distributions) [183] can be made to have efficient underwater adhesive properties. However, their high viscoelasticity in the preparation (solution) state makes these aqueous formulations difficult to inject. As discussed in Section 3.1.2, one way to potentially circumvent this problem is to use responsive copolymers with a hydrophilic / hydrophobic balance that is sensitive to environmental stimuli, namely the temperature. Such stimuli responsive behavior, which can trigger hydrophobic interactions on demand, can be imagined in different manners. A potentially interesting approach is to get inspired from responsive thickeners, initially made of a suspension of dense macromolecular particles, stabilized by intramolecular

hydrophobic interactions. These materials are capable of inducing dramatic changes in the mechanical properties, going from low-viscosity suspensions to highly viscoelastic hydrogels by turning the initial intramolecular hydrophobic interactions into intermolecular ones with a change in pH [184], a change in temperature or the application of shear [183,185]. Of course these ideas should be explored considering critical features like the kinetics of the transition process, which promotes the conversion of hydrophobic interactions from intra- to inter-molecular ones. Another feature is the overall hydrophilic/hydrophobic balance of the copolymer, which controls the equilibrium swelling behavior and the final viscoelastic and adhesive properties.

Finally, an important perspective for this field is to transfer the simple design guidelines obtained from synthetic model systems towards bio-based and natural polymers (Fig. 31). This is important for several reasons. Many bio-based polymers are potentially less toxic than their synthetic counterparts and thus safer for the human body and the environment. Some of them also feature other desirable functions such as antimicrobial properties and or rapid (bio)-degradability. Apart from their potential multifunctionality, these polymers also raise several fundamental questions. For instance, compared with synthetic polyelectrolytes typically characterized by flexible chains, charged polysaccharides have stiffer chains (larger persistence lengths) both due to their bulky repeat units and the presence of charges [186,187]. These polysaccharides also have lower charge densities, increasing the probability of compensation by counterions (rather than macroions) in their complexes. The impact of such inherent differences (between the synthetic models and bio-based polymers) on the physical and mechanical properties of bio-based coacervates merits further investigation and can foster new developments in soft underwater adhesives.

Our review of the current literature on soft underwater adhesives quickly revealed that the terms "hydrophobic" and "hydrophilic" are used to connote various concepts and properties in an inconsistent and confusing manner. It is still difficult to propose a quantitative criterion comprehensive enough to encompass all the underlying distinctions between hydrophilic and hydrophobic adhesives. Nonetheless, we proposed an equilibrium water content of 20 wt% as a preliminary distinguishing criterion. We also suggested to further divide hydrophilic adhesives into water-poor and water-rich systems based on significant differences in the mechanical properties associated with water contents below and above 60 wt%. Indeed, more work and discussions are needed to refine these criteria. To this end, future works are highly encouraged to meticulously report the equilibrium water content of their underwater adhesives.

## 6. Acknowledgements

The authors are grateful for helpful discussions with Fouzia Boulmedais (CNRS, Charles Sadron Institute, France), Marleen Kamperman (University of Groningen, the Netherlands), Christophe Chassenieux (Le Mans University, France), Pierre Schaaf (INSERM, France), Francisco Cedano (Saint

Gobain Research, France), Marco Dompé (Wageningen University and Research, the Netherlands), Victor Kang (Imperial College London, the UK), and Sina Ghiassinejad (TMC, Belgium).

## 7. References

- [1] Fan H, Gong JP. Underwater Adhesives. *Bioinspired Advanced Materials* 2021;2102983:1–21. <https://doi.org/10.1002/adma.202102983>.
- [2] Hofman AH, van Hees IA, Yang J, Kamperman M. Underwater Adhesives by Using the Supramolecular Toolbox. *Bioinspired Advanced Materials* 2018;30:1704640. <https://doi.org/10.1002/adma.201704640>.
- [3] Peppas NA, Sahlin JJ. Hydrogels as mucoadhesive and bioadhesive materials: A review. *Biomaterials* 1996;17:1553–61. [https://doi.org/10.1016/0142-9612\(95\)00307-X](https://doi.org/10.1016/0142-9612(95)00307-X).
- [4] Duarte AP, Coelho JF, Bordado JC, Cidade MT, Gil MH. Surgical adhesives: Systematic review of the main types and development forecast. *Prog Polym Sci* 2012;37:1031–50. <https://doi.org/10.1016/j.progpolymsci.2011.12.003>.
- [5] Bouten PJM, Zonjee M, Bender J, Yauw STK, van Goor H, van Hest JCM, et al. The chemistry of tissue adhesive materials. *Prog Polym Sci* 2014;39:1375–405. <https://doi.org/10.1016/j.progpolymsci.2014.02.001>.
- [6] Heinzmann C, Weder C, de Espinosa LM. Supramolecular polymer adhesives: Advanced materials inspired by nature. *Chem Soc Rev* 2016;45:342–58. <https://doi.org/10.1039/c5cs00477b>.
- [7] Ghobril C, Grinstaff MW. The chemistry and engineering of polymeric hydrogel adhesives for wound closure: A tutorial. *Chem Soc Rev* 2015;44:1820–35. <https://doi.org/10.1039/c4cs00332b>.
- [8] Yang J, Bai R, Chen B, Suo Z. Hydrogel Adhesion: A Supramolecular Synergy of Chemistry, Topology, and Mechanics. *Adv Funct Mater* 2019;1901693:1–27. <https://doi.org/10.1002/adfm.201901693>.
- [9] Ji X, Ahmed M, Long L, Khashab NM, Huang F, Sessler JL. Adhesive supramolecular polymeric materials constructed from macrocycle-based host-guest interactions. *Chem Soc Rev* 2019;48:2682–97. <https://doi.org/10.1039/c8cs00955d>.
- [10] Lee BP, Messersmith PB, Israelachvili JN, Waite JH. Mussel-Inspired Adhesives and Coatings. *Annu Rev Mater Res* 2011;41:99–132. <https://doi.org/10.1146/annurev-matsci-062910-100429>.
- [11] Stewart RJ, Wang CS, Shao H. Complex coacervates as a foundation for synthetic underwater adhesives. *Adv Colloid Interface Sci* 2011;167:85–93. <https://doi.org/10.1016/j.cis.2010.10.009>.
- [12] Waite JH. Mussel adhesion – essential footwork. *J Exp Biol*

- 2017;220:517–30.  
<https://doi.org/10.1242/jeb.134056>.
- [13] Ahn BK. Perspectives on  
 Mussel-Inspired Wet Adhesion. J Am Chem Soc  
 2017;139:10166–71.  
<https://doi.org/10.1021/jacs.6b13149>.
- [14] Spotnitz WD, Burks S. Hemostats,  
 sealants, and adhesives: Components of the surgical toolbox. Transfusion (Paris)  
 2008;48:1502–16.  
<https://doi.org/10.1111/j.1537-2995.2012.03707.x>.
- [15] Pinnaratip R, Bhuiyan MSA, Meyers K, Rajachar RM, Lee BP. Multifunctional  
 Biomedical Adhesives. Adv Healthc Mater  
 2019;1801568:1–17.  
<https://doi.org/10.1002/adhm.201801568>.
- [16] Narayanan A, Xu Y, Dhinojwala A, Joy A. Advances in  
 photoreactive tissue adhesives derived from natural polymers. ChemEngineering  
 2020;4:1–18.  
<https://doi.org/10.3390/chemengineering4020032>.
- [17] Scognamiglio F, Travan A, Rustighi I, Tarchi P, Palmisano S, Marsich E, et al. J Biomed Mater Res  
 al. Adhesive and sealant interfaces for general surgery applications. B Appl Biomater 2016;104:626–39.  
<https://doi.org/10.1002/jbm.b.33409>.
- [18] Stewart RJ, Wang CS, Song IT, Jones JP. The role of  
 coacervation and phase transitions in the sandcastle worm adhesive system. Adv Colloid  
 Interface Sci 2017;239:88–96.  
<https://doi.org/10.1016/j.cis.2016.06.008>.
- [19] Narayanan A, Dhinojwala A, Joy A. Design principles for  
 creating synthetic underwater adhesives. Chem Soc Rev  
 2021;50:13321–45.  
<https://doi.org/10.1039/d1cs00316j>.
- [20] Kord Forooshani P, Lee BP. Recent approaches  
 in designing bioadhesive materials inspired by mussel adhesive protein. J Polym Sci A Polym  
 Chem 2017;55:9–33.  
<https://doi.org/10.1002/pola.28368>.
- [21] Fan H, Wang J, Tao Z, Huang J, Rao P, Kurokawa T, et al. Adjacent cationic–  
 aromatic sequences yield strong electrostatic adhesion of hydrogels in  
 seawater. Nat Commun 2019;10.  
<https://doi.org/10.1038/s41467-019-13171-9>.
- [22] Stewart RJ, Ransom TC, Hlady V. Natural underwater  
 adhesives. J Polym Sci B Polym Phys 2011;49:757–71.  
<https://doi.org/10.1002/polb.22256>.
- [23] Danner E, Israelachvili JN, Wei W, Miller DR, Yu J, Das S, et al. Adaptive  
 hydrophobic and hydrophilic interactions of mussel foot proteins with organic thin  
 films. Proceedings of the National Academy of Sciences 2013;110:15680–  
 5.  
<https://doi.org/10.1073/pnas.1315015110>.
- [24] Villey R, Cortet PP, Creton C, Ciccotti M. In-situ  
 measurement of the large strain response of the fibrillar debonding region during the steady  
 peeling of pressure sensitive adhesives. Int J Fract  
 2017;204:175–90.  
<https://doi.org/10.1007/s10704-016-0171-1>.



- [25] Vahdati M, Ducouret G, Creton C, Hourdet D. Topology-Specific  
Injectable Sticky Hydrogels. *Macromolecules*  
2020;9779–92.
- [26] Vahdati M, Cedano Serrano FJ, Creton C, Hourdet D. Coacervate-based  
Underwater Adhesives in Physiological Conditions. *ACS Appl Polym  
Mater* 2020;2:3397–410.  
<https://doi.org/10.1021/acspapm.0c00479>.
- [27] Palchesko RN, Zhang L, Sun Y, Feinberg AW. Development of  
Polydimethylsiloxane Substrates with Tunable Elastic Modulus to Study Cell Mechanobiology in  
Muscle and Nerve. *PLoS One*  
2012;7. <https://doi.org/10.1371/journal.pone.0051499>.
- [28] Creton C. Pressure-Sensitive  
Adhesives : An Introductory Course. *MRS Bull* 2003:434–  
9.
- [29] Creton C, Ciccotti M. Fracture and  
adhesion of soft materials: A review. *Reports on Progress  
in Physics* 2016;79:46601.  
<https://doi.org/10.1088/0034-4885/79/4/046601>.
- [30] Waite JHH. Adhesion a la  
Moule. *Integr Comp Biol* 2002;42:1172–80.  
<https://doi.org/https://doi.org/10.1093/icb/42.6.1172>.
- [31] Creton C. 50th Anniversary  
Perspective: Networks and Gels: Soft but Dynamic and Tough. *Macromolecules*  
2017;50:8297–316.  
<https://doi.org/10.1021/acs.macromol.7b01698>.
- [32] Yarusso DJ. Quantifying the  
Relationship between Peel and Rheology for Pressure Sensitive Adhesives. *Journal of Adhesion*  
1999;70:299–320.  
<https://doi.org/10.1080/00218469908009561>.
- [33] Rubinstein, Michael RHC. Polymr  
Physics. Oxford; 2003.
- [34] Guo H, Sanson N, Hourdet D, Marcellan A. Thermoresponsive  
Toughening with Crack Bifurcation in Phase-Separated Hydrogels under Isochoric  
Conditions. *Advanced Materials* 2016;28:7043.  
<https://doi.org/10.1002/adma.201603680>.
- [35] Guo H, Sanson N, Marcellan A, Hourdet D. Thermoresponsive  
Toughening in LCST-Type Hydrogels: Comparison between Semi-Interpenetrated and Grafted  
Networks. *Macromolecules* 2016;49:9568–77.  
<https://doi.org/10.1021/acs.macromol.6b02188>.
- [36] Vahdati M, Ducouret G, Creton C, Hourdet D. Thermally Triggered  
Injectable Underwater Adhesives. *Macromol Rapid  
Commun* 2020;41:1–7.  
<https://doi.org/10.1002/marc.201900653>.
- [37] Zosel A. Shear strength of  
pressure sensitive adhesives and its correlation to mechanical properties. *J Adhes* 1994;44:1–  
16. <https://doi.org/10.1080/00218469408026613>.
- [38] Kendall K. Cracking of Short  
Lap Joints. *J Adhes* 1975;7:137–40.  
<https://doi.org/10.1080/00218467508075045>.
- [39] Liu Z, Minsky H, Creton C, Ciccotti M, Hui CY. Mechanics of zero  
degree peel test on a tape — effects of large deformation, material nonlinearity, and finite bond

- length. *Extreme Mech Lett* 2019;32:100518.  
<https://doi.org/10.1016/j.eml.2019.100518>.
- [40] Li X, Zheng T, Liu X, Du Z, Xie X, Li B, et al. Coassembly of Short Peptide and Polyoxometalate into Complex Coacervate Adapted for pH and Metal Ion-Triggered Underwater Adhesion. *Langmuir* 2019;35:4995–5003.  
<https://doi.org/10.1021/acs.langmuir.9b00273>.
- [41] Narayanan A, Menefee JR, Liu Q, Dhinojwala A, Joy A. Lower Critical Solution Temperature-Driven Self-Coacervation of Nonionic Polyester Underwater Adhesives. *ACS Nano* 2020;14:8359–67.  
<https://doi.org/10.1021/acsnano.0c02396>.
- [42] Shao H, Stewart RJ. Biomimetic underwater adhesives with environmentally triggered setting mechanisms. *Advanced Materials* 2010;22:729–33.  
<https://doi.org/10.1002/adma.200902380>.
- [43] Sousa MP, Neto AI, Correia TR, Miguel SP, Matsusaki M, Correia IJ, et al. Bioinspired multilayer membranes as potential adhesive patches for skin wound healing. *Biomater Sci* 2018;6:1962–75.  
<https://doi.org/10.1039/c8bm00319j>.
- [44] Kurokawa T, Gong JP, Takahata M, Nakajima T, Guo HL, Sun TL, et al. Self-Adjustable Adhesion of Polyampholyte Hydrogels. *Advanced Materials* 2015;27:7344–8.  
<https://doi.org/10.1002/adma.201504059>.
- [45] Brubaker CE, Messersmith PB. Enzymatically degradable mussel-inspired adhesive hydrogel. *Biomacromolecules* 2011;12:4326–34.  
<https://doi.org/10.1021/bm201261d>.
- [46] Chung H, Grubbs RH. Rapidly cross-linkable DOPA containing terpolymer adhesives and PEG-based cross-linkers for biomedical applications. *Macromolecules* 2012;45:9666–73.  
<https://doi.org/10.1021/ma3017986>.
- [47] Xu Y, Liu Q, Narayanan A, Jain D, Dhinojwala A, Joy A. Mussel-Inspired Polyesters with Aliphatic Pendant Groups Demonstrate the Importance of Hydrophobicity in Underwater Adhesion. *Adv Mater Interfaces* 2017;4:1–6.  
<https://doi.org/10.1002/admi.201700506>.
- [48] Lawrence PG, Lapitsky Y. Ionically cross-linked poly(allylamine) as a stimulus-responsive underwater adhesive: Ionic strength and pH effects. *Langmuir* 2015;31:1564–74.  
<https://doi.org/10.1021/la504611x>.
- [49] Ahn Y, Jang Y, Selvapalam N, Yun G, Kim K. Supramolecular velcro for reversible underwater adhesion. *Chemie - International Edition* 2013;52:3140–4.  
<https://doi.org/10.1002/anie.201209382>.
- [50] Liu J, Scherman OA. Cucurbit[n]uril Supramolecular Hydrogel Networks as Tough and Healable Adhesives. *Adv Funct Mater* 2018;28:1–6.  
<https://doi.org/10.1002/adfm.201800848>.
- [51] Yi MB, Lee TH, Han GY, Kim H, Kim HJ, Kim Y, et al. Movable Cross-linking in Adhesives: Superior Stretching and Adhesion Properties via a Supramolecular Sliding

- Effect. ACS Appl Polym Mater 2021;3:2678–86.  
<https://doi.org/10.1021/acsapm.1c00240>.
- [52] Georgiou I, Hadavinia H, Ivankovic A, Kinloch AJ, Tropsa V, Williams JG. Cohesive zone models and the plastically deforming peel test. Journal of Adhesion 2003;79:239–65.  
<https://doi.org/10.1080/00218460309555>.
- [53] Kinloch AJ, Williams JG. The mechanics of peel tests. In: Dillard DA, Pocius AV, editors. The Mechanics of Adhesion, Amsterdam: Elsevier; 2002, p. 273–301.
- [54] Renvoise J, Burlot D, Marin G, Derail C. Peeling of PSAs on viscoelastic substrates: A failure criterion. Journal of Adhesion 2007;83:403–16.  
<https://doi.org/10.1080/00218460701282554>.
- [55] Renvoise J, Burlot D, Marin G, Derail C. Adherence performances of pressure sensitive adhesives on a model viscoelastic synthetic film: A tool for the understanding of adhesion on the human skin. Int J Pharm 2009;368:83–8.  
<https://doi.org/10.1016/j.ijpharm.2008.09.056>.
- [56] Chivers RA. Easy removal of pressure sensitive adhesives for skin applications. Int J Adhes Adhes 2001;21:381–8.  
<https://doi.org/10.1109/GlobalSIP.2016.7906046>.
- [57] Tiu BDB, Delparastan P, Ney MR, Gerst M, Messersmith PB. Enhanced Adhesion and Cohesion of Bioinspired Dry/Wet Pressure-Sensitive Adhesives. ACS Appl Mater Interfaces 2019;11:28296–306.  
<https://doi.org/10.1021/acsami.9b08429>.
- [58] Yuk H, Varela CE, Nabzdyk CS, Mao X, Padera RF, Roche ET, et al. Dry double-sided tape for adhesion of wet tissues and devices. Nature 2019;575:169–74.  
<https://doi.org/10.1038/s41586-019-1710-5>.
- [59] Li J, Celiz AD, Yang J, Yang Q, Wamala I, Whyte W, et al. Tough adhesives for diverse wet surfaces. Science 2017;357:378–81.  
<https://doi.org/10.1126/science.aah6362>.
- [60] Michel R, Manassero M, Corté L, Poirier L, Legagneux J, van Poelvoorde Q. Interfacial fluid transport is a key to hydrogel bioadhesion. Proceedings of the National Academy of Sciences 2019;116:738–43.  
<https://doi.org/10.1073/pnas.1813208116>.
- [61] Macron J, Gerratt AP, Lacour SP. Thin Hydrogel–Elastomer Multilayer Encapsulation for Soft Electronics. Adv Mater Technol 2019;4:6–11.  
<https://doi.org/10.1002/admt.201900331>.
- [62] Shull KR, Creton C. Deformation behavior of thin, compliant layers under tensile loading conditions. J Polym Sci B Polym Phys 2004;42:4023–43.  
<https://doi.org/10.1002/polb.20258>.
- [63] Lakrout H, Sergot P, Creton C. Direct observation of cavitation and fibrillation in a probe tack experiment on model acrylic pressure-sensitive-adhesives. Journal of Adhesion 1999;69:307–59.  
<https://doi.org/10.1080/00218469908017233>.
- [64] Sudre G, Olanier L, Tran Y, Hourdet D, Creton C. Reversible adhesion between a hydrogel and a polymer brush. Soft Matter

- 2012;8:8184–93.  
<https://doi.org/10.1039/c2sm25868d>.
- [65] Webber RE, Shull KR, Roos A, Creton C. Effects of geometric confinement on the adhesive debonding of soft elastic solids. *Plasmas Fluids Relat Interdiscip Topics* 2003;68:11.  
<https://doi.org/10.1103/PhysRevE.68.021805>.
- [66] Macron J, Bresson B, Tran Y, Hourdet D, Creton C. Equilibrium and Out-of-Equilibrium Adherence of Hydrogels against Polymer Brushes. *Macromolecules* 2018;51:7556–66.  
<https://doi.org/10.1021/acs.macromol.8b01063>.
- [67] Cedano-Serrano FJ, Sidoli U, Synytska A, Tran Y, Hourdet D, Creton C. From Molecular Electrostatic Interactions and Hydrogel Architecture to Macroscopic Underwater Adherence. *Macromolecules* 2019;52:3852–62.  
<https://doi.org/10.1021/acs.macromol.8b02696>.
- [68] Dompé M, Cedano-Serrano FJ, Heckert O, van den Heuvel N, van der Gucht J, Tran Y, et al. Thermo-responsive Complex Coacervate-Based Underwater Adhesive. *Advanced Materials* 2019;31.
- [69] Rao P, Sun TL, Chen L, Takahashi R, Shinohara G, Guo H, et al. Tough Hydrogels with Fast, Strong, and Reversible Underwater Adhesion Based on a Multiscale Design. *Advanced Materials* 2018;30:1–8.  
<https://doi.org/10.1002/adma.201801884>.
- [70] Narayanan A, Kaur S, Peng C, Debnath D, Mishra K, Liu Q, et al. Viscosity Attunes the Adhesion of Bioinspired Low Modulus Polyester Adhesive Sealants to Wet Tissues. *Biomacromolecules* 2019;20:2577–86.  
<https://doi.org/10.1021/acs.biomac.9b00383>.
- [71] Karnal P, Jha A, Wen H, Gryska S, Barrios C, Frechette J. Contribution of Surface Energy to pH-Dependent Underwater Adhesion of an Acrylic Pressure-Sensitive Adhesive. *Langmuir* 2019;35:5151–61.  
<https://doi.org/10.1021/acs.langmuir.9b00120>.
- [72] Derks D, Lindner A, Creton C, Bonn D. Cohesive failure of thin layers of soft model adhesives under tension. *J Appl Phys* 2003;93:1557–66.  
<https://doi.org/10.1063/1.1533095>.
- [73] Clancy SK, Sodano A, Cunningham DJ, Huang SS, Zalicki PJ, Shin S, et al. Marine Bioinspired Underwater Contact Adhesion. *Biomacromolecules* 2016;17:1869–74.  
<https://doi.org/10.1021/acs.biomac.6b00300>.
- [74] Lakrout H, Creton C, Ahn D, Shull KR. Influence of molecular features on the tackiness of acrylic polymer melts. *Macromolecules* 2001;34:7448–58.  
<https://doi.org/10.1021/ma0020279>.
- [75] Saffman PG, Taylor GI. The penetration of a fluid into a porous medium or Hele-Shaw cell containing a more viscous liquid. *Proc R Soc Lond A Math Phys Sci* 1958;245:312–29.  
<https://doi.org/10.1098/rspa.1958.0085>.
- [76] Nase J, Derks D, Lindner A. Dynamic evolution of fingering patterns in a lifted Hele-Shaw cell. *Physics of Fluids* 2011;23. <https://doi.org/10.1063/1.3659140>.
- [77] Shull KR, Flanigan CM, Crosby AJ. Fingering instabilities of confined elastic layers in tension. *Phys Rev Lett*

- 2000;84:3057–60.  
<https://doi.org/10.1103/PhysRevLett.84.3057>.
- [78] Lin S, Mao Y, Radovitzky R, Zhao X. Instabilities in confined elastic layers under tension: Fringe, fingering and cavitation. *J Mech Phys Solids* 2017;106:229–56.  
<https://doi.org/10.1016/j.jmps.2017.05.011>.
- [79] Chiche A, Dollhofer J, Creton C. Cavity growth in soft adhesives. *European Physical Journal E* 2005;17:389–401.  
<https://doi.org/10.1140/epje/i2004-10148-3>.
- [80] Poivet S, Nallet F, Gay C, Teisseire J, Fabre P. Force response of a viscous liquid in a probe-tack geometry: Fingering versus cavitation. *European Physical Journal E* 2004;15:97–116.  
<https://doi.org/10.1140/epje/i2004-10040-2>.
- [81] Zosel A. The effect of fibrillation on the tack of pressure sensitive adhesives. *Int J Adhes Adhes* 1998;18:265–71.  
[https://doi.org/10.1016/S0143-7496\(98\)80060-2](https://doi.org/10.1016/S0143-7496(98)80060-2).
- [82] Deplace F, Carelli C, Mariot S, Retsos H, Chateauminois A, Ouzineb K, et al. Fine tuning the adhesive properties of a soft nanostructured adhesive with rheological measurements. *Journal of Adhesion* 2009;85:18–54.  
<https://doi.org/10.1080/00218460902727381>.
- [83] Villey R, Creton C, Cortet PP, Dalbe MJ, Jet T, Saintyves B, et al. Rate-dependent elastic hysteresis during the peeling of pressure sensitive adhesives. *Soft Matter* 2015;11:3480–91.  
<https://doi.org/10.1039/c5sm00260e>.
- [84] Manoj Lalwani S, Eneh C, Lutkenhaus J. Emerging trends in the dynamics of polyelectrolyte complexes. *Chemical Physics* 2020:24157–77.  
<https://doi.org/10.1039/d0cp03696j>.
- [85] Liu Y, Winter HH, Perry SL. Linear viscoelasticity of complex coacervates. *Adv Colloid Interface Sci* 2017;239:46–60.  
<https://doi.org/10.1016/j.cis.2016.08.010>.
- [86] Winter HH, Mours M. Rheology of Polymers Near Liquid-Solid Transitions. *Advances in Polymer Science* 1997;134:165–234.  
[https://doi.org/10.1007/3-540-68449-2\\_3](https://doi.org/10.1007/3-540-68449-2_3).
- [87] Hamad FG, Chen Q, Colby RH. Linear Viscoelasticity and Swelling of Polyelectrolyte Complex Coacervates. *Macromolecules* 2018;51:5547–55.  
<https://doi.org/10.1021/acs.macromol.8b00401>.
- [88] Lehericey P, Snabre P, Delots A, Holten-Andersen N, Divoux T. Time-resolved rheometry of drying liquids and suspensions. *J Rheol (N Y N Y)* 2021;65:427–36.  
<https://doi.org/10.1122/8.0000214i>.
- [89] Dahlquist CA. Pressure-Sensitive Adhesives. In: Patrick RL, editor. *Treatise on Adhesion and Adhesives*, Marcel Dekker, Inc.; 1969, p. 219–60.
- [90] Henning Winter H. The occurrence of self-similar relaxation in polymers. *J Non Cryst Solids*

- 1994;172–174:1158–67.  
[https://doi.org/10.1016/0022-3093\(94\)90638-6](https://doi.org/10.1016/0022-3093(94)90638-6).
- [91] Liu Y, Momani B, Winter HH, Perry SL. Rheological characterization of liquid-to-solid transitions in bulk polyelectrolyte complexes. *Soft Matter* 2017;13:7332–40.  
<https://doi.org/10.103a/c7sm01285c>.
- [92] Wang T, Lei CH, Dalton AB, Creton C, Lin Y, Fernando KAS, et al. Waterborne, nanocomposite pressure-sensitive adhesives with high tack energy, optical transparency, and electrical conductivity. *Advanced Materials* 2006;18:2730–4.  
<https://doi.org/10.1002/adma.200601335>.
- [93] Han L, Wang M, Prieto-López LO, Deng X, Cui J. Self-Hydrophobization in a Dynamic Hydrogel for Creating Nonspecific Repeatable Underwater Adhesion. *Adv Funct Mater* 2020;30.  
<https://doi.org/10.1002/adfm.201907064>.
- [94] Dompe M, Vahdati M, Ligten F van, Cedano-Serrano FJ, Hourdet D, Creton C, et al. Enhancement of the Adhesive Properties by Optimizing the Water Content in PNIPAM-Functionalized Complex Coacervates. *ACS Appl Polym Mater* 2020:1722–30.
- [95] Huang Y, Lawrence PG, Lapitsky Y. Self-assembly of stiff, adhesive and self-healing gels from common polyelectrolytes. *Langmuir* 2014;30:7771–7.  
<https://doi.org/10.1021/la404606y>.
- [96] Xu J, Li X, Li X, Li B, Wu L, Li W, et al. Supramolecular Copolymerization of Short Peptides and Polyoxometalates: Toward the Fabrication of Underwater Adhesives. *Biomacromolecules* 2017;18:3524–30.  
<https://doi.org/10.1021/acs.biomac.7b00817>.
- [97] Dompé M, Cedano-Serrano FJ, Vahdati M, van Westerveld L, Hourdet D, Creton C, et al. Underwater Adhesion of Multiresponsive Complex Coacervates. *Adv Mater Interfaces* 2020;7:1901785.
- [98] Kim K, Shin M, Koh MY, Ryu JH, Lee MS, Hong S, et al. TAPE: A medical adhesive inspired by a ubiquitous compound in plants. *Adv Funct Mater* 2015;25:2402–10.  
<https://doi.org/10.1002/adfm.201500034>.
- [99] Lee D, Hwang H, Kim JS, Park J, Youn D, Kim D, et al. VATA: A Poly(vinyl alcohol)- And Tannic Acid-Based Nontoxic Underwater Adhesive. *ACS Appl Mater Interfaces* 2020;12:20933–41.  
<https://doi.org/10.1021/acsami.0c02037>.
- [100] Peng Q, Chen J, Zeng Z, Wang T, Xiang L, Peng X, et al. Adhesive Coacervates Driven by Hydrogen-Bonding Interaction. *Small* 2020;16:1–8.  
<https://doi.org/10.1002/sml.202004132>.
- [101] Cui Y, Yin L, Sun X, Zhang N, Gao N, Zhu G. A Universal and Reversible Wet Adhesive via Straightforward Aqueous Self-Assembly of Polyethylenimine and Polyoxometalate. *ACS Appl Mater Interfaces* 2021; 13, 47155–62. <https://doi.org/10.1021/acsami.1c14231>.
- [102] Peng Q, Wu Q, Chen J, Wang T, Wu M, Yang D, et al. Coacervate-Based Instant and Repeatable Underwater Adhesive with Anticancer and Antibacterial Properties. *ACS Appl Mater Interfaces* 2021.  
<https://doi.org/10.1021/acsami.1c13744>.
- [103] Wang YJ, He Y, Zheng SY, Xu Z, Li J, Zhao Y, et al. Polymer Pressure-Sensitive Adhesive with A Temperature-Insensitive Loss Factor Operating Under Water and



- Oil. Adv Funct Mater 2021;2104296:1–8.  
<https://doi.org/10.1002/adfm.202104296>.
- [104] Zhu X, Wei C, Chen H, Zhang C, Peng H, Wang D, et al. A Cation-Methylene-Phenyl Sequence Encodes Programmable Poly(Ionic Liquid) Coacervation and Robust Underwater Adhesion. Adv Funct Mater 2022;32. <https://doi.org/10.1002/adfm.202105464>.
- [105] Wei X, Chen D, Zhao X, Luo J, Wang H, Jia P. Underwater Adhesive HPMC/SiW-PDMAEMA/Fe3+Hydrogel with Self-Healing, Conductive, and Reversible Adhesive Properties. ACS Appl Polym Mater 2021;3:837–46.  
<https://doi.org/10.1021/acsapm.0c01177>.
- [106] Israelachvili J, Pashley R. The hydrophobic interaction is long range, decaying exponentially with distance (Israelachvili and Pashley, 1982).pdf 1982;300:341–2.
- [107] Meyer EE, Rosenberg KJ, Israelachvili J. Recent progress in understanding hydrophobic interactions. Proceedings of the National Academy of Sciences 2006;103:15739–46.  
<https://doi.org/10.1073/pnas.0606422103>.
- [108] Vladimir Aseyev, Heikki Tenhu and FMW. Non-ionic Thermoresponsive Polymers in Water. Advances in Polymer Science 2011;242:29–89.  
[https://doi.org/10.1007/12\\_2010\\_57](https://doi.org/10.1007/12_2010_57).
- [109] Gil ES, Hudson SM. Stimuli-reponsive polymers and their bioconjugates. Progress in Polymer Science (Oxford) 2004;29:1173–222.  
<https://doi.org/10.1016/j.progpolymsci.2004.08.003>.
- [110] Teotia AK, Sami H, Kumar A. Thermo-responsive polymers: Structure and design of smart materials. Switchable and Responsive Surfaces and Materials for Biomedical Applications, Elsevier Ltd; 2015, p. 3–43.  
<https://doi.org/10.1016/B978-0-85709-713-2.00001-8>.
- [111] Zhang Q, Weber C, Schubert US, Hoogenboom R. Thermo-responsive polymers with lower critical solution temperature: From fundamental aspects and measuring techniques to recommended turbidimetry conditions. Mater Horiz 2017;4:109–16.  
<https://doi.org/10.1039/c7mh00016b>.
- [112] van Durme K, van Assche G, van Mele B. Kinetics of demixing and remixing in poly(N-isopropylacrylamide)/water studied by modulated temperature DSC. Macromolecules 2004;37:9596–605.  
<https://doi.org/10.1021/ma048472b>.
- [113] Schild HG, Tirrell DA. Microcalorimetric detection of lower critical solution temperatures in aqueous polymer solutions. Journal of Physical Chemistry® 1990;94:4352–6.  
<https://doi.org/10.1021/j100373a088>.
- [114] Petit L, Bouteiller L, Brûlet A, Lafuma F, Hourdet D. Responsive hybrid self-assemblies in aqueous media. Langmuir 2007;23:147–58.  
<https://doi.org/10.1021/la061466j>.
- [115] Otake K, Inomata H, Konno M, Saito S. Thermal Analysis of the Volume Phase Transition with N-Isopropylacrylamide Gels. Macromolecules 1990;23:283–9.  
<https://doi.org/10.1021/ma00203a049>.

- [116] Shibayama M, Tanaka T, Han CC. Small angle neutron scattering study on poly(N-isopropyl acrylamide) gels near their volume-phase transition temperature. *J Chem Phys* 1992;97:6829–41.  
<https://doi.org/10.1063/1.463636>.
- [117] Shibayama M, Morimoto M, Nomura S. Phase Separation Induced Mechanical Transition of Poly(N-isopropylacrylamide)/Water Isochore Gels. *Macromolecules* 1994;27:5060–6.  
<https://doi.org/10.1021/ma00096a031>.
- [118] Ruel-Gariépy E, Leroux JC. In situ-forming hydrogels - Review of temperature-sensitive systems. *European Journal of Pharmaceutics and Biopharmaceutics* 2004;58:409–26.  
<https://doi.org/10.1016/j.ejpb.2004.03.019>.
- [119] Durand A, Hervé M, Hourdet D. Thermogelation in Aqueous Polymer Solutions. In: McCormick CL, editor. *Stimuli-Responsive Water Soluble and Amphiphilic Polymers*, 2000, p. 181–207.  
<https://doi.org/10.1021/bk-2001-0780>.
- [120] Guo H, Brûlet A, Rajamohanan PR, Marcellan A, Sanson N, Hourdet D. Influence of topology of LCST-based graft copolymers on responsive assembling in aqueous media. *Polymer (Guildf)* 2015;60:164–75.  
<https://doi.org/10.1016/j.polymer.2015.01.038>.
- [121] Guo H, Mussault C, Brûlet A, Marcellan A, Hourdet D, Sanson N. Thermoresponsive Toughening in LCST-Type Hydrogels with Opposite Topology: From Structure to Fracture Properties. *Macromolecules* 2016;49:4295–306.  
<https://doi.org/10.1021/acs.macromol.6b00798>.
- [122] Quentin Demassieux, Berghezan D, Creton C. Microfocused Beam SAXS and WAXS Mapping at the Crack Tip and Fatigue Crack Propagation in Natural Rubber. *Fatigue Crack Growth in Rubber Materials*, Springer; 2020, p. 467–91.  
[https://doi.org/10.1007/12\\_2020\\_79](https://doi.org/10.1007/12_2020_79).
- [123] Rublon P, Huneau B, Saintier N, Beurrot S, Leygue A, Verron E, et al. In situ synchrotron wide-angle X-ray diffraction investigation of fatigue cracks in natural rubber. *J Synchrotron Radiat* 2013;20:105–9.  
<https://doi.org/10.1107/S0909049512044457>.
- [124] Brüning K, Schneider K, Roth S v., Heinrich G. Strain-induced crystallization around a crack tip in natural rubber under dynamic load. *Polymer (Guildf)* 2013;54:6200–5.  
<https://doi.org/10.1016/j.polymer.2013.08.045>.
- [125] Trabelsi S, Albouy PA, Rault J. Stress-induced crystallization around a crack tip in natural rubber. *Macromolecules* 2002;35:10054–61.  
<https://doi.org/10.1021/ma021106c>.
- [126] Kaur S, Narayanan A, Dalvi S, Liu Q, Joy A, Dhinojwala A. Direct Observation of the Interplay of Catechol Binding and Polymer Hydrophobicity in a Mussel-Inspired Elastomeric Adhesive. *ACS Cent Sci* 2018;4:1420–9.  
<https://doi.org/10.1021/acscentsci.8b00526>.
- [127] Wei W, Broomell C, Yu J, Israelachvili JN, Waite JH. Hydrophobic Enhancement of Dopa-Mediated Adhesion in a Mussel Foot Protein. *J Am Chem Soc* 2012;135:377–83.  
<https://doi.org/10.1021/ja309590f>.
- [128] Nasserri R, Tam KC. Sticky Hydrogels from Hydrazide-Functionalized Poly(oligo(ethylene glycol) methacrylate) and Dialdehyde Cellulose

- Nanocrystals with Tunable Thermal and Strain-Hardening Characteristics. ACS Sustain Chem Eng 2021. <https://doi.org/10.1021/acssuschemeng.1c03183>.
- [129] Poivet S, Fabre P, Nallet F, Schierholz K, Abraham G, Papon É, et al. Amphiphilic diblock copolymers with adhesive properties: I. Structure and swelling with water. European Physical Journal E 2006;20:273–87. <https://doi.org/10.1140/epje/i2005-10130-7>.
- [130] Nasser R, Tam KC. Stimuli-responsive hydrogel consisting of hydrazide-functionalized poly(oligo(ethylene glycol)methacrylate) and dialdehyde cellulose nanocrystals. Mater Adv 2020;1:1631–43. <https://doi.org/10.1039/d0ma00397b>.
- [131] Harada A, Takashima Y, Nakahata M. Supramolecular polymeric materials via cyclodextrin-guest interactions. Acc Chem Res 2014;47:2128–40. <https://doi.org/10.1021/ar500109h>.
- [132] Roling O, Stricker L, Voskuhl J, Lamping S, Ravoo BJ. Supramolecular surface adhesion mediated by azobenzene polymer brushes. Chemical Communications 2016;52:1964–6. <https://doi.org/10.1039/c5cc08968a>.
- [133] Appel EA, del Barrio J, Loh XJ, Scherman OA. Supramolecular polymeric hydrogels. Chem Soc Rev 2012;41:6195–214. <https://doi.org/10.1039/c2cs35264h>.
- [134] Harada A, Kobayashi R, Takashima Y, Hashidzume A, Yamaguchi H. Macroscopic self-assembly through molecular recognition. Nat Chem 2011;3:34–7. <https://doi.org/10.1038/nchem.893>.
- [135] Takashima Y, Sahara T, Sekine T, Kakuta T, Nakahata M, Otsubo M, et al. Supramolecular adhesives to hard surfaces: Adhesion between host hydrogels and guest glass substrates through molecular recognition. Macromol Rapid Commun 2014;35:1646–52. <https://doi.org/10.1002/marc.201400324>.
- [136] Wang Q, Schlenoff JB. The Polyelectrolyte Complex/Coacervate Continuum. Macromolecules 2014;47:3108. <https://doi.org/10.1021/ma500500q>.
- [137] Schlenoff JB, Yang M, Digby ZA, Wang Q. Ion Content of Polyelectrolyte Complex Coacervates and the Donnan Equilibrium. Macromolecules 2019;52:9149–59. <https://doi.org/10.1021/acs.macromol.9b01755>.
- [138] Rumyantsev AM, Jackson NE, de Pablo JJ. Polyelectrolyte Complex Coacervates: Recent Developments and New Frontiers. Annu Rev Condens Matter Phys 2021;12:155–76. <https://doi.org/10.1146/annurev-conmatphys-042020-113457>.
- [139] Martin N. Dynamic Synthetic Cells Based on Liquid–Liquid Phase Separation. ChemBioChem 2019;20:2553–68. <https://doi.org/10.1002/cbic.201900183>.
- [140] Sing CE. Development of the modern theory of polymeric complex coacervation. Adv Colloid Interface Sci 2017;239:2–16. <https://doi.org/10.1016/j.cis.2016.04.004>.

- [141] Spruijt E, Westphal AH, Borst JW, Cohen Stuart MA, van der Gucht J. Binodal compositions of polyelectrolyte complexes. *Macromolecules* 2010;43:6476–84.  
<https://doi.org/10.1021/ma101031t>.
- [142] Fu J, Schlenoff JB. Driving Forces for Oppositely Charged Polyion Association in Aqueous Solutions: Enthalpic, Entropic, but Not Electrostatic. *J Am Chem Soc* 2016;138:980–90.  
<https://doi.org/10.1021/jacs.5b11878>.
- [143] Shull KR, Jiang Z, Wang Q, Keshavarz B, Chen Y, Sadman K. Influence of Hydrophobicity on Polyelectrolyte Complexation. *Macromolecules* 2017;50:9417–26.  
<https://doi.org/10.1021/acs.macromol.7b02031>.
- [144] Chen Y, Yang M, Shaheen SA, Schlenoff JB. Influence of Nonstoichiometry on the Viscoelastic Properties of a Polyelectrolyte Complex. *Macromolecules* 2021. <https://doi.org/10.1021/acs.macromol.1c01154>.
- [145] Rubinstein M, Semenov AN. Dynamics of entangled solutions of associating polymers. *Macromolecules* 2001;34:1058–68.  
<https://doi.org/10.1021/ma0013049>.
- [146] Colby RH. Structure and linear viscoelasticity of flexible polymer solutions: Comparison of polyelectrolyte and neutral polymer solutions. *Rheol Acta* 2010;49:425–42.  
<https://doi.org/10.1007/s00397-009-0413-5>.
- [147] Spruijt E, Sprakel J, Lemmers M, Stuart MAC, van der Gucht J. Relaxation dynamics at different time scales in electrostatic complexes: Time-salt superposition. *Phys Rev Lett* 2010;105:1–4.  
<https://doi.org/10.1103/PhysRevLett.105.208301>.
- [148] Spruijt E, Cohen Stuart MA, van der Gucht J. Linear viscoelasticity of polyelectrolyte complex coacervates. *Macromolecules* 2013;46:1633–41.  
<https://doi.org/10.1021/ma301730n>.
- [149] Rubinstein M, Semenov AN. Thermoreversible gelation in solutions of associating polymers. 2. Linear dynamics. *Macromolecules* 1998;31:1386–97.  
<https://doi.org/10.1021/ma970617+>.
- [150] Sing CE, Perry SL. Recent progress in the science of complex coacervation. *Soft Matter* 2020;16:2885–914.  
<https://doi.org/10.1039/d0sm00001a>.
- [151] Schlenoff JB. Site-specific perspective on interactions in polyelectrolyte complexes: Toward quantitative understanding. *Journal of Chemical Physics* 2018;149.
- [152] Schlenoff JB, Rmaile AH, Bucur CB. Hydration contributions to association in polyelectrolyte multilayers and complexes: Visualizing hydrophobicity. *J Am Chem Soc* 2008;130:13589–97.  
<https://doi.org/10.1021/ja802054k>.
- [153] Fu J, Fares HM, Schlenoff JB. Ion-Pairing Strength in Polyelectrolyte Complexes. *Macromolecules*

- 2017;50:1066–74.  
<https://doi.org/10.1021/acs.macromol.6b02445>.
- [154] Yang M, Shi J, Schlenoff JB. Control of Dynamics in Polyelectrolyte Complexes by Temperature and Salt. *Macromolecules* 2019;52:1930–41.  
<https://doi.org/10.1021/acs.macromol.8b02577>.
- [155] Sadman K, Delgado DE, Won Y, Wang Q, Gray KA, Shull KR. Versatile and High-Throughput Polyelectrolyte Complex Membranes via Phase Inversion. *ACS Appl Mater Interfaces* 2019;11:16018–26.  
<https://doi.org/10.1021/acsami.9b02115>.
- [156] Shamoun RF, Reisch A, Schlenoff JB. Extruded saloplastic polyelectrolyte complexes. *Adv Funct Mater* 2012;22:1923–31.  
<https://doi.org/10.1002/adfm.201102787>.
- [157] Stevens MJ, Steren RE, Hlady V, Stewart RJ. Multiscale structure of the underwater adhesive of *Phragmatopoma Californica*: A nanostructured latex with a steep microporosity gradient. *Langmuir* 2007;23:5045–9.  
<https://doi.org/10.1021/la063765e>.
- [158] Shao H, Bachus KN, Stewart RJ. A water-borne adhesive modeled after the sandcastle glue of *P. californica*. *Macromol Biosci* 2009;9:464–71.  
<https://doi.org/10.1002/mabi.200800252>.
- [159] Jones JP, Sima M, O’Hara RG, Stewart RJ. Water-Borne Endovascular Embolics Inspired by the Undersea Adhesive of Marine Sandcastle Worms. *Adv Healthc Mater* 2016;5:795–801.  
<https://doi.org/10.1002/adhm.201500825>.
- [160] Dompé M, Cedano-Serrano FJ, Vahdati M, Sidoli U, Heckert O, Synytska A, et al. Tuning the interactions in multiresponsive complex coacervate-based underwater adhesives. *Int J Mol Sci* 2020;21.
- [161] Vahdati M. Salt and temperature responsive soft underwater adhesives. Sorbonne University, 2019.
- [162] MURAKAWA K, KING DR, SUN T, GUO H, KUROKAWA T, GONG JP. Polyelectrolyte Complexation via Viscoelastic Phase Separation Results in Tough and Self-Recovering Porous Hydrogels. *Materials Chemistry B* 2019.  
<https://doi.org/10.1039/C9TB01376H>.
- [163] Yin P, Li D, Liu T. Solution behaviors and self-assembly of polyoxometalates as models of macroions and amphiphilic polyoxometalate–organic hybrids as novel surfactants. *Chem Soc Rev* 2012;41:7368–83.  
<https://doi.org/10.1039/c2cs35176e>.
- [164] Chen J, Peng Q, Peng X, Zhang H, Zeng H. Probing and Manipulating Noncovalent Interactions in Functional Polymeric Systems. *Chem Rev* 2022.  
<https://doi.org/10.1021/acs.chemrev.2c00215>.
- [165] Fan H, Wang L, Feng X, Bu Y, Wu D, Jin Z. Supramolecular Hydrogel Formation Based on Tannic Acid. *Macromolecules* 2017;50:666–76.  
<https://doi.org/10.1021/acs.macromol.6b02106>.
- [166] Erel-Unal I, Sukhishvili SA. Hydrogen-bonded multilayers of a neutral polymer and a polyphenol. *Macromolecules*

- 2008;41:3962–70.  
<https://doi.org/10.1021/ma800186q>.
- [167] Niu W, Zhu J, Zhang W, Liu X. Simply Formulated Dry Pressure-Sensitive Adhesives for Substrate-Independent Underwater Adhesion. *ACS Mater Lett* 2022;4:410–7.  
<https://doi.org/Fmm.s>.
- [168] Schrader AM, Wei W, Israelachvili JN, Idso M, Cristiani TR, Dobbs HA, et al. Tuning underwater adhesion with cation- $\pi$  interactions. *Nat Chem* 2017;9:473–9.  
<https://doi.org/10.1038/nchem.2720>.
- [169] Xiang L, Zhang J, Wang W, Gong L, Zhang L, Yan B, et al.  $\pi$ -cation- $\pi$  interaction with implications for bio-inspired wet adhesion. *2020;117:294–301*.  
<https://doi.org/10.1016/j.actbio.2020.09.043>.
- [170] Zhang J, Lei H, Qin M, Wang W, Cao Y. Quantifying cation- $\pi$  interactions in marine adhesive proteins using single-molecule force spectroscopy. *Materials* 2022;1:100005.  
<https://doi.org/10.1016/j.supmat.2021.100005>.
- [171] Park S, Kim S, Jho Y, Hwang DS. Cation- $\pi$  Interactions and Their Contribution to Mussel Underwater Adhesion Studied Using a Surface Forces Apparatus: A Mini-Review. *Langmuir* 2019;35:16002–12.  
<https://doi.org/10.1021/acs.langmuir.9b01976>.
- [172] Fan H, Wang J, Gong JP. Barnacle Cement Proteins-Inspired Tough Hydrogels with Robust, Long-Lasting, and Repeatable Underwater Adhesion. *Adv Funct Mater* 2021;31.  
<https://doi.org/10.1002/adfm.202009334>.
- [173] Fan H, Cai Y, Gong JP. Facile tuning of hydrogel properties by manipulating cationic-aromatic monomer sequences. *Sci China Chem* 2021;64:1560–8.  
<https://doi.org/10.1007/s11426-021-1010-3>.
- [174] Harrington MJ, Masic A, Holten-andersen N, Waite JHH, Fratzl P. Iron-Clad Fibers : A Metal-Based Biological Strategy for Hard Flexible Coatings. *Science* 2010;328:216–20.  
<https://doi.org/10.1126/science.1181044>.
- [175] Waite JH, Andersen NH, Jewhurst S, Sun C. Mussel adhesion: Finding the tricks worth mimicking. *Journal of Adhesion* 2005;81:297–317.  
<https://doi.org/10.1080/00218460590944602>.
- [176] Chang H, Adibnia V, Li C, Su R, Qi W, Banquy X. Short-sequence superadhesive peptides with topologically enhanced cation- $\pi$  Interactions. *Chemistry of Materials* 2021;33:5168–76.  
<https://doi.org/10.1021/acs.chemmater.1c01171>.
- [177] Debertrand L, Zhao J, Creton C, Narita T. Swelling and mechanical properties of polyacrylamide-derivative dual-crosslink hydrogels having metal-ligand coordination bonds as transient crosslinks. *Gels* 2021;7.  
<https://doi.org/10.3390/gels7020072>.
- [178] Grindy SC, Lenz M, Holten-Andersen N. Engineering Elasticity and Relaxation Time in Metal-Coordinate Cross-Linked Hydrogels. *Macromolecules* 2016;49:8306–12.  
<https://doi.org/10.1021/acs.macromol.6b01523>.



- [179] Grindy SC, Learsch R, Mozhdehi D, Cheng J, Barrett DG, Guan Z, et al. Control of hierarchical polymer mechanics with bioinspired metal-coordination dynamics. *Nat Mater* 2015;14:1210–6.  
<https://doi.org/10.1038/nmat4401>.
- [180] Dompé M, Cedano-Serrano FJ, Vahdati M, Hourdet D, van der Gucht J, Kamperman M, et al. Hybrid complex coacervate. *Polymers (Basel)* 2020;12:1–16.  
<https://doi.org/10.3390/polym12020320>.
- [181] Rose S, PrevotEAU A, Elzière P, Hourdet D, Marcellan A, Leibler L. Nanoparticle solutions as adhesives for gels and biological tissues. *Nature* 2014;505:382–5.  
<https://doi.org/10.1038/nature12806>.
- [182] Michel R, Roquart M, Llusar E, Gaslain F, Norvez S, Baik JS, et al. Hydrogel-Tissue Adhesion Using Blood Coagulation Induced by Silica Nanoparticle Coatings. *ACS Appl Bio Mater* 2020;3:8808–19.  
<https://doi.org/10.1021/acsbm.0c01158>.
- [183] Chassenieux C, Nicolai T, Benyahia L. Rheology of associative polymer solutions. *Curr Opin Colloid Interface Sci* 2011;16:18–26.  
<https://doi.org/10.1016/j.cocis.2010.07.007>.
- [184] Tam KC, Farmer ML, Jenkins RD, Bassett DR. Rheological Properties of Hydrophobically Modified Alkali-Soluble Polymers-Effects of Ethylene-Oxide Chain Length. *J Polym Sci B Polym Phys*, 1998;36:2275-90.
- [185] Bokias G, Hourdet D, Iliopoulos I. Positively charged amphiphilic polymers based on poly(N-isopropylacrylamide): Phase behavior and shear-induced thickening in aqueous solution. *Macromolecules* 2000;33:2929–35.  
<https://doi.org/10.1021/ma991409f>.
- [186] Lorchat P, Konko I, Combet J, Jestin J, Johner A, Laschewski A, et al. New regime in polyelectrolyte solutions. *EPL* 2014;106.
- [187] Buhler E, Boué F. Chain Persistence Length and Structure in Hyaluronan Solutions: Ionic Strength Dependence for a Model Semirigid Polyelectrolyte. *Macromolecules* 2004;37:1600–10.  
<https://doi.org/10.1021/ma0215520>.